Mapping the Uncharted Water Channel of Dihydrodipicolinate Synthase: A Proposed Mechanism of Allostery

---

A thesis submitted in partial fulfilment of the

requirements for the degree of

Masters in Biochemistry

in the School of Biological Sciences

by Amanda Jane Board

University of Canterbury

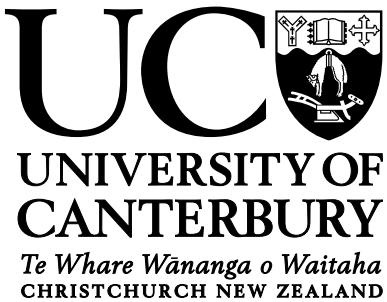

2018

Acknowledgements

Firstly, I would like to thank my supervisors.
Ren Dobson, thank you for believing in me from the beginning, you have been a constant stream of support that could not have been bettered. Thank you for everything.
Grant Pearce, thank you for providing me with genes and ASA (even though I forgot to ask), and giving sound advice when I need it. I could not ask for better supervisors.
I must also extend my thanks to the rest of the Dobson lab group. Rachel, for your "I'll tell you what to do then you go do it" method of teaching, it was the best way to learn. Jenna, for the office chats, the constant help, and showing me what it's really like to work in science. Chris, for always remaining calm and keen to help, even when super stressed yourself. Jim, for your enthusiastic help, and always sticking up for me. Serena, for always helping me find what I need in the freezer even when I couldn't understand Grant's crazy storage system. Jen, for your calm and effective advice. Hannah, for the help with my poster and presentation. Michael for the chats, the help, and the crystals. David, for the kinetics, I couldn't have got that data without you. Finally, to Tones, for the golf advice, procrastinating with me, and for making me feel like I wasn't alone.
Thanks to Paul, Tessa, Barb, Jordan, and the rest of the team at Merin Street, for your support, especially towards the end. It has been an escape coming into work with such vibrant people
To my family; Mum and Dad you always supported me, financially and emotionally, even though you had no idea what I was talking about you were always positive when I was unsure, celebrated my successes and you were a constant stream of support and love. Jack, for always listening and saying, "sounds interesting", and Grandma and Auntie Shell for your support and enthusiasm.
Lastly, thank you to Martin. Nothing I can say will be any measure on what you have done for me over this time. You picked me up when I felt defeated, you put me and my education first, you talked through all my problems, and you always let me know how proud you were and are of me. You pushed me to get to this point and I owe you everything. Thank you so much for your unwavering support, I couldn't have done this without you.

Abstract

Dihydrodipicolinate synthase catalyses the condensation reaction of pyruvate and aspartate semialdehyde in the first committed step of the diaminopimelic acid pathway that synthesizes lysine. Dihydrodipicolinate synthase is allosterically inhibited by lysine.

This study hypothesises that a water channel that connects the lysine binding site and the active site is critical for allosteric inhibition by lysine. When lysine binds to the allosteric site, it acts as a lid for the water channel, blocking the ability to shuttle protons to the active site from bulk solvent, slowing the reaction. To mimic the lysine in the allosteric site, two substituted enzymes were created with a point substitution at the 48 position, which is positioned in the water channel. The substitutions inserted are phenylalanine and tryptophan (DHDPS-S48F and DHDPS-S48W), since their bulky sidechains should block the water channel.

Kinetic studies show both substituted enzymes had a slower rate than the native. The DHDPS-S48F enzyme had a similar rate to the native with lysine, consistent with our hypothesis. The DHDPS-S48W enzyme had a much slower rate than the other two, and when lysine was in the assay there was no change to the rate. Therefore, either lysine did not bind, or it had no effect on the enzyme.

The substituted enzymes were crystallised with substrates and lysine to ensure the only interference was the water channel being blocked, and to identify any changes in the structure as a result of ligand binding. The catalytic sites of both substituted enzymes were unaffected by the substitutions. There was slight variation in Y107 in both enzymes, more so in the tryptophan substitution, but this was only a minor change. The allosteric site was also unaffected by the substitutions, yet lysine was not present in the DHDPS-S48W, despite extensive soaking. This could have been due to Y106 being unable to move to allow the lysine in to the allosteric site due to the slight variation in Y107, as these two residues are connected via hydrophobic stacking. Overall when the water channel was blocked the catalysis was slowed supporting the hypothesis that the water channel is involved in the allosteric mechanism of dihydrodipicolinate synthase.

Abbreviations

Å	Ångstrom
α	alpha
A49	Alanine at position 49
AAA	α-Aminoadipic acid pathway
AEC	Anion exchange chromatography
AMP	Ampicillin
β	beta
B-factor	Estimation of atomic mobility
ºC	Degrees Celsius
C	Carbon
2,3-BPG	2,3-bisphosphoglycerate
dapA	Dihydrodipcolate Synthase gene
dapB	Dihydrodipcolate Reductase gene
Da	dalton
DAP	diaminopimelic acid pathway
DHDPR	Dihydrodipcolate Reductase
DHDPS	Dihydrodipcolate Synthase
DHDPS-S48F	Dihydrodipcolate Synthase with a phenylalanine at the 48 position
DHDPS-S48F apo	Dihydrodipcolate Synthase with a phenylalanine at the 48 position no ligands
DHDPS-S48F L	Dihydrodipcolate Synthase with a phenylalanine at the 48 position with lysine bound
DHDPS-S48F LP	Dihydrodipcolate Synthase with a phenylalanine at the 48 position with lysine and pyruvate bound
DHDPS-S48F LPS	Dihydrodipcolate Synthase with a phenylalanine at the 48 position with lysine, pyruvate and succinic semi-aldehyde bound
DHDPS-S48F P	Dihydrodipcolate Synthase with a phenylalanine at the 48 position with pyruvate bound
DHDPS-S48F PS	Dihydrodipcolate Synthase with a phenylalanine at the 48 position with pyruvate and succinic semi-aldehyde bound.
DHDPS-S48W	Dihydrodipcolate Synthase with a tryptophan at the 48 position
DHDPS-S48W apo	Dihydrodipcolate Synthase with a tryptophan at the 48 position with no ligands
DHDPS-S48W L	Dihydrodipcolate Synthase with a tryptophan at the 48 position with lysine
DHDPS-S48W LP	Dihydrodipcolate Synthase with a tryptophan at the 48 position with lysine and pyruvate bound
DHDPS-S48W LPS	Dihydrodipcolate Synthase with a tryptophan at the 48 position with lysine, pyruvate and succinic semi-aldehyde bound

Abbreviations

DHDPS-S48W COCL	Dihydrodipcolate Synthase with a tryptophan at the 48 position with lysine co-crystallised
DHDPS-WT	The native Dihydrodipcolate Synthase from *E. coli*
DHDPS-WT L	The native Dihydrodipcolate Synthase from *E. coli* with lysine bound
DHDPS-WT P	The native Dihydrodipcolate Synthase from *E. coli* with pyruvate bound
DHDPS-WT PS	The native Dihydrodipcolate Synthase from *E. coli* with pyruvate and succinic semi-aldehyde bound.
DNA	Deoxyribonucleic acid
DSF	Differential scanning Fluorimetry
dH_2O	distilled water
E.coli	*Escherichia coli*
E84	Glutamate at position 84
EDTA	Ethylenediaminetetraacetic acid
F48	Phenylalanine at position 48
g	grams
h	Hour
H	Hydrogen
H56	Histidine at position 56
HEPES	*N*-2-hydroxyethylpiperazine-*N'*-2-ethane sulfonic acid
HIC	hydrophobic interaction chromatography
HTPA	(4S)-4-hydroxy-2,3,4,5-tetrahydro-(2S)-dipicolinate
$I_{0.5}$	Inhibitor concentration giving 50% inhibition
IPTG	isopropyl β-D-thiogalactopyranoside
ITC	Isothermal titration calorimetry
K161	Lysine at position 161
K	Lysine
k_{cat}	catalytic constant
kDa	kilodalton
K_m	Michaelis constant (rate of enzyme at half V_{max})
L	litre
L167	Leucine at position 167
L51	Leucine at position 51
LB	Luria-Bertani broth
Lysine	*S*-Lysine
M	Moles per litre
mM	Millimoles per litre

Abbreviations

min	minutes
mL	millilitres
µL	microliters
N	Nitrogen
Nε	Side chain nitrogen on lysine
N80	Asparagine at position 80
$NADP^+$	Nicotinamide Adenine Dinucleotide Phosphate
NADPH	Nicotinamide Adenine Dinucleotide Phosphate reduced form
nM	Nanometres
O	Oxygen
OD	Optical Density
OH	Hydroxyl group
pJG001	pBluescript plasmid containing the *dap*A gene encoding DHDPS
rpm	revolutions per minute
s	Second
S-ASA	*S*-aspartate semialdehyde
SEC	Size exclusion chromatography
SCA	statistical coupling analysis
SDS-PAGE	Sodium dodecyl sulfate-Polyacrylamide gel electrophoresis
S48	Serine at the 48 position
S48F	Serine to phenylalanine substitution
S48W	Serine to tryptophan substitution
T44	Threonine at the 44 position
T168	Threonine at the 16 position
T_m	Melting temperature
T state	Tense state
THDP	(*S*)-1,2,3,4-tetrahydrodipicolinate
UV	Ultraviolet
v/v	Volume per volume
V_{max}	Maximum rate of an enzyme
WT	Wild type
Y106	Tyrosine at the 106 position
Y107	Tyrosine at the 107 position
Y133	Tyrosine at the 133 position

Chapter One: Introduction

Every living creature relies on 20 amino acids that form proteins to carry out all cellular functions, making amino acids essential for life. As such, elucidating the biosynthesis of these amino acids is vital for understanding life itself. Nine amino acids are "essential" in animals, in that they cannot be synthesised and therefore must be ingested. Lysine is one of these essential amino acids and, because of the medical and agricultural implications of this amino acid, the biosynthesis of lysine (via the diaminopimelic acid (DAP) pathway) has been studied since the 1960s.

In plants and bacteria, dihydrodipicolinate synthase (DHDPS) catalyses the first committed step of lysine biosynthesis. Like most enzymes that catalyse a committed step, DHDPS is under strict regulatory control, whereby it is allosterically inhibited by lysine in a form of feedback inhibition.

This thesis will explore the mechanism of DHDPS allostery and attempt to understand how the enzyme is regulated.

1.1 Allostery

Allostery is the regulation of protein structure, function and flexibility by a ligand that binds to a site other than the catalytic site[1], termed an allosteric site. Allostery can positively enhance the catalysis of the enzyme via allosteric activators, while ligands that decrease enzyme activity are referred to as allosteric inhibitors[1]. Allostery was first described in haemoglobin, which is allosterically inhibited[2]. The affinity of haemoglobin for oxygen is decreased when it binds its allosteric inhibitor, 2,3-bisphosphoglycerate (2,3-BPG), as this binding promotes the T state[3]. In contrast, binding of pyruvate kinase to its allosteric activator, fructose-1,6-bisphosphate, induces a conformational change in the catalytic site, increasing the affinity of the enzyme for its substrate, phosphoenolpyruvate[4]. In both cases, the ligand binds to the protein at a site other than the active site, altering the conformation of the protein and influencing its function.

Allostery does not need to induce drastic changes in the protein structure to be effective. In the general model of allostery, the allosteric inhibitor/activator binds to the allosteric site, resulting in specific movement of certain residues in the protein that affect the catalytic site, causing decreases or increases in enzyme activity. However, this is not always the case, as

allostery can simply promote changes in the enzyme that decrease or increase the activation energy required to carry out the reaction[5]. This kind of alteration could be achieved by the enzyme on its own, but is promoted by the binding of the allosteric promoter or inhibitor[5].

It has long been hypothesised that allostery is a ligand-induced conformational change that will either promote or reduce the activity of the enzyme. However, the question remains as to how the allosteric site influences the catalytic site when they are spatially separated on the enzyme. A review by Goodey and Benkovic in 2008[1] investigated how to find the connection between the two sites, which could be up to 30 Å apart. They noted a technique described by Suel *et al*. that used sequence-based statistical coupling analysis (SCA) to determine whether two sites are functionally coupled. The method examines whether the sites coevolved using statistical comparison of homologous protein sequences[1, 6]. However, in some cases, it is more obvious how the allosteric site functions. Haemoglobin is a good example of this, as 2,3-BPG holds the protein in the T state, which does not accept oxygen as readily[3].

The mechanism of DHDPS allostery is unknown; however, a water channel, which is the topic of this thesis, connects the catalytic and allosteric sites. This connection could be involved in the allosteric mechanism, as a connection is necessary for one site to influence the other.

1.2 Lysine biosynthesis pathway

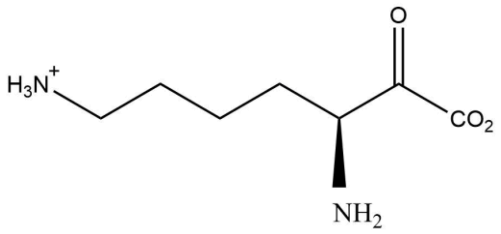

Figure 1.1: *The chemical structure of L-Lysine*

Lysine (figure 1.1) is one of the nine essential amino acids in animals. There are two lysine synthesis pathways: the DAP pathway and the α-aminoadipic acid (AAA) pathway. The DAP pathway branches off the aspartate pathway, and is only found in plants and bacteria[7]. The AAA pathway, which is a glutamate biosynthesis family pathway, is found in higher fungi, euglenoids, and a small number of bacteria[8 9]. This thesis will focus on the DAP pathway in bacteria, as the study is conducted in *Escherichia coli*.

The Dap pathway (Figure 1.2) branches off the aspartate biosynthesis pathway, which is the precursor of methionine, isoleucine, and threonine[10 11]. Prior to the step catalysed by DHDPS, the subject of this study, aspartokinase first phosphorylates aspartate to form aspartyl phosphate. This molecule is then reduced by aspartate semialdehyde dehydrogenase to produce aspartate semialdehyde ((S)-ASA) [12 13]. It is from this point that the DAP pathway begins, starting with DHDPS, which catalyses the condensation reaction between (S)-ASA and pyruvate to generate heterocyclic (4S)-4-hydroxyl-2,3,4,5- tetrahydro-(2S)-dipicolinic acid (HTPA), which is extremely unstable[7]. HTPA is quickly reduced by dihydrodipicolinate reductase (DHDPR) to produce (*S*)-1,2,3,4-tetrahydrodipicolinate (THDP)[14]. THDP then feeds into three different pathways: the dehydrogenase pathway, the acetylase pathway, and the succinyl-dependent pathway. Each of these pathways come together at the product *meso*-diaminopimelate, which is decarboxylated by diaminopimelate decarboxylase to produce lysine[15] (Figure 1.2)

The dehydrogenase pathway (Figure 1.2 blue) contains only one enzyme, diaminopimelate dehydrogenase, which catalyses the oxidative deamination of THDP to *meso*-diaminopimelate, also producing ammonia as a side product[16]. This pathway is rarely used, and has only been confirmed in a few bacterial species. The acetylase pathway (Figure 1.2 green) uses various acetyl intermediates to produce *meso*-diaminopimelate. The pathway contains three enzymes (acetyltransferase, aminotransferase, and deacetylase) and, like the dehydrogenase pathway, is not common[16]. The most commonly used pathway is the succinyl-dependent pathway (Figure 1.2purple). Four enzymes are involved in this pathway: tetrahydrodipicolinate *N*-succinyltransferase, *N*-succinyldiaminopimelate aminotransferase, *N*-succinyl-*S*-diaminopimelate desuccinylase, and diaminopimelate epimerase. The product of this pathway, *meso*-diaminopimelate, is then converted to lysine[17 18 19].

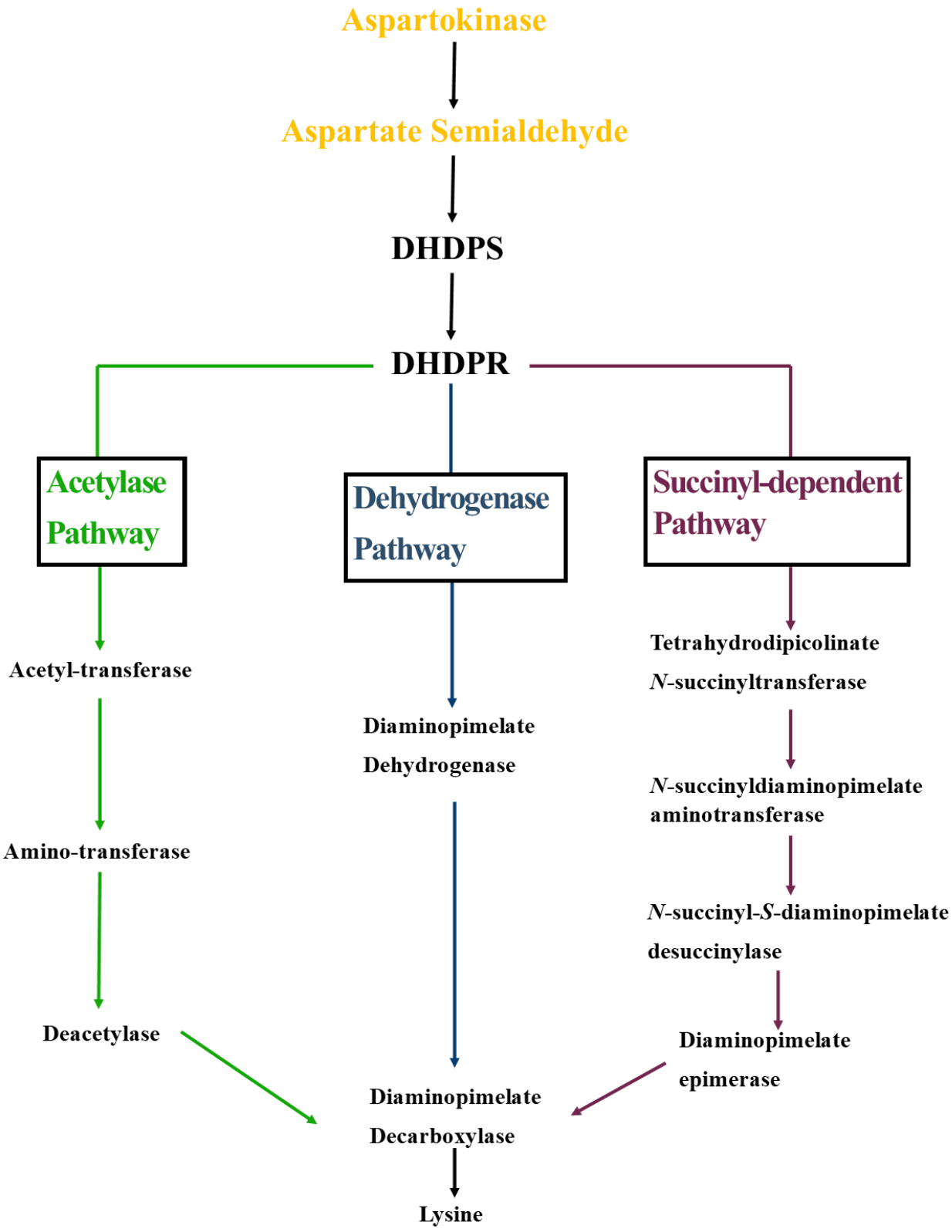

Figure 1.2: *The Dap pathway from Aspartokinase, showing the three alternative routes of the dap pathway; acetylase, pathway (green), dehydrogenase pathway (blue) and, succinyl-dependent pathway (purple).*

1.3 DHDPS

1.3.1 Background

DHDPS was first purified in 1965,[20] and the gene encoding this enzyme, *dapA*, was first mapped in 1971[21]. Knockout studies have shown that *dapA* is essential in many organisms, including *E. coli*, which is used in the current study[22]. It is now widely accepted that the DHDPS-catalysed condensation of *S*-ASA and pyruvate to form HTPA is the first committed step in the DAP pathway[7].

1.3.2 Structure of DHDPS

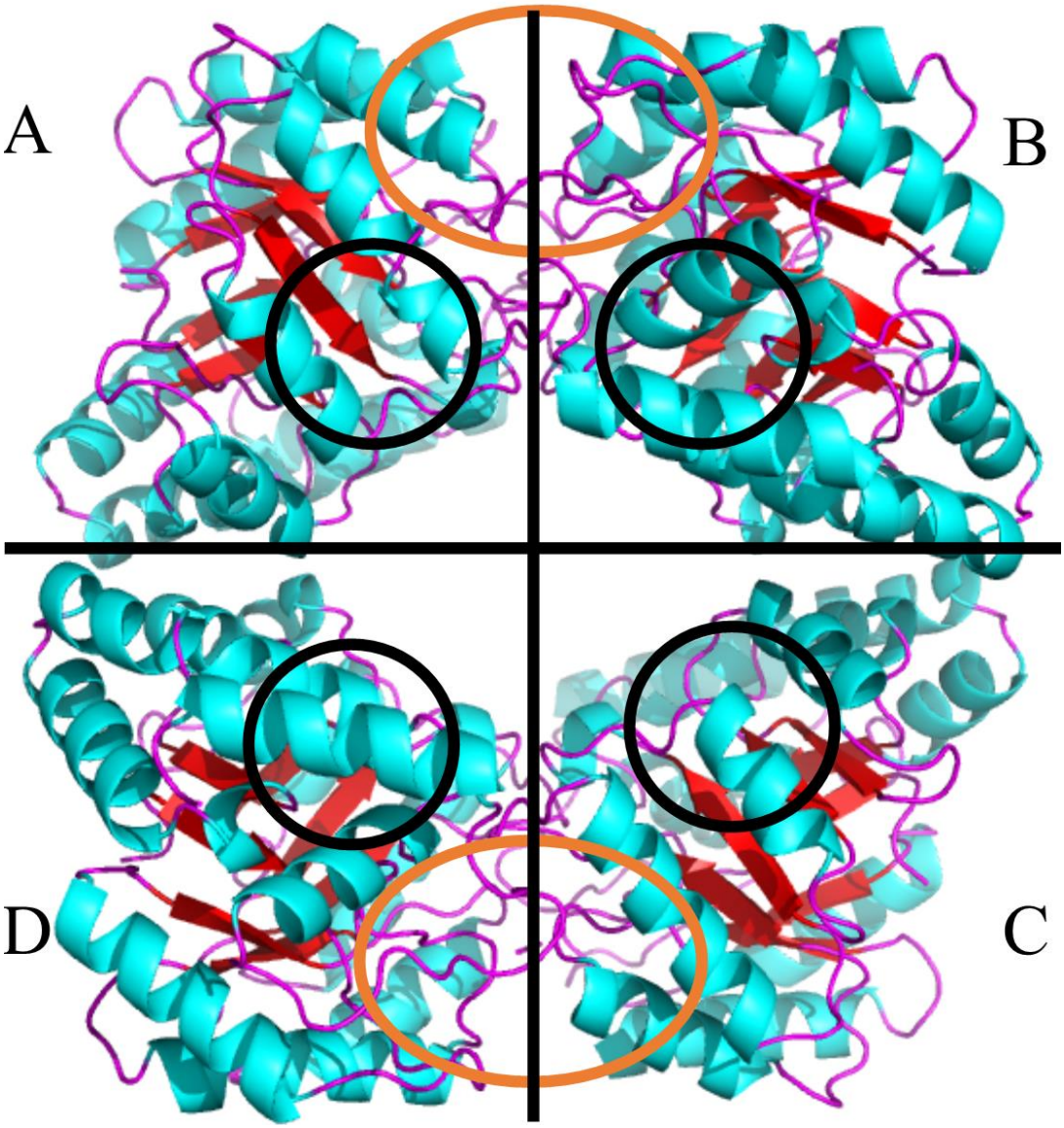

Figure 1.3: *The structure of* E. coli *DHDPS in its native form. Each monomer is labelled to indicate the positions of the interfaces. The colours show the secondary structure, with α helices in blue, β sheets in red, and loops in pink. The catalytic site is indicated by black circles, and the allosteric site is shown by orange circles.*

Although the structure of DHDPS differs across species, the monomeric subunit is fairly conserved. The monomer is in a TIM barrel formation, where the α helices surround a circle of eight β sheets. The structure of the *E. coli* DHDPS is shown in Figure 1.3. The enzyme itself is a tetramer made up of two homodimers consisting of identical monomers[23, 24]. Each monomer contains 292 residues and its own catalytic site, which is located in the middle of the monomer (Figure 1.3, black circles), along with an allosteric site located at the A,B/C,D interface (Figure 1.3, orange circles)[24 25].

1.3.2.1 The catalytic site

The catalytic site of DHDPS was identified within the TIM barrel (Figure 1.4)[24]. As DHDPS exists as a tetramer, there are four catalytic sites[23 24]. The catalytic site contains a triad of residues along with a major residue that covalently binds the substrates as the chemistry takes place[26, 27]. The main residue involved in catalysis is K161, which initially binds to pyruvate[25 26]. The catalytic triad consists of three residues that are thought to shuttle protons to bulk solvent via a tunnel that leads from the active site to the allosteric site. The three residues involved in this activity are these are Y133, Y107, and T44[27].

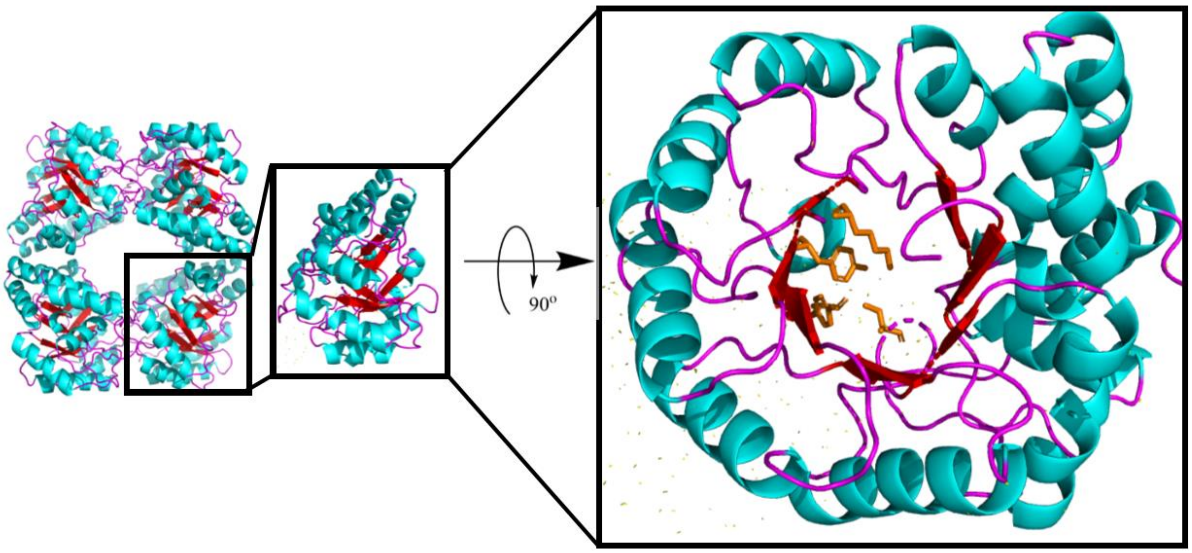

Figure 1.4: *From the tetramer to the monomer. The monomer is then rotated left 90º. This view shows the TIM barrel fold with the beta sheets on the inside and the alpha helices on the outside. The catalytic triad and Lysine 161 are shown in orange*

1.3.2.2 The Allosteric site

The allosteric site of DHDPS is found in the A,B/C,D interface (Figure 1.5)[28]. Lysine is the allosteric inhibitor of DHDPS and, when bound, decreases the rate of catalysis[29]. However, there have been some conflicting results regarding how lysine binds to the allosteric site. Blinking *et al.* hypothesised that the main chain oxygen atom of Tyr107 bonds to the Nε of the lysine[25]. More recently, Dobson *et al.*[28] used high resolution imaging to show that the nitrogen of the lysine side chain was bound to the main chain oxygen of S48[28].

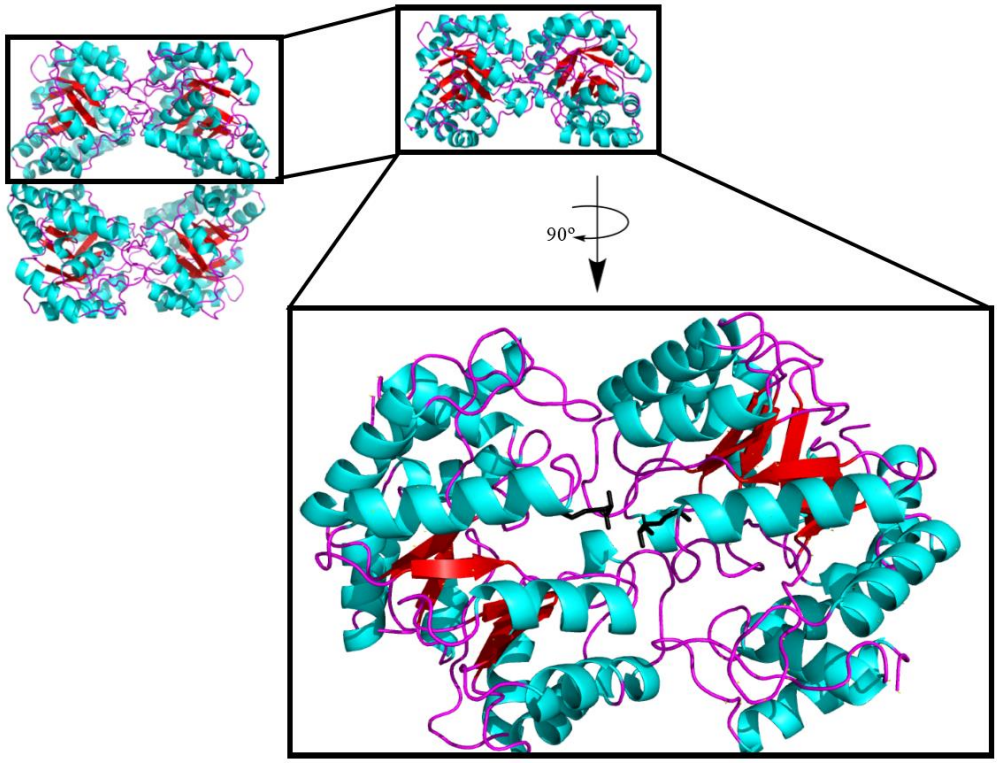

Figure 1.5: *From the tetramer to the dimer, with the dimer then rotated 90º down. This shows the top of the dimer with both the lysine's (black) in the allosteric site.*

1.3.2.3 The A,B/C,D interfaces

The A,B/C,D interfaces are the location of the allosteric sites (Figure 1.3)[28]. The monomers are bound to each other via a hydrophobic stack made up of residue Y106 from one monomer and Y107 of the other[25,24,28]. This hydrophobic stack is what holds the dimer together and maintains the quaternary structure of the enzyme. These residues are in close proximity to the all-important K161 residue[24,25,26].

1.3.2.4 The A,D/B,C interfaces

The A,D/B,C interfaces holds the two identical dimers together (Figure 1.3) to form the tetramer[24]. Inter-dimer interactions occur between only three residues: L167, T168, and L197[25]. Water molecules also form hydrogen bond interactions, the most notable of which involves Q196 and several water molecules[28].

1.3.3 DHDPS-catalysed reaction

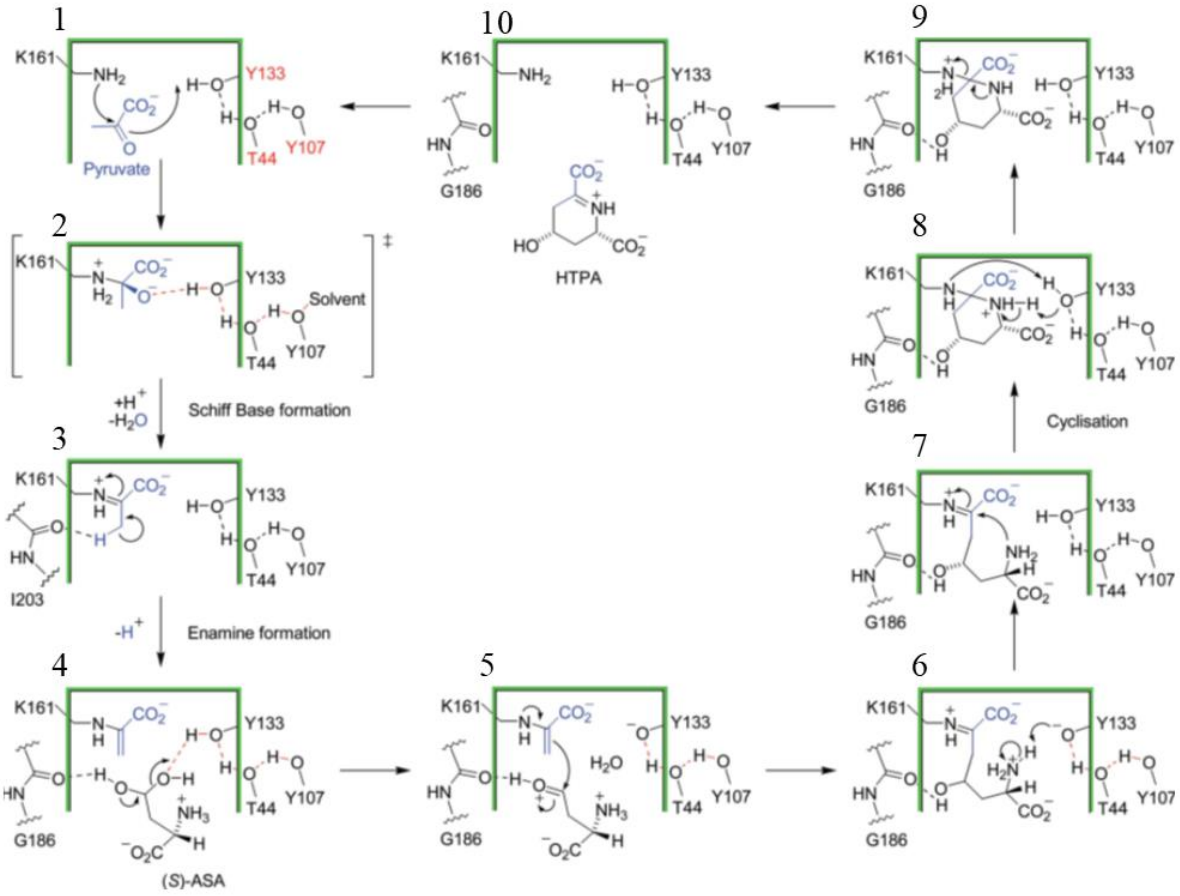

Figure 1.6: *DHDPS reaction mechanism. The mechanism shows the movement of electrons and atoms within the catalytic site (indicated by green lines). The reaction starts at the top left and moves anticlockwise around the figure to the release of the product in the final step. The first three steps depict the binding of pyruvate and Schiff base formation, while steps 4–6 depict the aldol reaction and the addition of (S)-ASA. Steps seven to ten show the cyclisation and release of the product.*

DHDPS catalyses a condensation reaction whereby pyruvate and *S*-ASA are combined, forming HTPA, which is immediately reduced by DHDPR. The DHDPS reaction is referred to as a ping pong mechanism, where one substrate binds and a product is released before the

second substrate binds, resulting in the formation of the final product[25 30]. The DHDPS reaction occurs in three parts. In the first step, pyruvate binds to DHDPS, resulting in the formation of a Schiff base (Figure 1.6, steps 1–3). Pyruvate binds at residue K161 of the enzyme and reacts with residue Y133, releasing a water molecule but gaining a hydrogen.

The second step involves an aldol reaction where *S*-ASA is added, as shown in steps 4–6 in Figure 1.6. In this reaction, *S*-ASA interacts with residues Y133 and G186, releasing a water molecule and creating a carbonyl group (oxygen double bonded to a carbon), which then interacts with the bound pyruvate, releasing the oxygen atom and creating a covalent bond (steps 5 and 6). In the final transamination step, THDP is formed (Figure 1.6 steps 6–10), with residue Y133 taking back a hydrogen to reform the alcohol group, and the product is rearranged into a ring conformation[25,27]. The reaction takes place at residue K161, which holds the reactants while the chemistry is taking place[26,31].

1.3.4 DHDPS is allosterically inhibited by lysine

The allosteric regulation of DHDPS occurs via the binding of lysine to the allosteric site, which slows down the rate of the reaction. In general, the allosteric site is located in the A/B and C/D interfaces of the enzyme[24]. In *E. coli*, DHDPS contains two binding pockets, one at each interface[25]. Each of these binding pockets binds two lysine molecules, one to each monomer[25]. Once the first lysine binds to the binding pocket, the second is more willing to bind[25]. From very early on, it was apparent that DHDPS was regulated by lysine[29]; however, the elucidation of the crystal structure of the enzyme allowed a greater understanding of the allosteric site.

Across species, lysine has different effects on the enzyme. DHDPS from plants is more affected by lysine than the enzyme from bacteria, with an $I_{0.5}$ concentration in the range of 0.01–0.05 mM[32, 33]. In comparison, bacterial species *E. coli*[7], *Bacillus sphaericus*[34], and *Methanobacterium thermoautotropicum*[35] have $I_{0.5}$ values of between 0.25 and 1.0 mM, and are therefore less affected by lysine. *Thermotoga maritima* (Gram-positive) and most Gram-negative bacteria, are least effected with $I_{0.5}$ concentrations of >10 mM. As yet, there has been no explanation as to why lysine affects these enzymes differently.

Most structural studies of DHDPS use X-ray crystallography. This technique determines the structure of the enzyme but provides little information on enzyme dynamics because the protein is in an immobile crystal form. Like all parts of life, enzymes are dynamic. Therefore,

structures determined by X-ray crystallography represent only one of the many conformations of the enzyme. Thus, other techniques are used when trying to understand the way the enzyme moves, and how reactions are carried out.

Although it is known that lysine is the allosteric inhibitor of DHDPS, there is still no clear understanding of how lysine carries out this inhibition. Thus, the mechanism of DHDPS allostery is the last great secret of this well-studied enzyme. Currently, there are three hypotheses regarding the allosteric mechanism. The first hypothesis comes from Blickling *et al.*[25], who crystallised the protein from *E. coli*. They reported that residues Y106 and Y107 are responsible for lysine inhibition, as they form a hydrophobic stack that connects the lysine binding site to the catalytic site. They also noted that upon lysine binding, the rigidity of R138, which they state is "responsible for coordination of the carboxyl group of L-aspartate-4-semialdehyde (L-ASA)", is increased when lysine binds to the allosteric site. This rigidity is compromised when lysine interacts with residues Y107 and N80. Therefore, this hypothesis is based on the movement of key residues.

The second hypothesis comes from Phenix *et al.*[36], who studied DHDPS from *Sinorhizobium meliloti*, which, like *E. coli*, is a Gram-negative bacterium. The authors hypothesised that key residues in the active site move when lysine binds to the allosteric site. They state that when lysine is bound, it increases "the number of easily accessible vibration states". This hypothesis is therefore similar to the previous one as it involves movement of key residues upon binding of the allosteric inhibitor, lysine.

The third hypothesis is the one that this work will be centred around. The hypothesis was first presented by Dobson *et al.*[28], who suggested that bound lysine acts as a "lid" to cover the water channel that joins the catalytic site and the allosteric site in the DHDPS enzyme. The water channel is thought to move protons from bulk solvent to the active site, which then allows Schiff base formation (see section 1.3.3). This movement stops when lysine binds, as it sits on top of the water channel blocking any protons from bulk solvent. Therefore, this hypothesis suggests that the structure of the monomer has significance in the water channel.

1.4 Motivation for this research

The aim of this research is to understand the mechanism of *E. coli* DHDPS allosteric regulation by lysine. As DHDPS catalyses the first step in lysine biosynthesis, regulation of this enzyme can have major implications for the organism in question, as lysine is a building block for all proteins. Up-regulation of DHDPS could result in organisms that can over

produce lysine, while down-regulation may result in non-functional proteins. Understanding how DHDPS is regulated in nature could provide useful information for achieving this regulation artificially.

There are three main motivations for elucidating the allosteric inhibition of DHDPS. First, lysine is only synthesised by plants and bacteria, but is an essential amino acid for all animals[20]. For this reason, several studies have examined ways to enhance lysine production in different species. Geng *et al.*[37] investigated a method of stopping the allosteric inhibition of DHDPS to enhance the amount of lysine produced in *E. coli*[37]. This approach is particularly relevant in plants, as plants with saturating amounts of lysine would be a valuable source of essential amino acids. This idea was also investigated by Shaul *et al.*[38], who looked to increase the level of lysine in tobacco[38]. The research presented in this thesis provides an insight into how the allosteric mechanism may work, making it easier to design an enzyme that is not regulated.

Second, manipulation of lysine biosynthesis via DHDPS could have some application in pesticide development. Pesticides are aimed at killing plant pathogens, particularly bacteria. Halting lysine production by targeting DHDPS could be an effective method of bacterial plant pathogen control. Coulter *et al.*[39] investigated different inhibitors that could be used as potential pesticides[39]. The trouble with this approach is that plants also contain DHDPS and, despite some structural differences[40], there is likely to be some similarities in the allosteric and catalytic sites. Understanding the mechanism of lysine binding to the allosteric site will provide insight into how DHDPS is naturally regulated, allowing the development of specific inhibitors, which are not deferential to plants

The final motivation centres around the medical implications of DHDPS. As DHDPS is not found in animals, it is a potential target for antibiotics and other medicines combating important bacterial pathogens of humans and animals. Antibiotic resistance is one of the biggest threats facing the world today. As such, there are multiple reviews outlining the significance of DHDPS and other enzymes of the DAP pathway for antibiotic development[41 42]. Other studies have investigated whether inhibiting DHDPS could be used to treat other common diseases. Domigan *et al.*[43] investigated DHDPS in *Bacillus anthracis*, the causative agent of anthrax. *B. anthracis* is relatively common in livestock in developing countries and has also been found in developed countries. The authors hypothesised that inhibiting DHDPS would stop the production of lysine, thereby killing the pathogen. Devenish *et al.*[44] took a

similar approach for the treatment of *Neisseria meningitides*, which causes meningitis. Meningitis has a high mortality rate, especially in developing countries. Therefore, understanding the allosteric mechanism of DHDPS regulation would provide vital information for the development of drugs to combat these important bacterial pathogens.

Much of the research on DHDPS and the other enzymes of the DAP pathway has been conducted with an eventual goal of antibiotic development[42]. These studies have all hypothesised that disrupting the DAP pathway will stop lysine production. Therefore, DHDPS has always been at the centre of this research as it is the first step in the pathway[42]. Previous attempts to inhibit DHDPS have not been hugely successful[45, 46]; however, in 2016, Skovpen *et al.*[47] successfully inhibited DHDPS in Gram-negative bacterium *Campylobacter jejuni* by mimicking the shape of two lysines located in the allosteric binding pocket. This research showed how the enzyme could be successfully inhibited using the allosteric site. The findings outlined in this thesis could aid research such as this, with an eventual application in antibiotic development.

1.5 Aims and hypothesis

This project aims to test the hypothesis that the water channel that runs between the active site and the allosteric site of DHDPS plays a key role in the allosteric mechanism, and to examine whether the water channel is critical for the allosteric mechanism in *E. coli*. This will be tested by generating point mutations along the wall of the water channel, causing a blockage. The activity of the enzyme will then be assessed relative to the wild-type. If the hypothesis is correct, the activity of the mutated enzyme will be similar to that of wild-type DHDPS with lysine bound to the allosteric site. The mutated enzyme will also be crystallised to ensure that the mutation does not interfere with the active site.

The questions that this study aims to answer are: 1) Do the protons from bulk solvent, which is required for Schiff base formation from pyruvate, enter the active site via the water channel? 2) If the water channel is blocked, will this stop catalysis? 3) If the water channel is blocked, will lysine still bind to the allosteric site? 4) Does blocking the water channel influence substrate binding?

1.6 References

1. Goodey, N. M., and Benkovic, S. J. (2008) Allosteric regulation and catalysis emerge via a common route, *Nature chemical biology* ***4***, 474.

2. Monod, J., Wyman, J., and Changeux, J.-P. (1978) On the nature of allosteric transitions: a plausible model, In *Selected Papers in Molecular Biology by Jacques Monod*, pp 593-623, Elsevier.

3. Kinoshita, A., Tsukada, K., Soga, T., Hishiki, T., Ueno, Y., Nakayama, Y., Tomita, M., and Suematsu, M. (2007) Roles of hemoglobin allostery in hypoxia-induced metabolic alterations in erythrocytes simulation and its verification by metabolome analysis, *Journal of Biological Chemistry* ***282***, 10731-10741.

4. Jurica, M. S., Mesecar, A., Heath, P. J., Shi, W., Nowak, T., and Stoddard, B. L. (1998) The allosteric regulation of pyruvate kinase by fructose-1, 6-bisphosphate, *Structure* ***6***, 195-210.

5. Cooper, A., and Dryden, D. (1984) Allostery without conformational change, *European Biophysics Journal* ***11***, 103-109.

6. Süel, G. M., Lockless, S. W., Wall, M. A., and Ranganathan, R. (2003) Evolutionarily conserved networks of residues mediate allosteric communication in proteins, *Nature Structural and Molecular Biology* ***10***, 59.

7. Yugari, Y. (1962) Condensation step in diaminopimelic acid synthesis, *Federation Proceedings* ***21***, 10-&.

8. Nishida, H. (2001) Distribution of genes for lysine biosynthesis through the aminoadipate pathway among prokaryotic genomes, *Bioinformatics* ***17***, 189-191.

9. [9] Bryson, V., and Vogel, H. J. (1965) EVOLVING GENES AND PROTEINS, *Science 147*, 68-&.

10. Cohen, G. (1983) The common pathway to lysine, methionine, and threonine, *Biotechnology Series[Biotechnol. Ser.]. 1983.*

11. Viola, R. E. (2001) The central enzymes of the aspartate family of amino acid biosynthesis, *Accounts of Chemical Research* ***34***, 339-349.

12. Biellmann, J. F., Eid, P., Hirth, C., and Jornvall, H. (1980) Aspartate-beta-semialdehyde dehydrogenase from E*scherichia-coli* purification and general-properties, *European Journal of Biochemistry* ***104***, 53-58.

13. Black, S., and Wright, N. G. (1955) Beta-aspartokinase and beta-aspartyl phosphate, *Journal of Biological Chemistry* ***213***, 27-38.

14. Tamir, H., and Gilvarg, C. (1974) Dihydrodipicolinic acid reductase, *Journal of Biological Chemistry* ***249***, 3034-3040.

15. White, P., and Kelly, B. (1965) Purification and properties of diaminopimelate decarboxylase from *Escherichia coli*, *Biochemical Journal* ***96***, 75.

16. Neidhardt, F. C., and Curtiss, R. (1996) *Escherichia Coli* and *Salmonella:* Cellular and Molecular Biology, ASM Press.

17. Wiseman, J. S., and Nichols, J. S. (1984) Purification and properties of diaminopimelic acid epimerase from *Escherichia coli*, *Journal of Biological Chemistry* ***259***, 8907-8914.

18. Simms, S., Voige, W., and Gilvarg, C. (1984) Purification and characterization of succinyl-CoA: tetrahydrodipicolinate N-succinyltransferase from *Escherichia coli*, *Journal of Biological Chemistry* ***259***, 2734-2741.

19. Lin, Y., Myhrman, R., Schrag, M., and Gelb, M. (1988) Bacterial N-succinyl-L-diaminopimelic acid desuccinylase. Purification, partial characterization, and substrate specificity, *Journal of Biological Chemistry* ***263***, 1622-1627.

20. Yugari, Y., and Gilvarg, C. (1965) The condensation step in diaminopimelate synthesis, *Journal of Biological Chemistry* ***240***, 4710-4716.

21. Bukhari, A. I., and Taylor, A. L. (1971) Mutants of *Escherichia coli* with a growth requirement for either lysine or pyridoxine, *Journal of bacteriology* ***105***, 988-998.

22. Griffin, M. D. W., Dobson, R. C. J., Pearce, F. G., Antonio, L., Whitten, A. E., Liew, C. K., Mackay, J. P., Trewhella, J., Jameson, G. B., Perugini, M. A., and Gerrard, J. A. (2008) Evolution of quaternary structure in a homotetrameric enzyme, *Journal of Molecular Biology* ***380***, 691-703.

23. Shedlarski, J. G., and Gilvarg, C. (1970) Pyruvate-aspartic semialdehyde condensing enzyme of *Escherichia-coli*, *Journal of Biological Chemistry* ***245***, 1362.

24. Mirwaldt, C., Korndorfer, I., and Huber, R. (1995) The Crystal Structure of Dihydrodipicolinate Synthase from *Escherichia coli* at 2.5 Å Resolution, *Journal of molecular biology* ***246***, 227-239.

25. Blickling, S., Renner, C., Laber, B., Pohlenz, H.-D., Holak, T. A., and Huber, R. (1997) Reaction mechanism of Escherichia coli dihydrodipicolinate synthase investigated by X-ray crystallography and NMR spectroscopy, *Biochemistry* ***36***, 24-33.

26. da Costa, T. P. S., Muscroft-Taylor, A. C., Dobson, R. C., Devenish, S. R., Jameson, G. B., and Gerrard, J. A. (2010) How essential is the 'essential'active-site lysine in dihydrodipicolinate synthase?, *Biochimie* ***92,*** 837-845.

27. Dobson, R. C., Valegård, K., and Gerrard, J. A. (2004) The crystal structure of three site-directed mutants of *Escherichia coli* dihydrodipicolinate synthase: further evidence for a catalytic triad, *Journal of molecular biology* ***338***, 329-339.

28. Dobson, R. C., Griffin, M. D., Jameson, G. B., and Gerrard, J. A. (2005) The crystal structures of native and (S)-lysine-bound dihydrodipicolinate synthase from *Escherichia coli* with improved resolution show new features of biological significance, *Acta Crystallographica Section D: Biological Crystallography* ***61***, 1116-1124.

29. Yugari, Y., and Gilvarg, C. (1962) Coordinated end-product inhibition in lysine synthesis in *Escherichia coli*, *Biochimica Et Biophysica Acta 62*, 612-&.

30. Muscroft-Taylor, A. C., da Costa, T. P. S., and Gerrard, J. A. (2010) New insights into the mechanism of dihydrodipicolinate synthase using isothermal titration calorimetry, *Biochimie* ***92***, 254-262.

31. Laber, B., Gomisruth, F. X., Romao, M. J., and Huber, R. (1992) *Escherichia-coli* dihydrodipicolinate synthase - identification of the active-site and crystallization, *Biochemical Journal 288*, 691-695.

32. Frisch, D. A., Gengenbach, B. G., Tommey, A. M., Sellner, J. M., Somers, D. A., and Myers, D. E. (1991) Isolation and characterization of dihydrodipicolinate synthase from maize, *Plant physiology* ***96***, 444-452.

33. Kumpaisal, R., Hashimoto, T., and Yamada, Y. (1989) Inactivation of wheat dihydrodipicolinate synthase by 3-bromopyruvate, *Agricultural and biological chemistry* ***53***, 355-359.

34. Bartlett, A. T., and White, P. (1986) Regulation of the enzymes of lysine biosynthesis in *Bacillus sphaericus* NCTC 9602 during vegetative growth, *Microbiology* ***132***, 3169-3177.

35. Bakhiet, N., Forney, F. W., Stahly, D. P., and Daniels, L. (1984) Lysine biosynthesis in *Methanobacterium thermoautotrophicum* is by the diaminopimelic acid pathway, *Current Microbiology* ***10***, 195-198.

36. Phenix, C. P., and Palmer, D. R. J. (2008) Isothermal titration microcalorimetry reveals the cooperative and noncompetitive nature of inhibition of *Sinorhizobium meliloti* L5-30 dihydrodipicolinate synthase by (S)-lysine, *Biochemistry* ***47***, 7779-7781.

37. Geng, F., Chen, Z., Zheng, P., Sun, J., and Zeng, A.-P. (2013) Exploring the allosteric mechanism of dihydrodipicolinate synthase by reverse engineering of the allosteric inhibitor binding sites and its application for lysine production, *Applied microbiology and biotechnology* ***97***, 1963-1971.

38. [38] Shaul, O., and Galili, G. (1992) Increased lysine synthesis in tobacco plants that express high-levels of bacterial dihydrodipicolinate synthase in their chloroplasts, *Plant Journal* ***2***, 203-209.

39. Coulter, C. V., Gerrard, J. A., Kraunsoe, J. A. E., and Pratt, A. J. (1999) Escherichia coli dihydrodipicolinate synthase and dihydrodipicolinate reductase: kinetic and inhibition studies of two putative herbicide targets, *Pest Management Science* ***55***, 887-895.

40. Griffin, M. D., Billakanti, J. M., Wason, A., Keller, S., Mertens, H. D., Atkinson, S. C., Dobson, R. C., Perugini, M. A., Gerrard, J. A., and Pearce, F. G. (2012) Characterisation of the first enzymes committed to lysine biosynthesis in *Arabidopsis thaliana*, *PLoS One 7*, e40318.

41. Mitsakos, V., Dobson, R. C. J., Pearce, F. G., Devenish, S. R., Evans, G. L., Burgess, B. R., Perugini, M. A., Gerrard, J. A., and Hutton, C. A. (2008) Inhibiting

dihydrodipicolinate synthase across species: Towards specificity for pathogens?, *Bioorganic & Medicinal Chemistry Letters* ***18***, 842-844.

42. Cox, R. J. (1996) The DAP pathway to lysine as a target for antimicrobial agents, *Natural Product Reports* ***13***, 29-43.

43. Domigan, L. J., Scally, S. W., Fogg, M. J., Hutton, C. A., Perugini, M. A., Dobson, R. C. J., Muscroft-Taylor, A. C., Gerrard, J. A., and Devenish, S. R. A. (2009) Characterisation of dihydrodipicolinate synthase (DHDPS) from *Bacillus anthracis*, *Biochimica et Biophysica Acta (BBA) - Proteins and Proteomics* ***1794***, 1510-1516.

44. Devenish, S. R., Huisman, F. H., Parker, E. J., Hadfield, A. T., and Gerrard, J. A. (2009) Cloning and characterisation of dihydrodipicolinate synthase from the pathogen *Neisseria meningitidis*, *Biochimica et Biophysica Acta (BBA)-Proteins and Proteomics* ***1794***, 1168-1174.

45. Turner, J. J., Healy, J. P., Dobson, R. C. J., Gerrard, J. A., and Hutton, C. A. (2005) Two new irreversible inhibitors of dihydrodipicolinate synthase: diethyl (E,E)-4-oxo-2,5-heptadienedioate and diethyl (E)-4-oxo-2-heptenedioate, *Bioorganic & Medicinal Chemistry Letters* ***15***, 995-998.

46. Turner, J. J., Gerrard, J. A., and Hutton, C. A. (2005) Heterocyclic inhibitors of dihydrodipicolinate synthase are not competitive, *Bioorganic & Medicinal Chemistry* ***13***, 2133-2140.

47. Skovpen, Y. V., Conly, C. J., Sanders, D. A., and Palmer, D. R. (2016) Biomimetic Design Results in a Potent Allosteric Inhibitor of Dihydrodipicolinate Synthase from *Campylobacter jejuni*, *Journal of the American Chemical Society* ***138***, 2014-2020.

Chapter Two: Molecular Biology and Protein Purification

2.1 Introduction

To test the hypothesis, the recombinant enzymes containing substitutions at residue 48 needed to be purified. As such, both DHDPS-S48F and DHDPS-S48W were purified, along with wild-type protein; DHDPS-WT, for comparison. DHDPS-S48F and DHDPS-S48W were expressed using *dapA*$^-$ *E. coli* strain AT997. Using a *dapA*$^-$ strain meant that the bacteria only expressed the mutant DHDPS enzyme provided on the plasmid. DHDPS-WT was purified from *dapA*$^+$ *E. coli* strain XL1-Blue, which contains an endogenous copy of DHDPS-WT. However, as both copies of the gene express wild-type enzyme, the presence of the endogenous copy did not affect the study. Protein expression was lower in strain AT997 compared with XL1-Blue because of the *dapA* deficiency, resulting in lower protein yields. DHDPR was also purified separately for the kinetic studies to be performed via coupled assay.

Sequencing was carried out prior to purification, while mass spectrometry was conducted post-purification, to ensure that the purified enzyme contained the correct substitution at position 48.

2.2 Sequencing

Plasmids were purified using a Sigma GenElute Plasmid DNA Miniprep Kit and then sequenced to ensure that the mutation was present and in the correct location. The sequences were analysed using CLC Genomics Workbench and compared with the DNA sequence previously published by Dobson *et al.*[1]. Sequence alignment confirmed that the only change occurred at residue 48 in the sequences obtained from the recombinant plasmids, indicating that the plasmids could be used to express enzymes containing a mutation at the correct position.

2.3 Purification of DHDPS

DHDPS is constitutively expressed in the cell so expression did not need to be induced. The three DHDPS enzymes (WT, S48F, and S48W) were purified using the protocol described by Mirwaldt *et al.*[2], which was adapted from the method of Lamber *et al.*[3]. This method has been further adapted by others[4-6,7]. Cells were lysed by sonication, followed by heat shock treatment at 75°C for 2 min. The protein was then purified using three different types of chromatography: anion exchange, hydrophobic interaction, and size exclusion. This protocol allowed the recovery of pure protein from DHDPS-S48F, DHDPS-S48W, and DHDPS-WT. All of the extracted proteins were examined using SDS-PAGE to verify purification (Figure 2.1). Enzyme activity was then tested using a coupled assay with DHDPR, as was carried out for the enzyme kinetics analysis (chapter three). In total, 9 mg of DHDPS-S48W, 4 mg of DHDPS-S48F, and 12.75 mg of DHDPS-WT were purified from 4 L of their respective cultures.

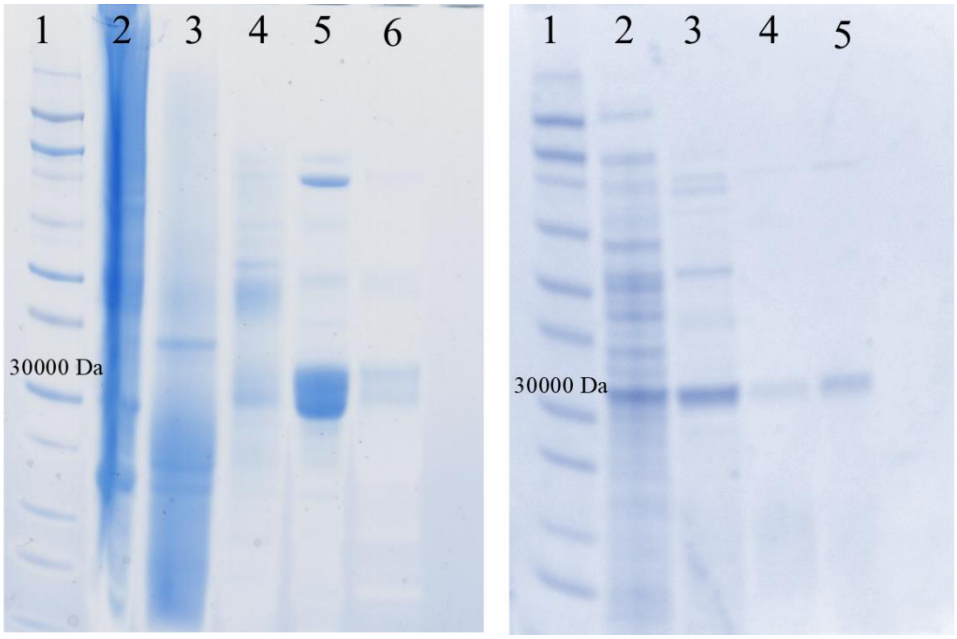

Figure 2.1: *SDS-PAGE gel of purified DHDPS-S48W (left) and DHDPS-S48F (right). In the left gel, Lane 1: protein ladder; lane 2: crude protein extract; lane 3: heat-shocked sample; lane 4: sample following anion exchange chromatography; lane 5: sample following hydrophobic interaction chromatography; lane 6: sample following size exclusion chromatography. The DHDPS-S48F gel doesn't include the crude so lane 2 skips to heat shock and so on. As DHDPS is slightly larger than 30000 Da, the 30000 Da band in the ladder is labelled. A replica gel was obtained for DHDPS-WT (not shown).*

2.4 DHDPR Purification and Overexpression

Unlike DHDPS, DHDPR is not constitutively expressed, so gene expression was induced using IPTG. DHDPR purification was conducted as per the protocol described by Kefala *et al.*[8]. The DHDPR gene was His-tagged[9] to aid in the recovery of pure protein, a technique that is commonly used for DHDPR purifications[8, 10]. Following cell lysis by sonication, the crude protein extract was loaded onto a HisTrap column (affinity chromatography), and then run through a size exclusion column. The product eluted from each step was analysed by SDS-PAGE to track the purity of the protein (Figure 2.2). Purified DHDPR was then used for kinetic studies, using a coupled assay following the composition of NADPH.

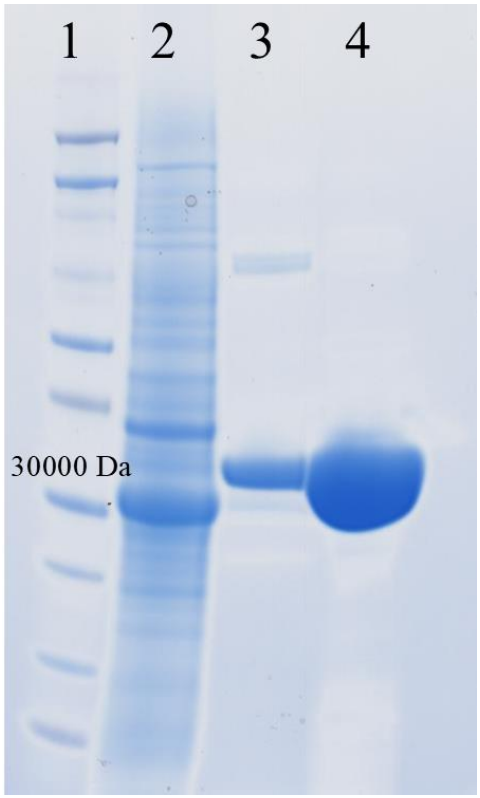

Figure 2.2: *SDS-PAGE analysis of purified DHDPR following each step of the purification process. Lane 1: protein ladder; lane 2: crude protein extract; lane 3: sample following HisTrap affinity chromatography; lane 4: sample following size exclusion chromatography. As DHDPS is slightly larger than 30000 Da, the 30000 Da band in the ladder is labelled. Note: a higher concentration of protein was loaded in lane 4 than in the other lanes.*

2.5 Mass Spectrometry

Mass spectrometry provides information about the mass of a molecule, and can be used to show changes in mass resulting from the addition or substitution of residues. Therefore, mass

spectrometry can confirm that a mutation present in the gene has been translated to the protein.

The mass spectrum data for the wild-type protein is shown in Figure 2.3. Although the spectrum shows the presence of some contaminants, the largest peak occurs at 31,270 Da. When the protein sequence mass is calculated it is 31269.97 Da[11, 12]. Therefore, it was concluded that the majority of the material in the protein sample was wild-type DHDPS.

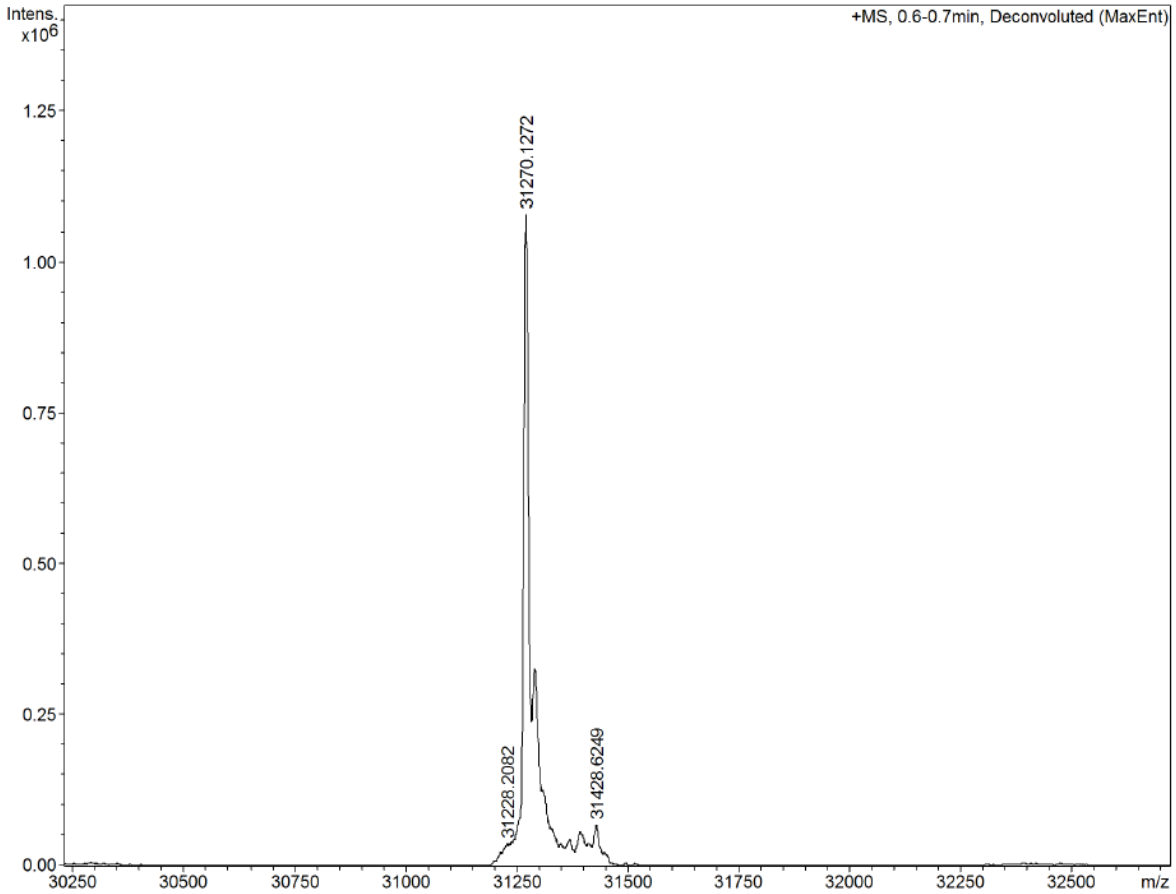

Figure 2.3: *Mass spectrum data for the DHDPS-WT sample. The molecular mass of the major product is 31,270 Da, which is consistent with the predicted mass of the wild-type protein (31,269.97 Da) calculated from the sequence data*[1].

The mass spectrum data for the DHDPS-S48F mutant protein sample is shown in Figure 2.4. The protein contains a serine (105 Da) to phenylalanine (169 Da) substitution, resulting in an

increase in mass of 64 Da[13 14]. The main peak occurred at a mass of 31,329 Da, which is approximately 60 Da greater than the mass of the wild-type protein (31,270 Da). Therefore, it is concluded that the sample contained the DHDPS-S48F mutant protein.

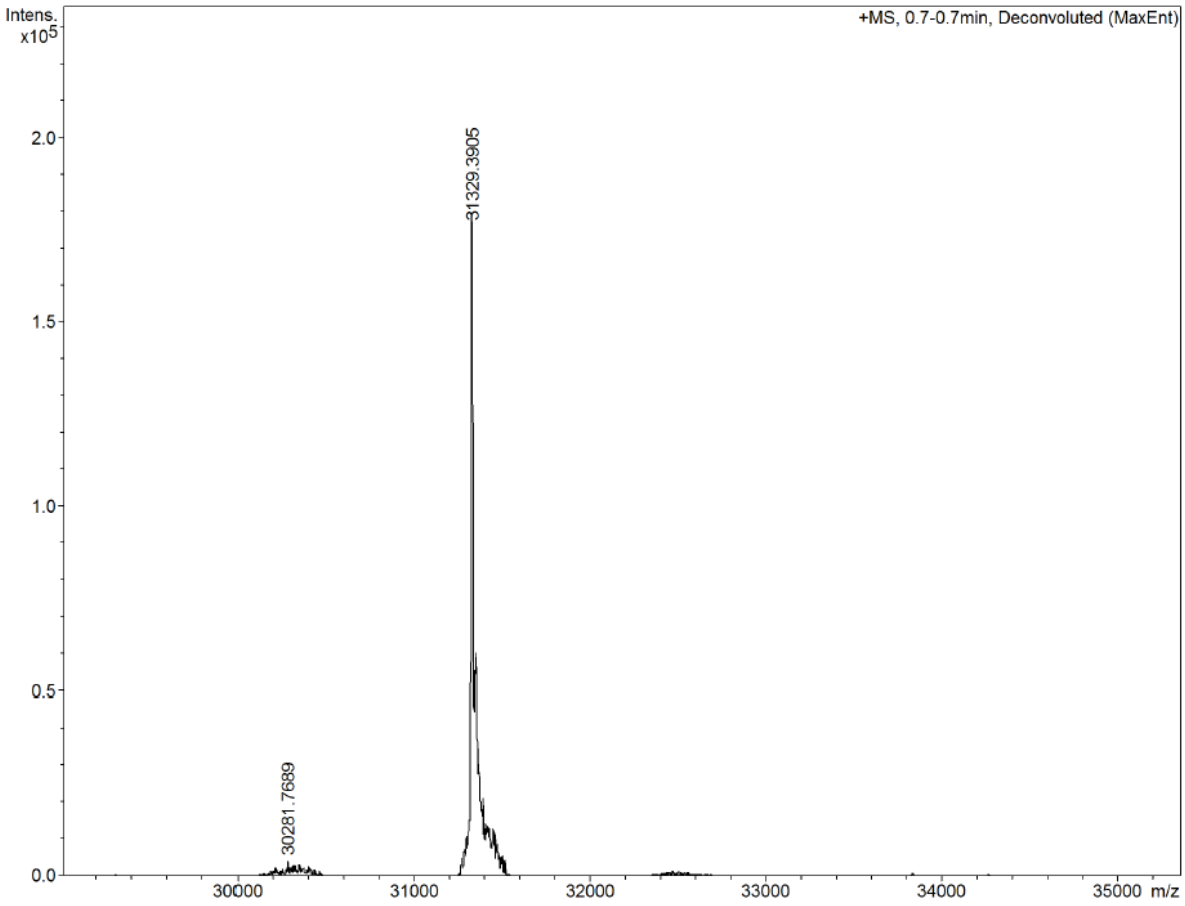

Figure 2.4: *Mass spectrum data for the DHDPS-S48F sample. The molecular mass of the major product is 31,329.0505 Da. Which is consistent with the predicted mass.*

The mass spectrum data for the DHDPS-S48W mutant protein sample is shown in Figure 2.5. The protein contained a serine (105.09 Da) to tryptophan (204.23 Da) substitution at residue 48, resulting in an increase in mass of 99.19 Da. The major peak occurred at a molecular mass of 31,369.05 Da, which is consistent with the calculated mass of the DHDPS-S48W mutant protein.

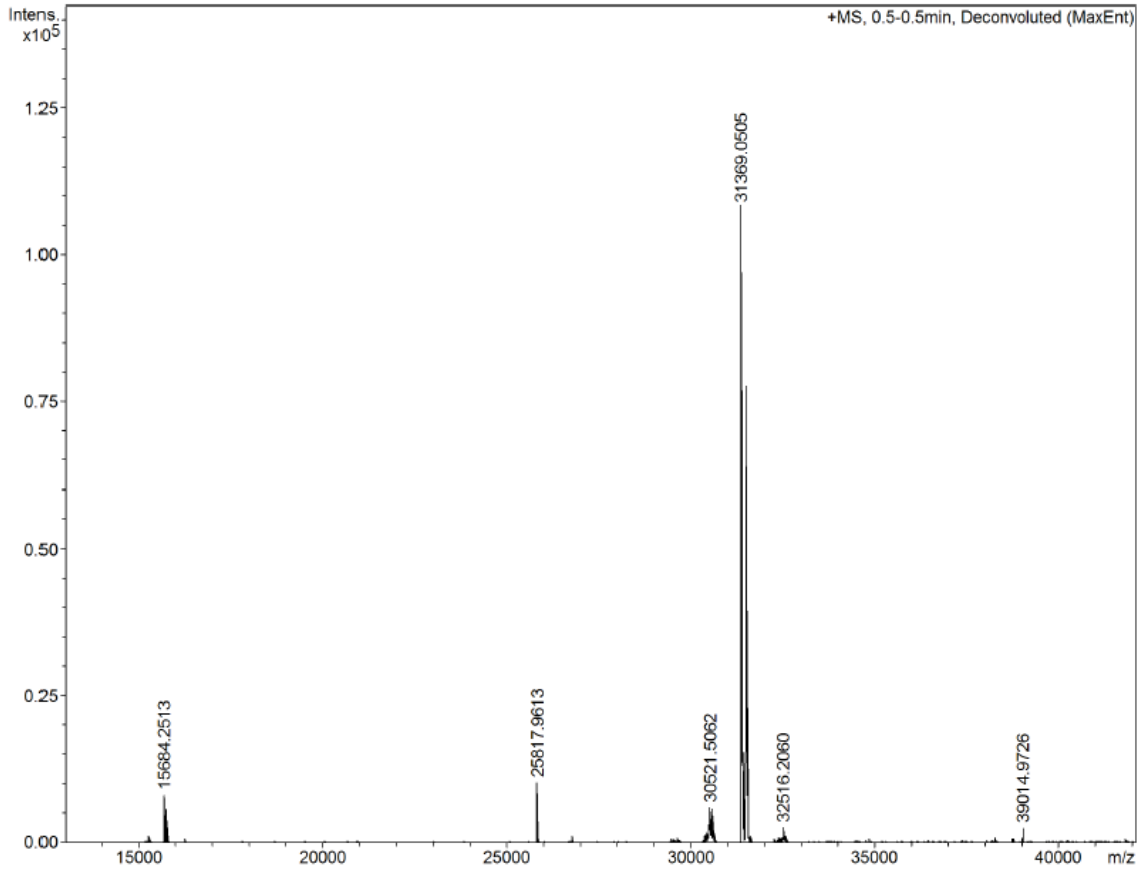

Figure 2.5: *Mass spectrum data for the DHDPS-S48W sample. Some impurities, introduced during purification, can be observed. The molecular mass of the major product is 31,369.0505 Da, which is consistent with the predicted mass.*

2.6 Summary

This chapter outlines the expression and purification of the mutant and wild-type DHDPS proteins used in this project. It was first confirmed that the mutations were present in expression constructs, and then mass spectrometry was used to more precisely measure and verify changes in the molecular weight of the purified proteins. The findings confirmed that

the point mutations were not altered during growth of the bacterial strains. As each protein contained a single point mutation, confirmation of the mutation prior to protein crystallisation ensured that wild-type enzyme was not being produced in addition to the mutant protein.

2.7 References

1. Dobson, R. C., Griffin, M. D., Jameson, G. B., and Gerrard, J. A. (2005) The crystal structures of native and (S)-lysine-bound dihydrodipicolinate synthase from *Escherichia coli* with improved resolution show new features of biological significance, *Acta Crystallographica Section D: Biological Crystallography* ***61***, 1116-1124.

2. Mirwaldt, C., Korndorfer, I., and Huber, R. (1995) The Crystal Structure of Dihydrodipicolinate Synthase from *Escherichia coli* at 2.5 Å Resolution, *Journal of molecular biology* ***246***, 227-239.

3. Laber, B., Gomisruth, F. X., Romao, M. J., and Huber, R. (1992) *Escherichia-coli* dihydrodipicolinate synthase - identification of the active-site and crystallization, *Biochemical Journal* ***288***, 691-695.

4. Blickling, S., and Knablein, J. (1997) Feedback inhibition of dihydrodipicolinate synthase enzymes by L-lysine, *Biological Chemistry* ***378***, 207-210.

5. Dobson, R. C., Griffin, M. D., Roberts, S. J., and Gerrard, J. A. (2004) Dihydrodipicolinate synthase (DHDPS) from *Escherichia coli* displays partial mixed inhibition with respect to its first substrate, pyruvate, *Biochimie* ***86***, 311-315.

6. Dobson, R. C. J., Griffin, M. D. W., Roberts, S. J., and Gerrard, J. A. (2004) Dihydrodipicolinate synthase (DHDPS) from *Escherichia coli* displays partial mixed inhibition with respect to its first substrate, pyruvate, *Biochimie* ***86***, 311-315.

7. da Costa, T. P. S., Muscroft-Taylor, A. C., Dobson, R. C., Devenish, S. R., Jameson, G. B., and Gerrard, J. A. (2010) How essential is the 'essential'active-site lysine in dihydrodipicolinate synthase?, *Biochimie* ***92***, 837-845.

8. Kefala, G., Janowski, R., Panjikar, S., Mueller-Dieckmann, C., and Weiss, M. S. (2005) Cloning, expression, purification, crystallization and preliminary X-ray diffraction analysis of DapB (Rv2773c) from *Mycobacterium tuberculosis*, *Acta Crystallographica Section F: Structural Biology and Crystallization Communications* ***61***, 718-721.

9. Smith, M. C., Furman, T. C., Ingolia, T. D., and Pidgeon, C. (1988) Chelating peptide-immobilized metal-ion affinity-chromatography - a new concept in affinity-chromatography for recombinant proteins, *Journal of Biological Chemistry* ***263***, 7211-7215.

10. Trigoso, Y. D., Evans, R. C., Karsten, W. E., and Chooback, L. (2016) Cloning, expression, and purification of Histidine-tagged *Escherichia coli* dihydrodipicolinate reductase, *PloS one* ***11***, e0146525.

11. Shedlarski, J. G., and Gilvarg, C. (1970) Pyruvate-aspartic semialdehyde condensing enzyme of *Escherichia-coli*, *Journal of Biological Chemistry* ***245***, 1362-+.

12. Richaud, F., Richaud, C., Ratet, P., and Patte, J.-C. (1986) Chromosomal location and nucleotide sequence of the *Escherichia coli* dapA gene, *Journal of bacteriology* ***166***, 297-300.

13. Thorpe, T. E. (1913) *A dictionary of applied chemistry*, Longmans, Green and co.

14. Plimmer, R. H. A. (1912) *The Chemical Constitution of the Proteins: Analysis*, Longmans, Green & Company.

Chapter Three: Kinetics and Differential Scanning Fluorimetry

3.1 Introduction

Conducting kinetic assays on DHDPS-S48W and DHDPS-S48F will demonstrate whether the substitutions interfere with the activity of the enzyme. This will show whether compromising the water channel with the bulky side chains of tryptophan, and phenylalanine will influence activity. Differential Scanning Fluorimetry (DSF) will also be conducted which will determine the stability of each enzyme. Chapter Two confirmed the substitutions were present and the proteins were purified. This chapter will observe the activity of both DHDPS-S48W, and DHDPS-S48F, along with the stability of the protein. The stability can determine whether the substitution causes a large change in the protein structure

Kinetic studies have been done on DHDPS many times to understand the reaction that takes place. It is widely accepted that DHDPS has a ping-pong mechanism [1]. Therefore, one substrate will bind, followed by the release of a product, then another substrate binds, and finally the last product is released. This is demonstrated in the reaction scheme; $E + S^1 \leftrightarrow ES^1 \rightarrow E + P^1 \rightarrow E + S^2 \leftrightarrow ES^2 \rightarrow E + P^2$. For the DHDPS reaction the first substrate to bind is pyruvate, which covalently binds to the residue K161, a water molecule is the first product to be released, then a schiff base is formed and ASA binds, the final product HTPA is then released.

The kinetics of DHDPS is best studied using a coupled assay. In the coupled assay, DHDPR provides a reaction between the product of DHDPS, HTPA, and NADPH. NADPH is oxidised in the reaction which is monitorable using a photospectrometer at 340 nm. When DHDPR is provided in excess quantities, the rate of NADPH degradation will be equal to the rate of DHDPS. Figure 3.1 displays the coupled assay and how the assay is run inside the cuvette.

The kinetics here follow the standard Michaelis–Menten curve which follows equation 3.1. This finds the V_{max} (maximum rate of the enzyme) and k_{cat} (the catalytic rate) of the enzyme. This information will tell us whether the mutants ability to turn over product is altered by the mutation in the water channel.

Equation 3.1: $V_0 = V_{max}$ ([Substrate] / [Substrate] K_m)

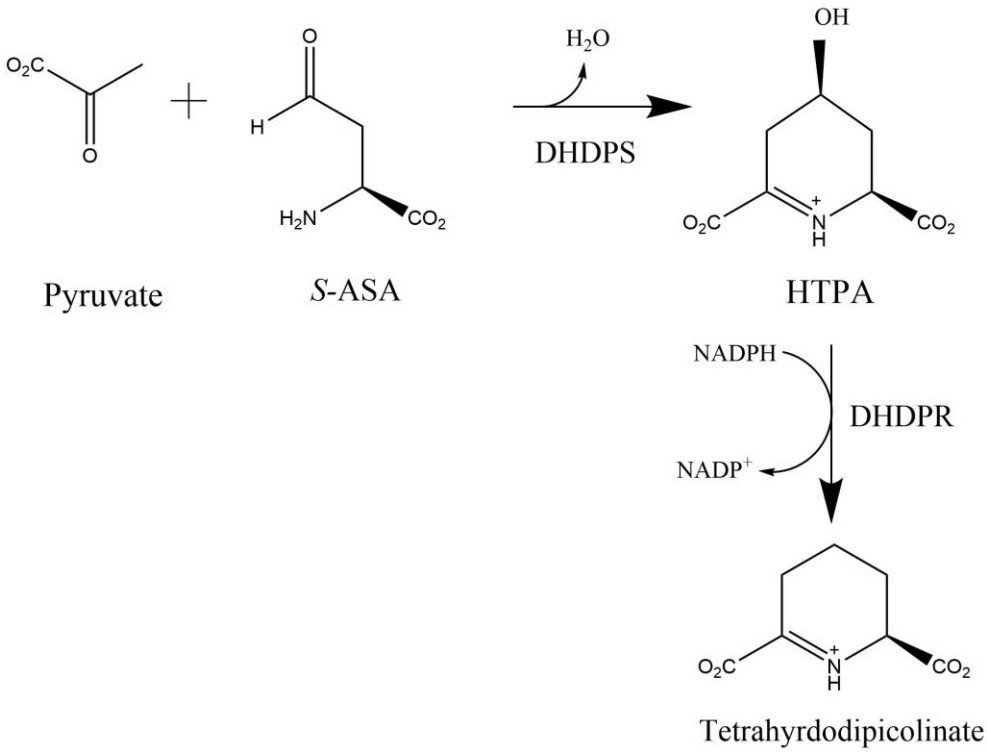

Figure 3.1: *The coupled assay performed in the kinetic studies. Showing the reactants of DHDPS change to HTPA, which is immediately reduced by DHDPS via NADPH.*

DSF measures how a protein denatures over a period of heating. This can display how stable a protein is, and at what its melting temperature is. SYPRO orange is used as a dye, it binds to hydrophobic groups in the enzyme, so as the enzyme is heated florescence should increase until the enzyme is denatured[2]. The differences between DHDPS-WT, DHDPS-S48F, and DHDPS-S48W should highlight any changes caused by the substitutions.

3.2Kinetics

All the kinetic studies were done by varying the amount of *S*-ASA. The purpose of these studies was to compare the reaction rate of DHDPS-WT along with DHDPS-S48F and DHDPS-S48W to observe the difference in rate. The hypothesis predicts that the water channel is directly involved in the allosteric mechanism by delivering a proton to the catalytic site for schiff base formation. The substitutions at the 48 position are to larger amino acids is expected to slow catalysis by blocking the channel. A slower rate for DHDPS-S48F and DHDPS-S48W may give evidence in favour of this hypothesis. The pyruvate concentration was not varied because it is the Schiff base formation which uses the water channel at this time pyruvate is already bound to the catalytic site (Chapter One), and there was limited

amount of *S*-ASA available. Figure 3.1 shows the reaction taking place. The data is taken by spectrometer monitoring at 340 nM which will show the degradation of NADPH. DHDPR is at 15-20 mg/mL in the cuvette to ensure the reaction being recorded is that of DHDPS. This technique follows multiple studies[3-5]. Each set of kinetic results had duplicates which were within 1%. DHDPS-WT and DHDPS-S48F had almost two times the activity DHDPS-S48W had, when the activity of the enzymes was being tested. This resulted in DHDPS-S48W needing twice the amount of enzyme in the cuvette than the other two. Table 3.1 has the K_M, the k_{cat} , the V_{Max} and the R^2 of each data set. Each of the graphs were constructed using graph pad prism 7.4.

Table 3.1: *This table shows the statistics of all the kinetic studies*

	K_M	V_{Max}	R square	K_{cat} (s)
DHDPS-WT	0.1527	128.0	0.9805	66.707
DHDPS-WT LYS	0.7163	18.11	0.9548	9.438
DHDPS-S48F	0.04856	15.18	0.8106	7.911
DHDPS-S48F LYS	0.3189	15.65	0.9446	8.156
DHDPS-S48W	0.6166	5.565	0.9967	2.901
DHDPS-S48W LYS	0.5573	5.717	0.9957	2.979

The kinetic graphs are shown in Figure 3.2 and 3.3. Figure 3.2 A contains the kinetic plots from DHDPS-WT, DHDPS-S48F, and DHDPS-S48W with and without lysine. DHDPS-WT without lysine is far more active than the substituted enzymes. Therefore, the substituted enzymes along with the DHDPS-WT with lysine are replotted on Figure 3.2 B. Here it is clear that DHDPS-S48F is more active than the rest. This is followed closely by both DHDPS-WT with lysine and DHDPS-S48F with lysine. The DHDPS-S48W assays are the least active.

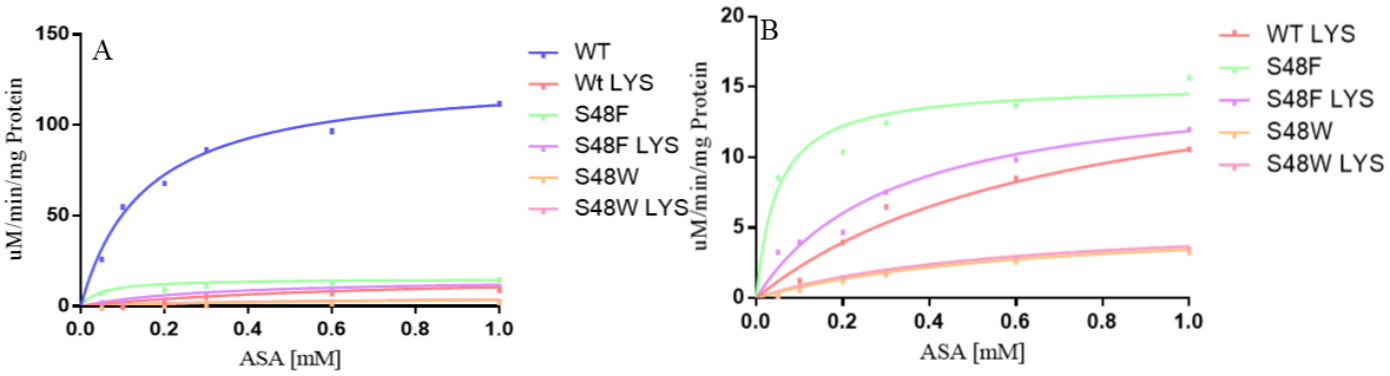

Figure 3.2: *Kinetic graphs of DHDPS-WT, DHDPS-S48F, and DHDPS-S48W with and without lysine. Each data set is coloured, with a key on the right of each graph.*

Individual enzymes graphs are used to determine the effect of lysine inhibition.in Figure 3.3. There is a difference between DHDPS-WT (A) and DHDPS-S48F (B) and their corresponding data with lysine. These two data sets show how the lysine interferes with the catalysis. The DHDPS-S48W graph (Figure 3.3 C) is different. There is little difference between the data set with lysine and the data set without lysine. Thus, implies the lysine either does not bind to the enzyme or does not affect the enzyme.

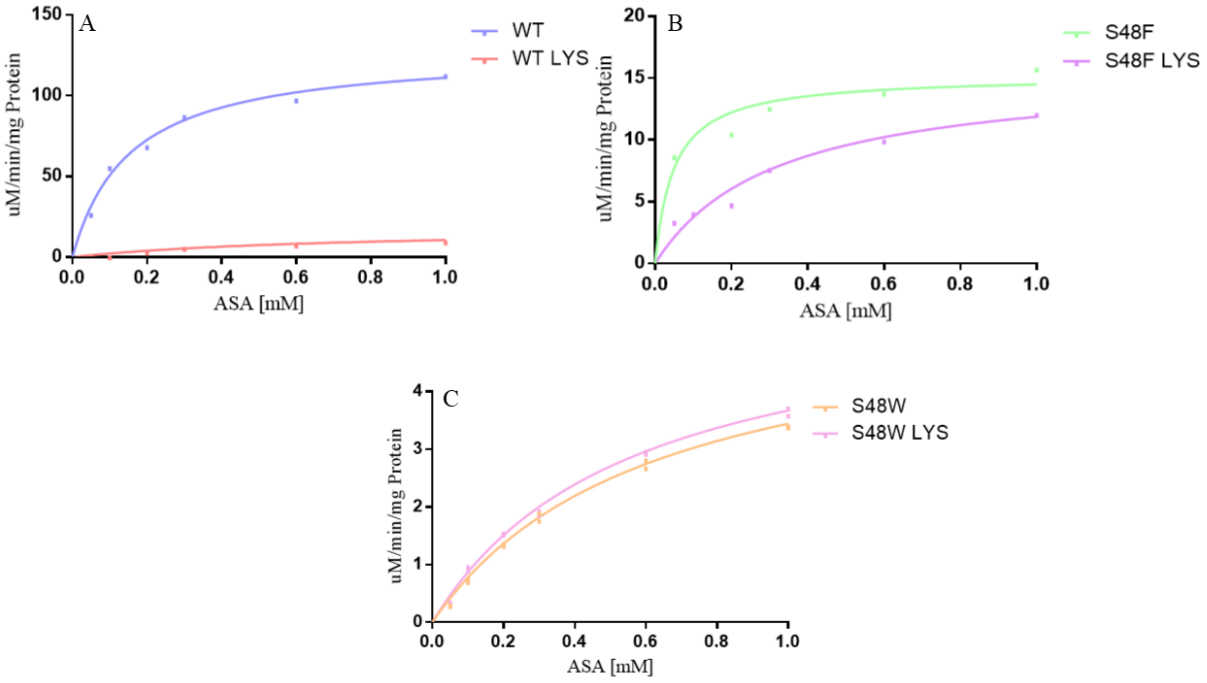

Figure 3.3: *The individual graphs of each enzyme. Graph A contains DHDPS-WT, graph B contains DHDPS-S48F, and graph C contains DHDPS-S48W. Each graph contains the assay with and without lysine.*

The graphs show the substitutions affect catalysis. Each of the substitutions enzymes are less active then the native DHDPS-WT. DHDPS-S48F is also affected by lysine but the affect is limited. DHDPS-S48W is not affected by lysine.

3.3 Differential scanning fluorimetry (DSF)

The DSF graphs are have florescence on the Y axis, and temperature on the X axis. As the temperature increases over time the florescence increases as the protein is unfolding, and more hydrophobic residues are exposed[2]. Plotting the derivative of the increase in fluorescence can be used to provide the melting point of an enzyme[6]. Each enzyme (DHDPS-WT, DHDPS- S48F, and DHDPS- S48W) is tested with 4 mM of lysine (allosteric inhibitor) and without any ligands. This compares whether the addition of lysine changes the stability.

Figures 3.4 and 3.5 contain the DSF data. The left side graph from Figure 3.4 has the data from the enzymes on their own. DHDPS-WT and DHDPS-S48F have very similar peaks with the main peak being at 62ºC and a shoulder peak at 51ºC. There are two domains in DHDPS monomer the smaller being the C terminal end, the shoulder could represent the smaller terminal. The larger peak could represent the larger domain the N terminal, which contains the TIM barrel [7]. DHDPS-S48W has three peaks at 42 ºC, 58 ºC and 71 ºC. This indicates DHDPS-S48W monomer may be more stable than the other two. However, the relative fluorescence for DHDPS-S48W without lysine was approximately eight-fold lower than the other assays and the interaction of the dye could be compromised. The right-side graph from Figure 3.4 contains the enzymes with lysine. The final peak of DHDPS-WT and DHDPS-S48F line up at around 62ºC indicating the breakdown of the N terminal and TIM barrel. Before this DHDPS-S48F has the small peak at around 45ºC. These are the same as earlier in the previous graph without the C terminal peak which could have been stabilised by the addition of the lysine. DHDPS-WT with lysine shares the final peak of DHDPS-S48F and has the small shoulder around 45ºC but its second peak is around 51ºC, which would be the breakdown of the C terminal. Again DHDPS-S48W does not follow the trend and has a single peak at around 50ºC. With lysine, DHDPS-S48W had levels of fluorescence similar to the other two proteins tested. This demonstrates, that the aberration in results for DHDPS-S48W without lysine is not solely related to the protein. Repetition was used to confirm the result but further investigation to determine any significance.

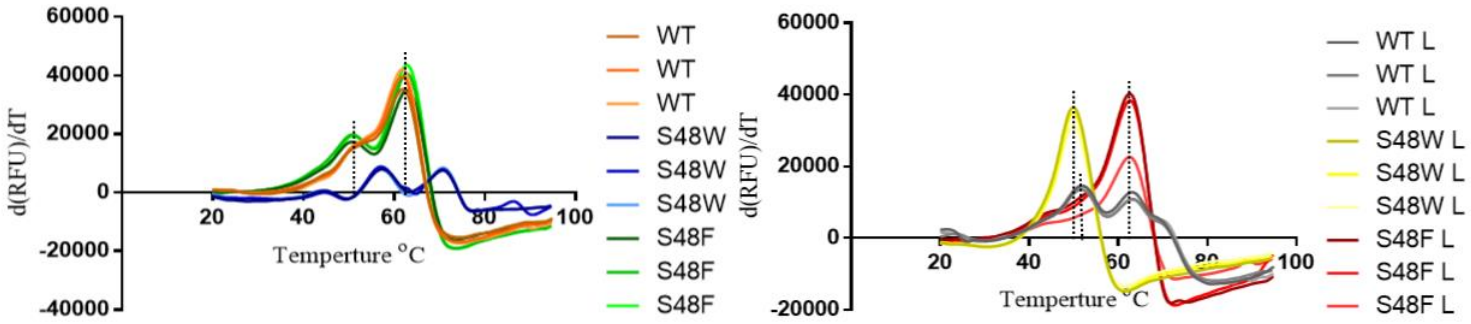

Figure 3.4: *The DSF derivative graphs. Left graph contains all the enzymes; DHDPS-WT, DHDPS-S48F and, DHDPS-S48W. The right graph contains data from the enzymes with lysine bound.*

Figure 3.5 contains the graphs of the individual enzymes. Each graph contains both the data with and without lysine. These graphs enforce what was found in the first two graphs. Graph

A contains the DHDPS-S48W data. Which is by far the most obscure. It seams like the addition of lysine destabilises the enzyme, with the derivative corresponding to a lower melting temperature.

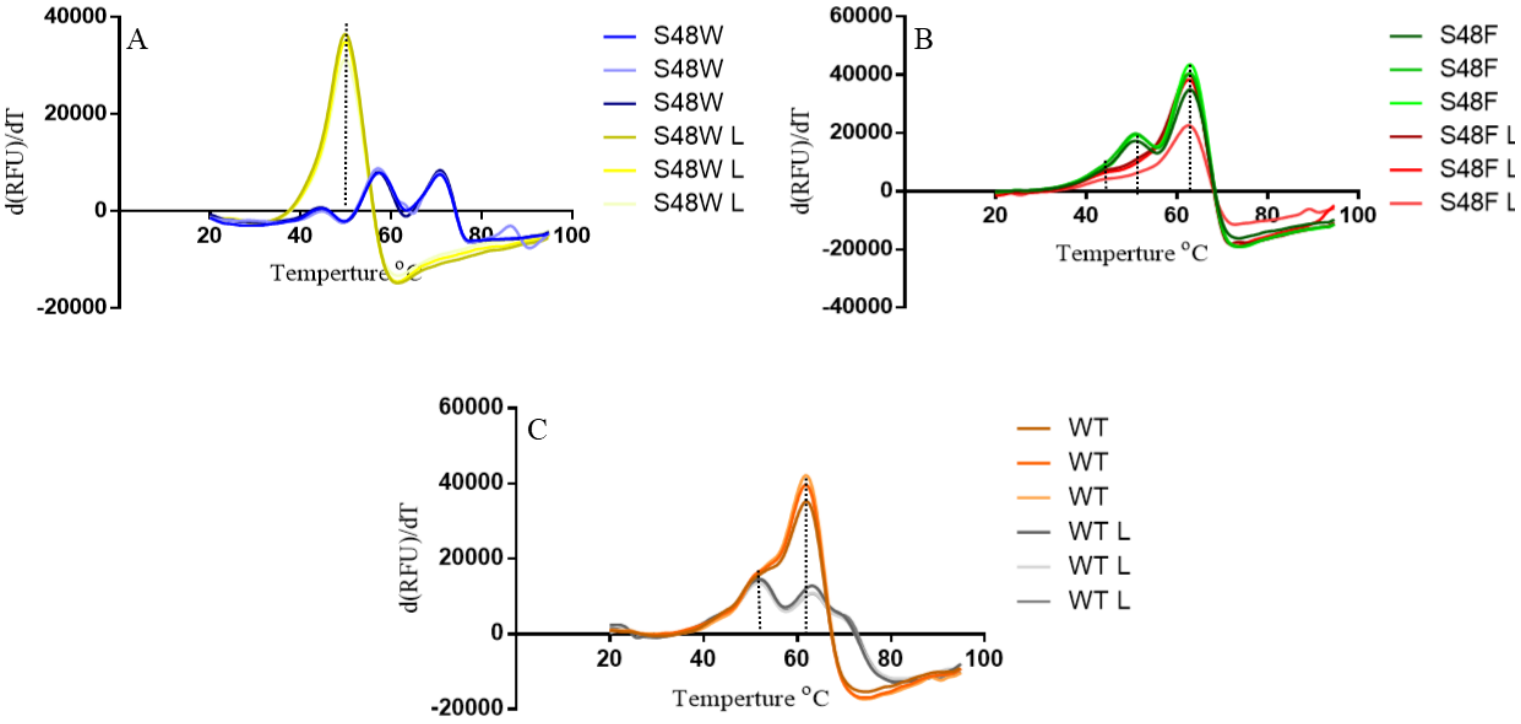

Figure 3.5: *The DSF derivative graphs. Graph A has the DHDPS-S48W data, graph B contains the DHDPS-S48F data, and Graph C contains the DHDPS-WT data.*

3.4 Summary

The kinetic studies on all the separate enzymes show both DHDPS-S48F and DHDPS-S48W have less activity then DHDPS-WT. DHDPS-S48W has the least activity and the addition of lysine doesn't change the activity. This backs up the hypothesis outlined in chapter one. As the substitution does decrease activity. The DSF data shows the similarities between DHDPS-S48F and DHDPS-WT. But the data for DHDPS-S48W shows there may be some interferences in the enzyme. The crystal structures in the following chapters will show whether the change in activity is due to the water channel being blocked, or the structure of the enzyme is compromised by the substitutions. The DSF data does show DHDPS-WT and DHDPS-S48F are influenced by lysine in the same manner.

3.5 References

1. Karsten, W. E. (1997) Dihydrodipicolinate synthase from *Escherichia coli*: pH dependent changes in the kinetic mechanism and kinetic mechanism of allosteric inhibition by L-lysine, *Biochemistry* ***36***, 1730-1739.

2. Niesen, F. H., Berglund, H., and Vedadi, M. (2007) The use of differential scanning fluorimetry to detect ligand interactions that promote protein stability, *Nature protocols* ***2***, 2212.

3. da Costa, T. P. S., Muscroft-Taylor, A. C., Dobson, R. C., Devenish, S. R., Jameson, G. B., and Gerrard, J. A. (2010) How essential is the 'essential'active-site lysine in dihydrodipicolinate synthase?, *Biochimie* ***92***, 837-845.

4. Dobson, R. C. J., Griffin, M. D. W., Roberts, S. J., and Gerrard, J. A. (2004) Dihydrodipicolinate synthase (DHDPS) from *Escherichia coli* displays partial mixed inhibition with respect to its first substrate, pyruvate, *Biochimie* ***86***, 311-315.

5. Coulter, C. V., Gerrard, J. A., Kraunsoe, J. A. E., and Pratt, A. J. (1999) *Escherichia coli* dihydrodipicolinate synthase and dihydrodipicolinate reductase: kinetic and inhibition studies of two putative herbicide targets, *Pest Management Science* ***55***, 887-895.

6. Seabrook, S. A., and Newman, J. (2013) High-throughput thermal scanning for protein stability: making a good technique more robust, *ACS combinatorial science* ***15***, 387-392.

7. Mirwaldt, C., Korndorfer, I., and Huber, R. (1995) The Crystal Structure of Dihydrodipicolinate Synthase from *Escherichia coli* at 2.5 Å Resolution, *Journal of molecular biology* ***246***, 227-239.

Chapter Four: Analysis of the DHDPS-S48F structures

4.1 Introduction

The findings outlined in the previous chapter confirmed that there is a difference in activity between DHDPS-WT and DHDPS-S48F, with the substitution likely interfering with catalysis. The bulky phenylalanine side-chain may block the water channel, which, as the hypothesis states, will slow catalysis. Alternatively, the side-chain could interfere simply by being in the way. Therefore, multiple structures were generated to investigate how the substitution at residue 48 interacts with the catalytic and allosteric sites.

Six structures were analysed, including an apoenzyme (DHDPS-S48F apo) and five different configurations of enzyme bound to various ligands, consisting of pyruvate (DHDPS-S48F P), pyruvate and succinic semi-aldehyde (DHDPS-S48F PS), both substrates and lysine (DHDPS-S48F LPS), pyruvate and lysine (DHDPS-S48F LP), and lysine (DHDPS-S48F L). The positioning of the ligands was then observed and compared with that in the DHDPS-WT protein to determine whether the substitution interfered with the water channel or the binding of ligands.

X-ray crystallography is used to determine the structure of a molecule. X-rays are exposed to protein crystals to produce a diffraction pattern. DHDPS has been crystallised many times before. In 1995, Mirwaldt *et al.*[1] were one of the first groups to crystallise DHDPS and examine its structure, while in 2005. Dobson *et al.*[2] refined the crystallisation method and crystallised the protein with the native (S)-lysine in the allosteric site.

As stated in chapter one, *E. coli* DHDPS exists as a tetramer, consisting of two identical dimers of two identical monomers (Figure 4.1). The figures included in this chapter will focus on the monomer for the catalytic site and the dimer for the allosteric site.

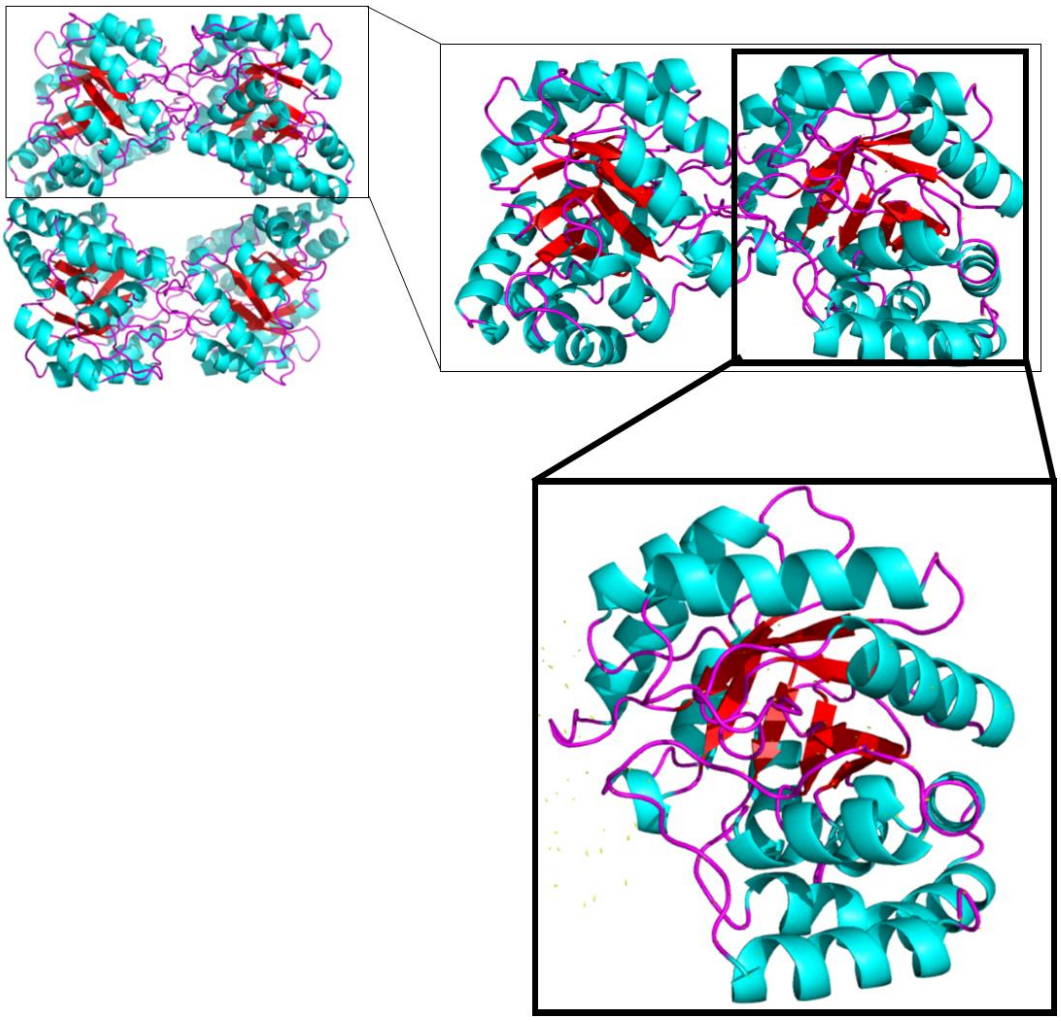

Figure 4.1: *Components of the DHDPS tetramer. The top left panel shows the tetramer, with the dimer shown in the top right and the monomer shown below.*

4.2 Data Collection and Refinement

4.2.1 Crystallisation and data collection

There are many methods of protein crystallisation, the most common of which are hanging drop and sitting drop. In hanging drop crystallisation, the drop containing the protein hangs over the crystallisation liquid, while in the sitting drop method, the drop containing the protein sits in a well adjacent to another well containing the crystallisation liquid. The hanging drop method was used in the current study as it was used successfully in several previous reports[1-4].

Mirwaldt *et al.*[1] used a 6-µL drop, while the drop used by Dobson *et al.*[2] was 4.8 µL. As larger/heavier drops have an increased chance of falling, and because the drops had to travel for data collection, a drop size of 4 µL was used in the current study to reduce the likelihood

to drops falling mid-flight. The smaller drop size also aided with crystal fishing. Fishing is the act of picking crystals out of the drop using a small wire loop. In larger drops, crystals can be difficult to fish as they move away from the loop, so reducing the drop size helps in the fishing process.

Variations of both the Mirwaldt *et al.*[1] and Dobson *et al.*[2] crystallisation methods were used in the current study. For each method, the optimum ratio of each of the components within the 4-µL drop was determined. The separate techniques were also tested at different pH levels (9.8, 9.9, and 10). The final protein concentration was lower than that used by either Mirwaldt *et al.*[1] or Dobson *et al.*[2] because of the large number of nucleation sites in the drops, resulting in multiple smaller crystals. The addition of ligands to the crystals was carried out as per the method of Dobson *et al*.[2].

4.2.2 Refinement and statistics.

Crystals were taken to the Australian Synchrotron for data collection. The MX1 and MX2 beamlines were used to collect the data, and all data processing was conducted using the CCP4 suite[5]. iMosflm[6] was used for indexing and integration, Aimless[7] was used for scaling, Phaser [8] was used to carry out molecular replacement using PDB ID: 1YXC[2] as a template, Refmac5[9-17] was used for refinement, and Coot was used for modelling and manipulation of the structures[18].

Information on all of the DHDPS-S48F structures is provided in Table 4.1. All structures were in the range of 1.7–1.9 Å, had an R_{free} value between 0.17 and 0.18, and were in the space group P 31 2 1. This is consistent with previous studies of wild-type DHDPS[1-4, 19]. The Ramachandran plots of the amino acids in all of the structures, including both chain A and chain B, were within the normal range, except for that of Y107. This is also consistent with previous findings[2,

Table 4.1: *Data processing statistics, including molecular replacement, B factors, and Ramachandran scores, for all DHDPS-S48F structures.*

Data collection	*S48F_apo*	*S48F_L*	*S48f_LP*	*S48f_LPS*	*s48f_P*	*s48f_PS*
Wavelength (Å)	0.95369	0.95369	0.95369	0.95369	0.95369	0.95369
Number of Images	360	360	360	360	360	360
Oscillations (°)	0.5	0.5	0.5	0.5	0.5	0.5
Space Group	P 31 2 1	P 31 2 1	P 31 2 1	P 31 2 1	P 31 2 1	P 31 2 1
Cell Parameters a,b.c (Å)	120.8 120.8 110.8	121.5 121.5 110.2	121.2 121.2 110.2	121.3 121.3 109.8	120.7 120.7 110.6	120.9 120.9 110.1
α,b,y (°)	90 90 120	90 90 120	90 90 120	90 90 120	90 90 120	90 90 120
Resolution range (Å)	32.3-1.74 (1.77-1.74)	33.3-1.82 (1.86-1.82)	33.3-1.82 (1.86-1.82)	33.3-1.82 (1.86-1.82)	33.2-1.82 (1.86-1.82)	33.2-1.82 (1.86-1.82)
Unique Reflections	95335(4536)	83378(4541)	835890(4524)	83472 (4551)	83226 (4565)	83200 (4543)
Mean I/σ(I)	10.5 (2.2)	11.7 (2.9)	17.5 (5.9)	17.6 (6.2)	15.1 (4.4)	19.6 (4.8)
Completeness (%)	100.0 (100.0)	100.0 (100.0)	100.0 (99.8)	100.0 (100.0)	100.0 (99.9)	100.0 (100.0)
Rmerge	0.133 (0.9)	0.137 (0.745)	0.087 (0.344)	0.087 (0.320)	0.098 (0.468)	0.079 (0.484)
Rp.i.m.	0.042 (0.305)	90	0.028 (0.111)	0.028 (0.103)	0.031 (0.151)	0.025 (0.155)
Rr.i.m.	0.14 (0.952)	0.143 (0.786)	0.092 (0.361)	0.092 (0.336)	0.103 (0.492)	0.083 (0.508)
CC1/2	0.998 (0.769)	0.997 (0.846)	0.999 (0.963)	0.998 (0.969)	0.998 (0.934)	0.999 (0.935)
Multiplicity	10.6 (9.4)	10.80 (9.0)	11.0 (10.5)	11.0 (10.5)	11.0 (10.5)	11.0 (10.7)
Molecular Replacement						
Mol/asym. Unit	2	2	2	2	2	2
LLG	4928.5	266.8	261.4	250.8	265.5	260
Rwork/Rfree	0.230/0.249	0.223/0.243	0.231/0.252	0.231/0.259	0.229/0.254	0.232/0.261
Refinement Details						
Rwork/Rfree (%)	0.149/0.171	0.143/0.169	0.139/0.169	0.139/0.167	0.144/0.174	0.144/0.171
No. of Atoms §						
Total	5046	5063	5136	5167	5056	4994
Macromolecules	2	2	2	2	2	2
Ligands	20	20	6	7	4	4
Water	620	658	750	684	670	649
Protein Residues	292	292	292	292	292	292
B Factors (Å)						
Macromolecules	18.077	15.525	15.487	16.944	18.902	17.274
Ligands	26.335	23.318	19.229	34.377	29.295	20.47
Solvent	32.624	31.177	22.398	31.1	23.342	31.757
Ramachandran Plot Residues in (%)						
Most favoured Regions	99.32	98.99	99.32	98.61	99.15	98.43
Additionally, Allowed	0.68	1.01	0.68	1.17	0.85	1.19
Disallowed Regions	0	0	0	0.17	0	0
All-atom Clash score	2.61	3.05	4.37	5.78	4.12	3.99

4.3 Features of the Phenylalanine Structures

All six of the phenylalanine structures (DHDPS-S48F) contained a point substitution (serine to phenylalanine) at residue 48 in all chains. As shown in Figure 4.2, density was observed at residue 48 in all six structures, confirming the serine to phenylalanine insertion.

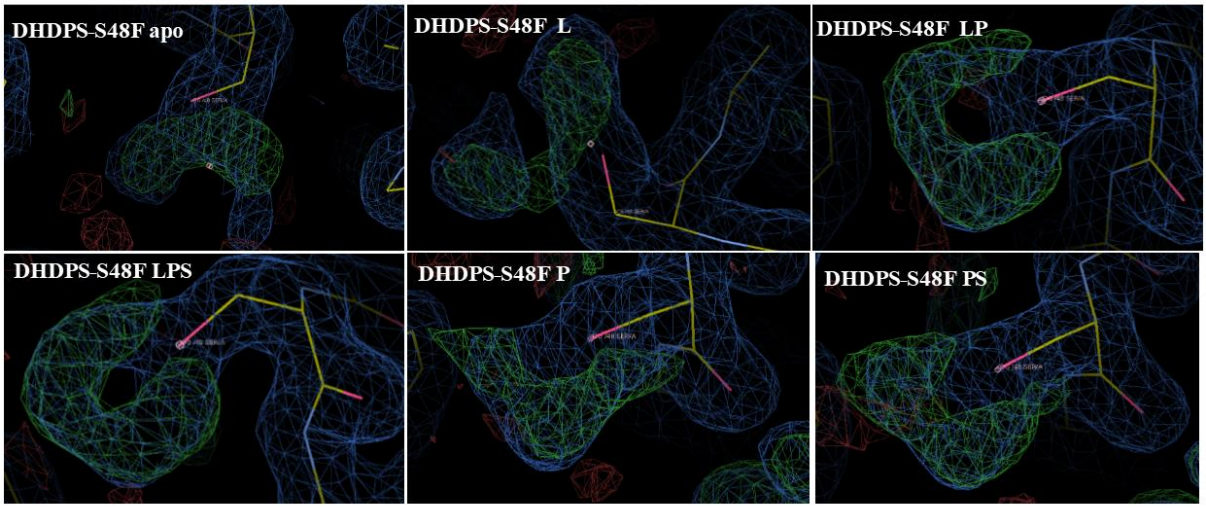

Figure 4.2: *Residue 48 within the A chain of all DHDPS-S48F structures. Each contains a phenylalanine, with the density showing a ring structure would be better suited.*

The six phenylalanine structures each contained a different feature. The apoenzyme contained only the substitution with no other ligands (DHDPS-S48F apo), while the remaining five structures contained various bound ligands, including: pyruvate (DHDPS-S48F P), pyruvate and succinic semi-aldehyde (DHDPS-S48F PS), pyruvate, succinic semi-aldehyde and lysine (DHDPS-S48F LPS), pyruvate and lysine (DHDPS-S48F LP), lysine (DHDPS-S48F L). All were crystallised in the dimer form, with 292 amino acids in each chain. As stated in Chapter One, the structure of each monomer is that of a TIM barrel, with the catalytic site being on the inside of the barrel. The allosteric site sits on the interface between the two monomers.

The phenylalanine structures showed a high degree of similarity. In all cases, both the tertiary and quaternary structures remained unchanged from that of the wild-type protein. The structures are shown in Figure 4.3, with each structure represented by a different colour. This representation shows that the phenylalanine substitution does not interfere with the overall structure of the enzyme.

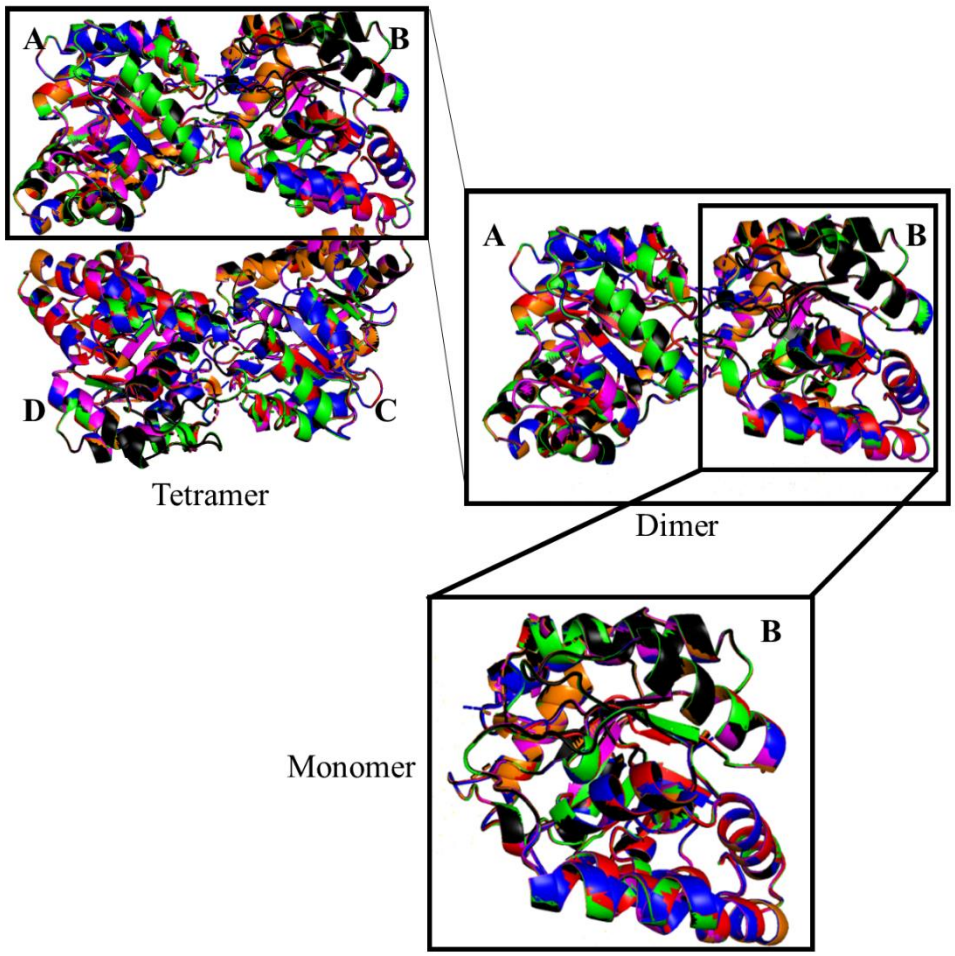

Figure 4.3: *Alignment of all DHDPS-S48F substitution structures. The tetramer, dimer, and monomer forms are shown. The structures are coloured as follows: DHDPS-S84F PS, red; DHDPS-S84F LP, pink; DHDPS-S84F LPS, blue; DHDPS-S84F P, green; DHDPS-S84F L, orange; DHDPS-S84F apo, black.*

Despite the conservation in tertiary and quaternary structures, some variation was observed in the secondary structures of the six phenylalanine variants. The major differences between the various structures are highlighted in Figure 4.4, with one variation observed in a loop, two in alpha helices, and three in beta sheets. DHDPS-S48F LP, DHDPS-S48F L, and the apoenzyme were looped differently to the other structures (Figure 4.4A). DHDPS-S48F L contained a difference in the alpha helix, while DHDPS-S48F apo had a separate loop after the helix (Figure 4.4B). In addition, DHDPS-S48 LP had a lifted helix whereas DHDPS-S48F apo and DHDPC-S48F PS showed breaks in the helix (Figure 4.4C). Despite the break, the loop still follows the same line as the other helix until another helix is formed. DHDPS-S48F PS contained a loop in place of the beta sheet (Figure 4.4D), while the beta sheet was also observed to be moved in this same structure (Figure 4.4E). Another variation was also observed in the beta sheet of DHDPS-S48F PS (Figure 4.4F).

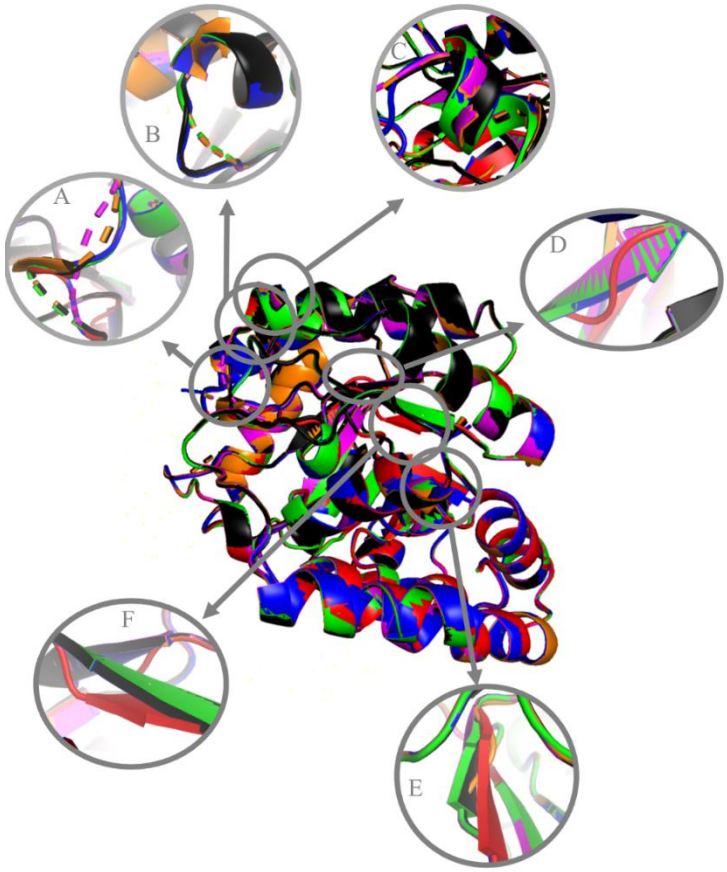

Figure 4.4: *Alignment of all DHDPS-S48F substitutions within the monomer. The variations in the secondary structure are enlarged. (A) Variation in the loops. (B) and (C) Variations in alpha helices. (D), (E), and (F) Variations in beta sheets. The structures are coloured as follows: DHDPS-S84F PS, red; DHDPS-S84F LP, pink; DHDPS-S84F LPS, blue; DHDPS-S84F P, green; DHDPS-S84F L, orange; DHDPS-S84F apo, black.*

Although there were variations in secondary structure between the DHDPS-S48F structures, with DHDPS-S48F PS showing the greatest variation in the interfaces between the monomers, most of the variations were only slight. In addition, as the quaternary and tertiary structures were very similar between the six variants, it is likely that the monomer interfaces are not significantly altered. Figure 4.5 shows the interfaces between the A and B monomers for all the DHDPS-S48F structures. The hydrophobic stacking of residues Y106 and Y107 is thought to be responsible for the interlocking of the monomers[1,3]. Therefore, these two residues are highlighted in Figure 4.5. More variation was observed at residue Y107 than at residue Y106.

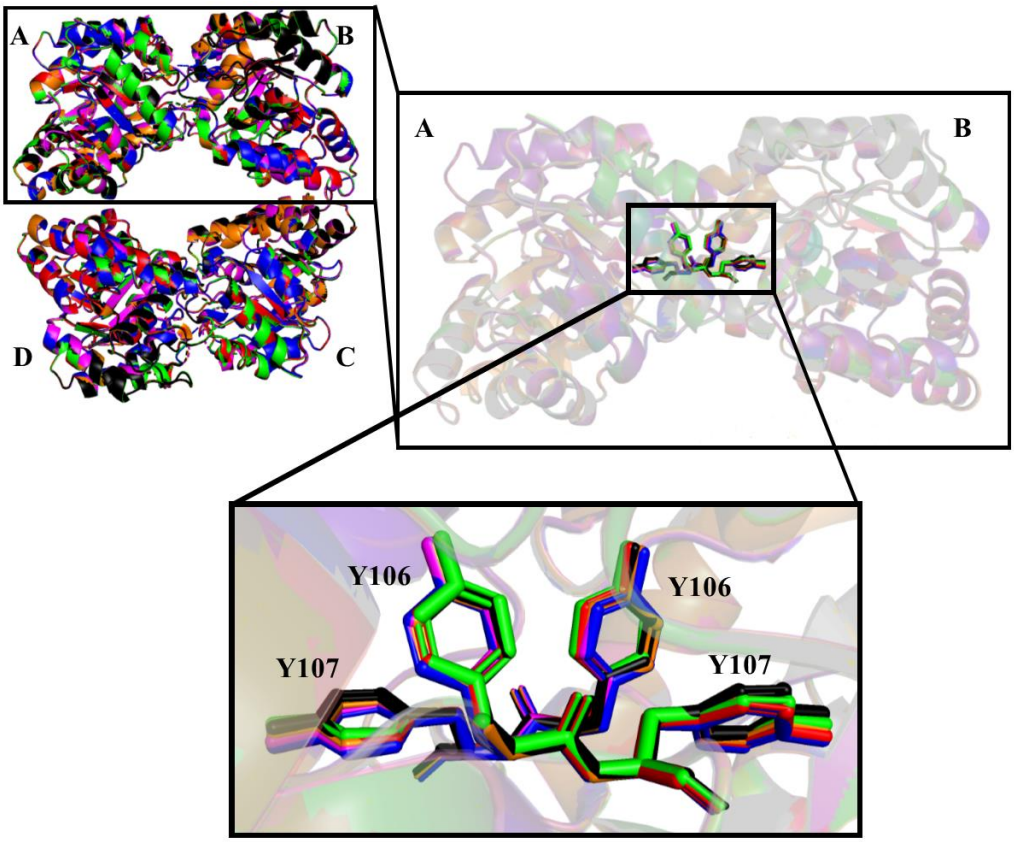

Figure 4.5: *Alignment of all DHDPS-S48F structures within a dimer, showing key residues at the A-B interface. The key residues are highlighted and labelled. The structures are coloured as follows: DHDPS-S84F PS, red; DHDPS-S84F LP, pink; DHDPS-S84F LPS, blue; DHDPS-S84F P, green; DHDPS-S84F L, orange; DHDPS-S84F apo, black.*

The B-C interface was also examined and is depicted in Figure 4.6. The two dimers are thought to be connected via residues L167, T168, L197, and Q196[2, 3], which are highlighted in the figure. There was little to no variation in any of the key residues at the B-C interface.

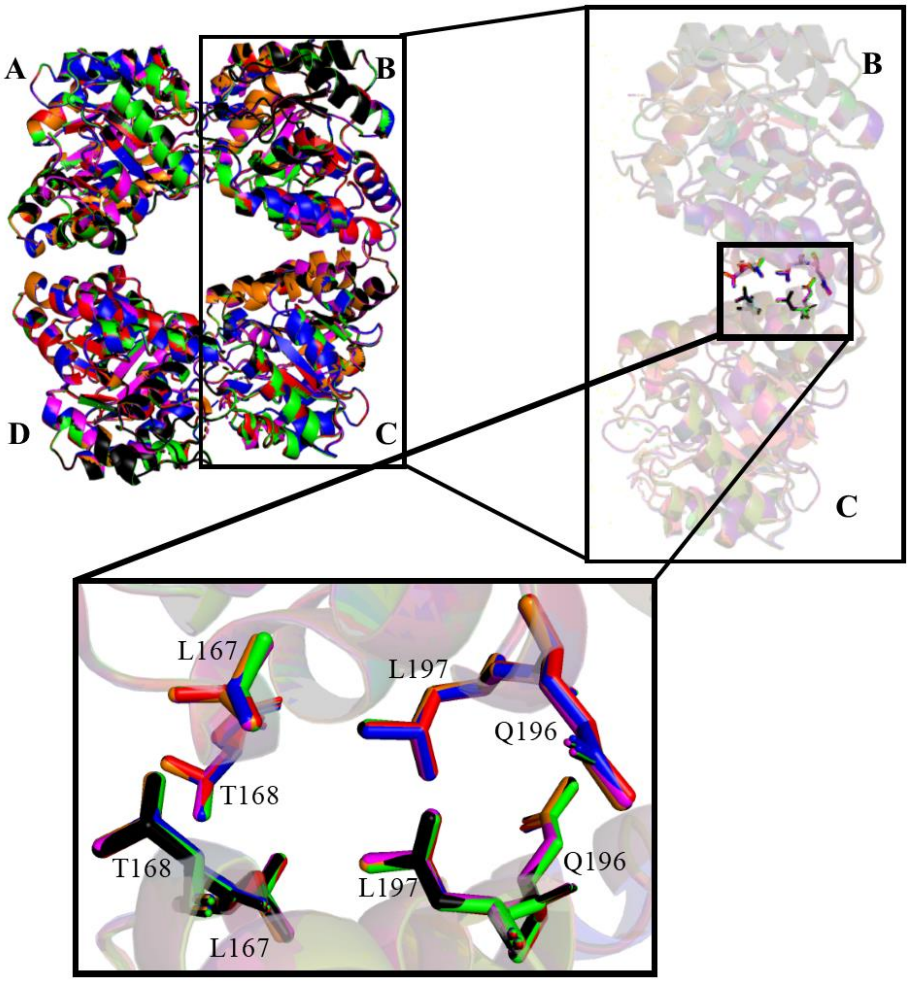

Figure 4.6: *Alignment of all DHDPS-S48F structures within a dimer, showing key residues at the B-C interface. The key residues are highlighted and labelled. DHDPS-S84F PS is in red, DHDPS-S84F LP is in pink, DHDPS-S84F LPS is in blue, DHDPS-S84F P is in green, DHDPS-S84F L is orange, and DHDPS-S84F apo is in black.*

Comparison of the DHDPS-S48F structures revealed variation in the secondary structures, but not in the quaternary and tertiary structures. In addition, the A-B and B-C interfaces showed little variation, with residue Y107 at the A-B interface being the most variable. To further assess how the phenylalanine substitution affected the protein conformation, all the DHDPS-S48F structures were then compared with various other published DHDPS-WT structures at the quaternary, tertiary, and secondary structure levels.

In the current study, DHDPS-WT was crystallised with lysine in the allosteric site but is not yet in the PDB. The dimer of this protein, termed DHDPS-WT L, along with DHDPS-WT from Dobson *et al.*[2], DHDPS-WT P from Devenish *et al.*[20], and DHDPS-WT PS from Boughton *et al.*[21], was aligned with the DHDPS-S48F structures (Figure 4.7). For all the DHDPS-S48F structures, alpha helices are coloured blue, beta sheets are red, and loops are pink. For all DHDPS-WT structures, alpha helices are red, beta sheets are yellow, and loops are green. There was little to no variation between the DHDPS-S48W structures and the DHDPS-WT structures.

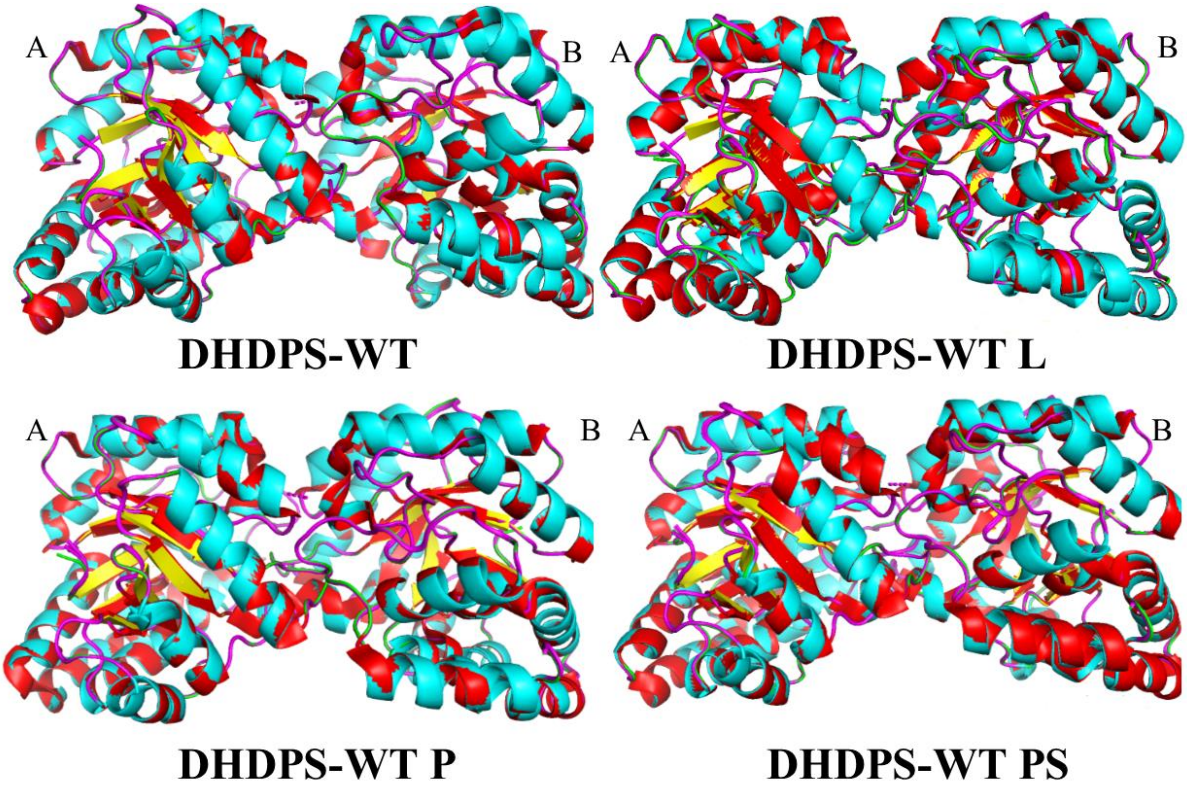

Figure 4.7: *Alignment of DHDPS-S48F dimer structures with four DHDPS-WT structures. Each DHDPS-WT structure is labelled. For DHDPS-WT structures, alpha helices are shown in red, beta sheets are in yellow, and loops are in green. For DHDPS-S48F structures, alpha helices are in blue, beta sheets are in red, and loops are in pink. DHDPS-WT is from Dobson et al., DHDPS-WT P is from Devenish et al., and DHDPS-WT PS is from Boughton et al. DHDPS-S48F L was crystallised in this work.*

The position of the phenylalanine in each of the DHDPS-S48F structures was then examined to determine whether it blocked the water channel. As can be seen in Figure 4.8, which is an overlay of all the DHDPS-S48F structures with residue 48 highlighted, all of the

phenylalanine structures sit in the same place, apart from DHDPS-S48F apo. While the phenylalanine hugs the side of the channel in most of the structures, the phenylalanine of DHDPS-S48F apo sits out in the channel, blocking it as intended. This may suggest that the phenylalanine allosteric ring does not block the channel as proficiently as first predicted.

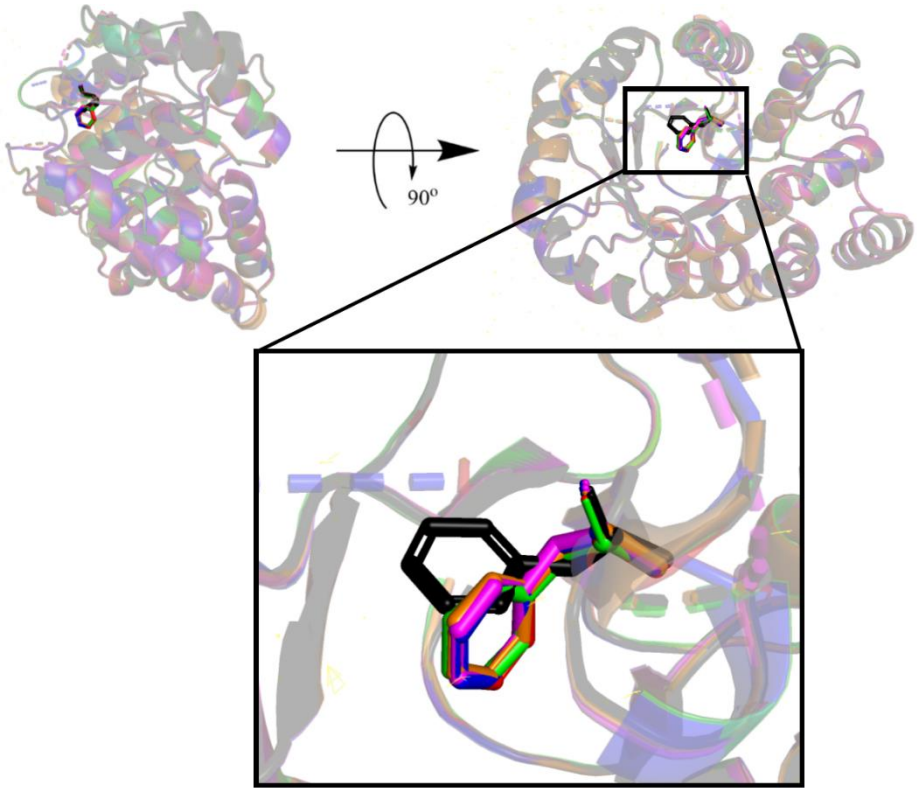

Figure 4.8: *Alignment of all of the DHDPS-S48F structures within a monomer. In the top right-hand panel, the monomer is rotated to the right by 90º and residue 48 is highlighted in all structures. DHDPS-S84F PS is in red, DHDPS-S84F LP is in pink, DHDPS-S84F LPS is in blue, DHDPS-S84F P is in green, DHDPS-S84F L is in orange, and DHDPS-S84F apo is in black.*

As shown in Figure 4.8, the substitutions resulted in two different conformations: that of DHDPS-S48F apo and that of the rest of the structures. Therefore, the residue must sustain some movement. To examine this further, the B-factor profiles of both chains of each of the DHDPS-S48F structures were analysed (Figure 4.9).

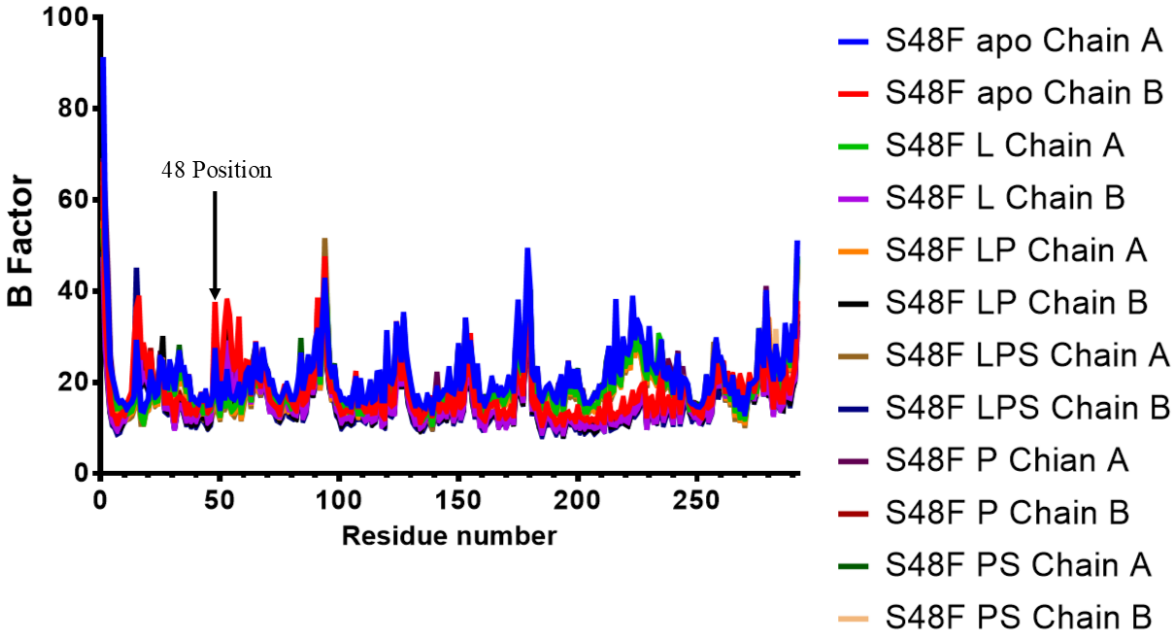

Figure 4.9: *B-factor scores for each of the residues in each chain of the DHDPS-S48F structures. Each residue is represented by a point on the graph. The key on the right shows the colours used to represent each chain.*

The B-factor profiles show a peak at residue 48, with the highest peak (score = 37) occurring in DHDPS-S48F apo chain B. The lowest score (18.4) occurred in DHDPS-S48F LP chain A, a difference of 18.6. The second highest peak occurred in chain A of DHDPS-S48F apo, with a score of 26.9. The larger amount of movement at the DHDPS-S48F apo substitution could explain why it occurs in a different conformation to the other structures.

Therefore, the six different DHDPS-S48F structures showed similar quaternary and tertiary structures to each other and to alternate DHDPS-WT structures. The substitution does not seem to interfere with the overall structure of the enzyme; however, the phenylalanine substitution does not block the water channel as well as expected. This may account for the results outlined in chapter three.

4.4 Minor Changes in the Catalytic Site

The catalytic site is found within the TIM Barrel and relies on the catalytic triad and residue K161 to carry out catalysis. Of the six structures with a phenylalanine substitution, four have substrate bound. These four structures were used to determine whether catalysis was hindered by the addition of the phenylalanine. The substitution was located at residue 48, which does not sit close to the active site but is close to residue T44 of the catalytic triad. The structures were used to examine whether the substitution interferes directly with the catalytic site.

4.4.1 Structures with bound substrate

Four of the phenylalanine substitution structures, namely DHDPS-S48F P, DHDPS-S48F LP, DHDPS-S48F PS, and DHDPS-S48F LPS, had substrate bound to them. The four proteins were crystallised separately and had been soaked in the ligand (20 mM) for 3 days prior to being put on the beam line. As explained in Chapter One, the DHDPS reaction mechanism is a ping pong reaction, where one substrate must bind before the second substrate binds. In the case of DHDPS, pyruvate must bind first, followed by Schiff base formation, which allows the subsequent binding of *S*-ASA. Therefore, while we examined a structure with just bound pyruvate, we did not include a structure with only succinic semi-aldehyde bound..

Figure 4.9 shows the overlayed catalytic sites of all of the DHDPS-S48F structures containing substrates. The key residues for catalysis, along with the substitution, are indicated. As shown in the Figure, there was little to no variation in any of the residues in the catalytic site. Futhermore, in all structures, the substrates were in the same location. Therefore, the substitution did not appear to interfere with any of the catalytic residues.

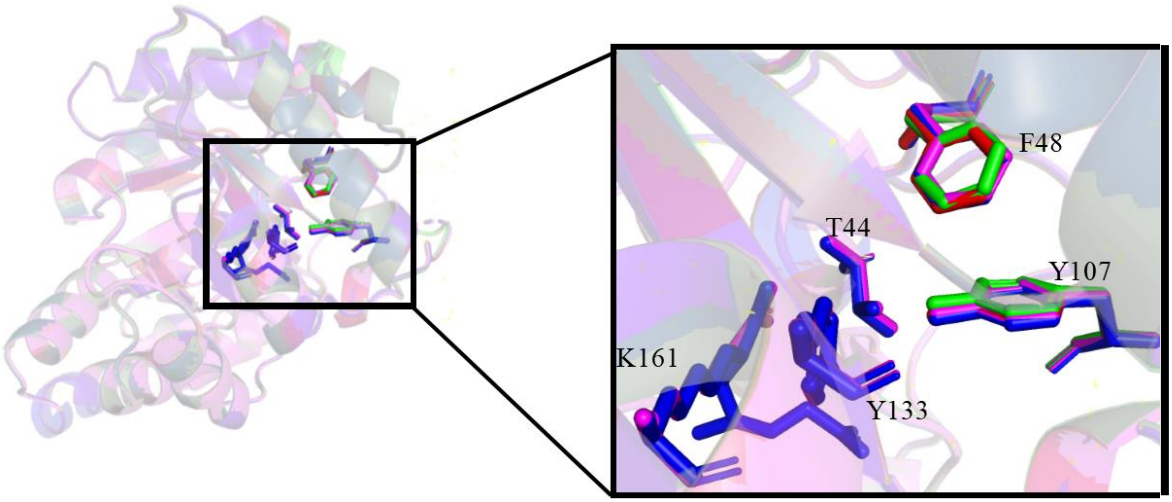

Figure 4.9: *Alignment of the catalytic sites of DHDPS-S84F PS (red), DHDPS-S84F LP (pink), DHDPS-S84F LPS (blue), and DHDPS-S84F P (green). The catalytic site within the monomer is enlarged.*

Although all of the DHDPS-S48F structures with bound substrate showed agreement with regards to the placement of the key residues in the catalytic site, we next investigated whether the placement differed from that of DHDPS-WT with bound substrate. Figure 4.10 shows the same DHDPS-S48F stuctures as shown in Figure 4.9, but also includes the DHDPS-WT P enzyme structure from Devenish *et al.*[20] and the DHDPS-WT PS structure from Boughton *et al.*[21]. The addition of the two DHDPS-WT structures showed that there was very little movement of the key residues in the catalytic site. Although there was minor movement at residue Y107, as both the DHDPS-WT structures sat higher than the DHDPS-S48F structures at Y107, this movement is not likely to be significant. However, there was a difference in the position of the succinic acid semialdehyde in the DHDPS-WT PS structure from Boughton *et al.*[21] and DHDPS-S48F PS from the current study. The polar groups of both structures end in the same position, but there is movement in the terminal two carbon atoms.

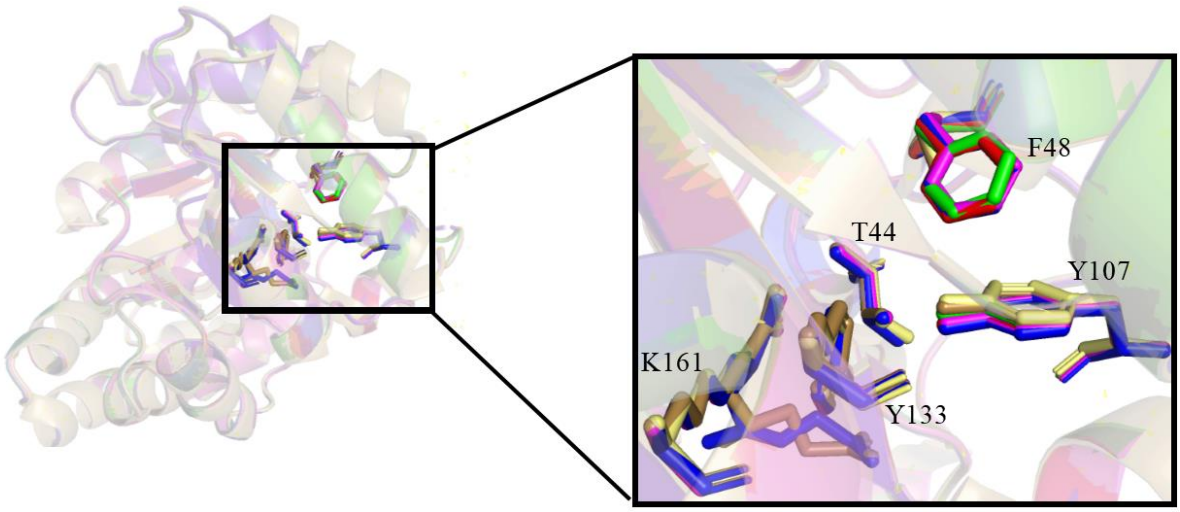

Figure 4.10: *Alignment of the monomer of DHDPS-S84F PS (red), DHDPS-S84F LP (pink), DHDPS-S84F LPS (blue), DHDPS-S84F P (green), DHDPS-WT P (Devenish et al.*[20]*) (yellow), and DHDPS-WT PS (Boughton et al.*[21]*) (brown). The catalytic site is enlarged.*

As shown in Figures 4.9 and 4.10, very few differences were observed in the active sites of the structures with bound substrate, including the DHDPS-WT structures. While there was also no variation in the pyruvate binding site, there was some variation in the succinic acid semialdehyde binding site. However, this may just be indicative of the different protein conformations as the polar groups aligned perfectly.

4.4.2 Structures without bound substrate

Only two of the six DHDPS-S48F structures, DHDPS-S48F apo and DHDPS-S48F L, had no bound substrate. Comparison of the catalytic sites of DHDPS-S84F L and DHDPS-S84F apo revealed two differences between the structures (Figure 4.11). The first difference was the phenylalanine substitution, while the second was a minor change in the position of residue Y107, whereby the Y107 in DHDPS-S48F apo was slightly higher than that in DHDPS-S84F L (enlarged area in Figure 4.11). Figure 4.11 also demonstrates that the substitution at residue 48 does not affect the catalytic site via steric interference.

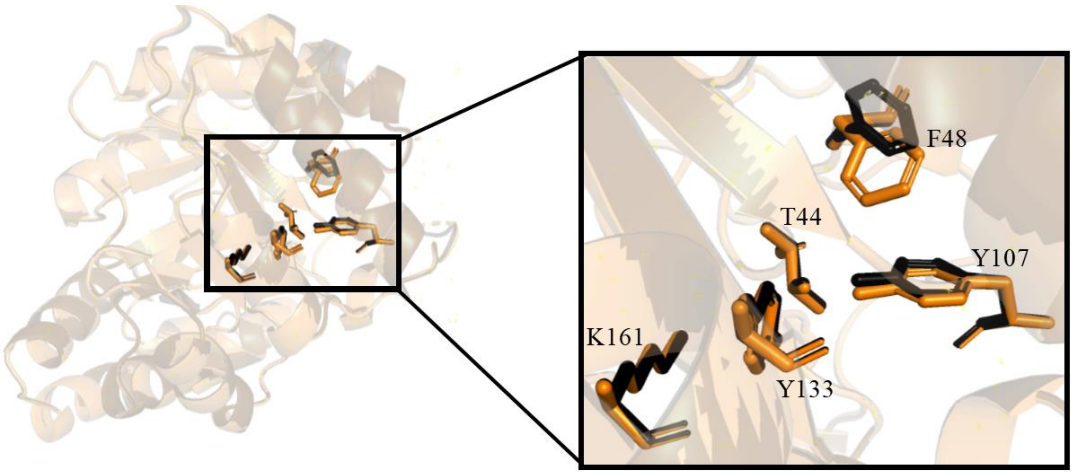

Figure 4.11: *Alignment of the monomer of DHDPS-S84F L (orange) and DHDPS-S84F apo (black). The catalytic site is enlarged.*

These two structures were then aligned with DHDPS-WT from Dobson *et al.*[2] and DHDPS-WT L from the current study (Figure 4.12). No differences were observed among the structures apart from the variance at Y107. As can be seen in the enlargement of the catalytic site (Figure 4.12), Y107 from DHDPS-WT L sits higher, while that of DHDPS-WT sits lower, than the corresponding residue from DHDPS-S48F apo.

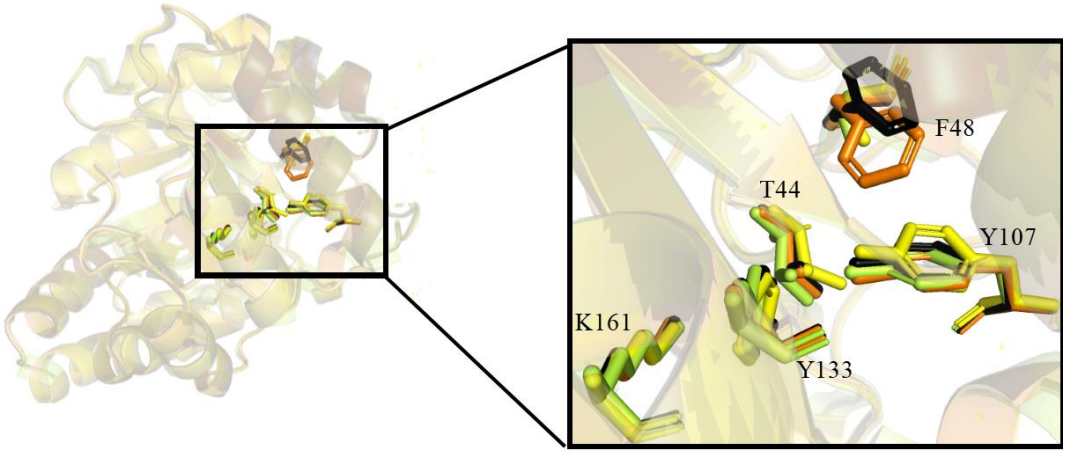

Figure 4.12: *Alignment of the monomer of DHDPS-S84F L (orange), DHDPS-S84F apo (black), DHDPS-WT (yellow-green), and DHDPS-WT L (yellow). The catalytic site is enlarged.*

Comparison of these two structures showed that there is little to no movement when the substrates are not bound. Residue K161 is motionless, while there is a small amount of movement in Y107.

4.4.3 All structures

All the DHDPS-S48F structures were then aligned (Figure 4.13). Again, the only observed variation occurred at residue Y107, with the movement being fairly minimal (enlarged area in Figure 4.13). The most notable difference was the position of the phenylalanine residue in the apo structure, which has been discussed previously.

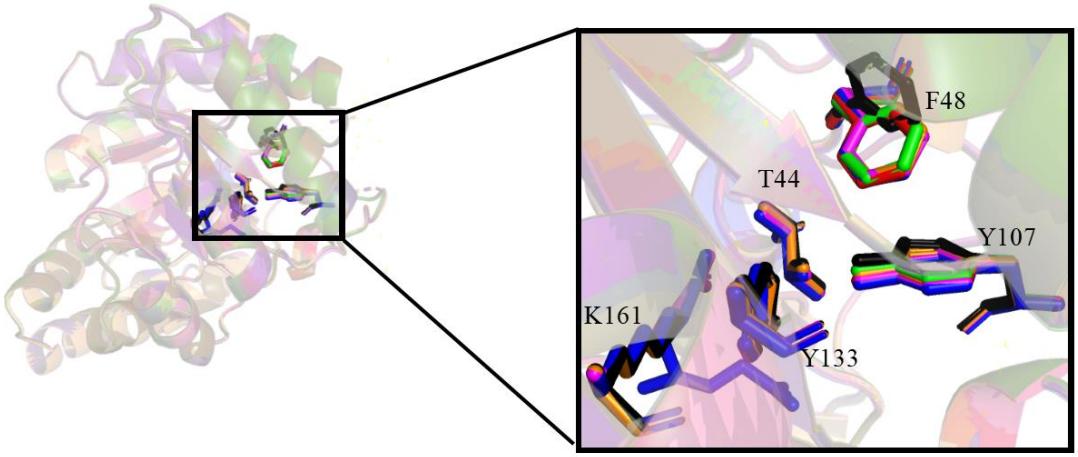

Figure 4.13: *Alignment of the monomer of all DHDPS-S48F proteins, with key residues within the catalytic site highlighted. DHDPS-S84F PS is in red, DHDPS-S84F LP is in pink, DHDPS-S84F LPS is in blue, DHDPS-S84F P is in green, DHDPS-S84F L is in orange, and DHDPS-S84F apo is in black.*

The DHDPS-S48F structures were then aligned with the DHDPS-WT structures (Figure 4.14). As with the previous alignment, variations occurred at residue Y107 and at the phenylalanine substitution (enlarged area in Figure 4.14). There is also some variation in the succinic acid semialdehyde binding site, as described above, and a small amount of movement at residue T44 (enlarged area in Figure 4.14).

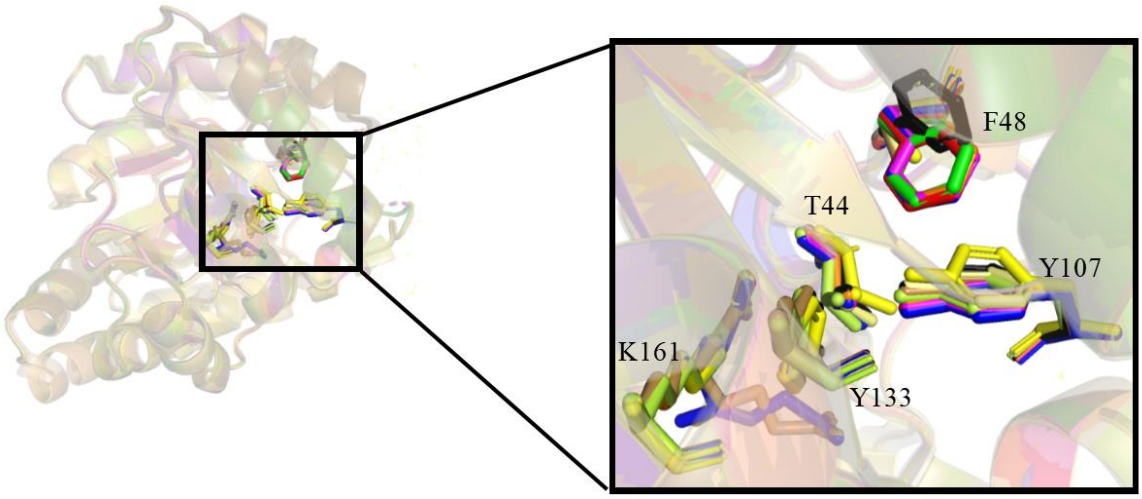

Figure 4.14: *Alignment of the monomer of the DHDPS-S48F and DHDPS-WT proteins. Key residues within the catalytic site are highlighted. Structures are coloured as follows: DHDPS-S84F PS, red; DHDPS-S84F LP, pink; DHDPS-S84F LPS, blue; DHDPS-S84F P, green; DHDPS-S84F L, orange; DHDPS-S84F apo, black; DHDPS-WT, yellow-green; DHDPS-WT L, yellow; DHDPS-WT P, bright yellow; DHDPS-WT PS, brown.*

4.4.4 Summary of changes in the catalytic site

The phenylalanine substitution does not appear to interfere with the catalytic site in the DHDPS-S48F structures, either by steric hinderance or by directly blocking catalysis. In addition, the placement of the phenylalanine side chain in all structures except DHDPS-S48F apo is not optimal for blocking the water channel as the ring of the phenylalanine does not lie flat across the channel. The key residues in the catalytic site do not interact with the substitution, nor does the substitution stop catalysis from taking place. As shown in Figure 4.8, the substitution does not interfere with the ability of the catalytic site to carry out the chemical reactions required for catalysis, which was confirmed by further comparison with the catalytic sites of the wild-type proteins.

4.5 Minor Changes in the Allosteric Site

The allosteric site is found at the A, B/C, D interface. This is where lysine, the allosteric inhibitor, binds to the enzyme to slow catalysis. Of the six phenylalanine substitution structures, DHDPS-S48F L, DHDPS-S48F LP, and DHDPS-S48F LPS have a lysine bound to the allosteric site. Figure 4.15 shows the density maps of the allosteric sites of these structures and confirms that there was density in the allosteric site, and that it does resemble lysine binding.

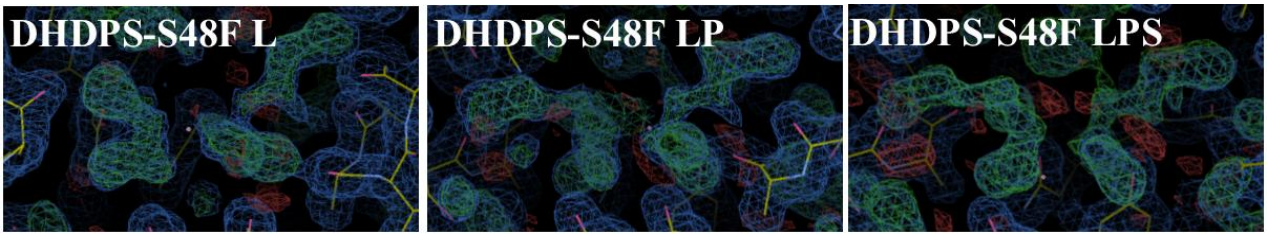

Figure 4.15: *Allosteric binding sites of DHDPS-S48F L, DHDPS-S48F LP, and DHDPS-S48F LPS. Density was observed in each structure, confirming that two lysine's would fit within the allosteric site. Each structure is labelled.*

4.6.1 Structures with bound lysine

In total, three of the phenylalanine substitution structures have a bound lysine. Of these, two structures also have substrate bound (DHDPS-S48F LP, and DHDPS-S48F LPS). There is some debate as to how the allosteric site binds lysine. Blinking *et al.*[22] showed that residues E84 and N80 bind to the polypeptide amino group of lysine, residue Y106 binds to the polypeptide carboxyl group, and residues H53 and H56 bind to Nε. Using a higher resolution structure, Dobson *et al.*[2] then showed that Nε binds to the main-chain O atom at residue S48 and not at H53. Both studies showed that Y106 is distorted slightly when bound to lysine. In the current study, PyMOL was used to identify the closest polar constructs to the lysine in the allosteric site, and to predict which of the residues bind lysine.

Figure 4.16 shows the allosteric sites of all DHDPS-S48F structures containing bound lysine. No differences in the key residues in the allosteric site were observed among the structures. However, there was a slight difference in the placement of the lysine bound to chain A in DHDPS-S48F LPS, with the carbon before the Nε sitting in a different position compared with the other structures. Despite this, Nε was in the same location, indicating that the observed difference may be an alternative placement as all the polar groups were in the same position.

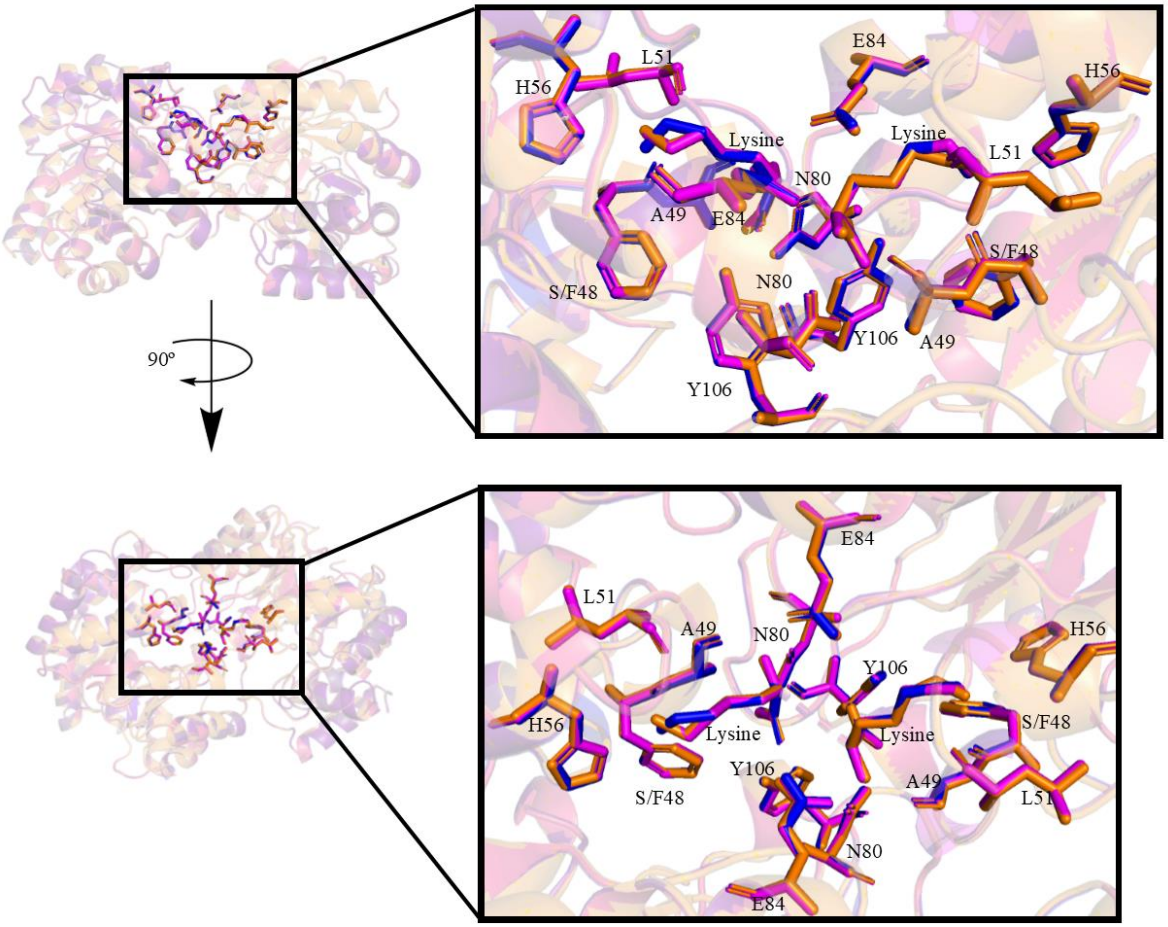

Figure 4.16: *Alignment of the dimer of all DHDPS-S48F proteins containing lysine bound at the allosteric site. Key residues within the allosteric site are highlighted. DHDPS-S84F LP is in pink, DHDPS-S84F LPS is in blue, and DHDPS-S84F L is orange.*

Only one of the DHDPS-WT structures (DHDPS-WT L) contained bound lysine. Therefore, the allosteric site of the wild-type protein was next compared with those of the DHDPS-S48F structures containing bound lysine (Figure 4.17). E84 of DHDPS-WT was slightly higher than the corresponding residues in the DHDPS-S48F structures. The second carbon of the side chain of this residue also showed a different orientation, although as the polar groups ended up in the same position, this could just be an alternative conformation. The rest of the DHDPS-WT L residues aligned perfectly with those of DHDPS-S48F (Figure 4.17).

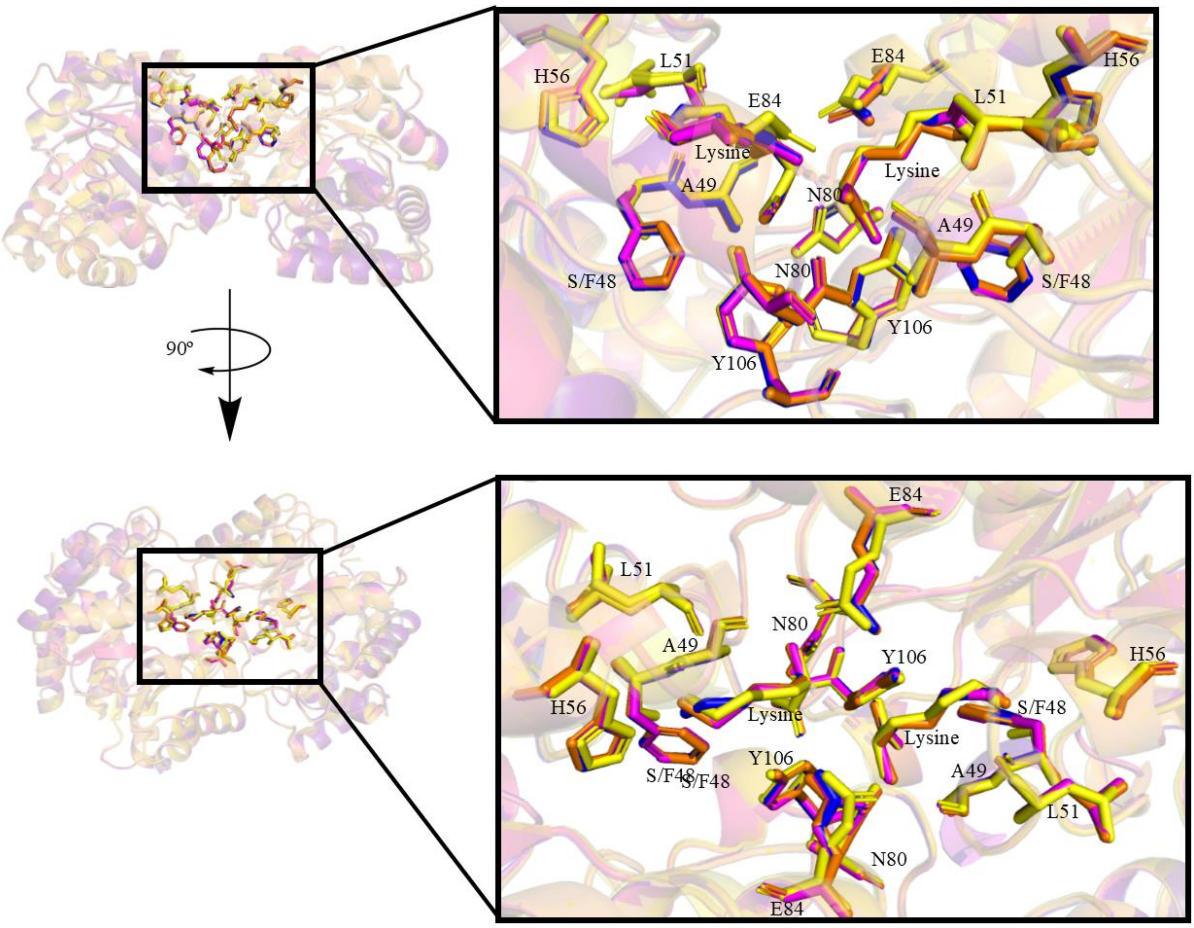

Figure 4.17: *Alignment of dimer of all DHDPS-S48F proteins containing lysine in the allosteric site with DHDPS-WT L. Key residues within the allosteric site are highlighted. DHDPS-WT L is in yellow, DHDPS-S84F LP is in pink, DHDPS-S84F LPS is in blue, and DHDPS-S84F L is orange.*

4.6.2 All structures

Comparing the positions of the residues in the allosteric site with/without bound lysine could show how the residues move when they bind lysine. Therefore, lysine-bound structures with

their corresponding unbound structures were compared, e.g., DHDPS-S48F LPS and DHDPS-S48F PS.

An alignment of the allosteric sites of all the DHDPS-S48F and DHDPS-WT structures is shown in Figure 4.18. The only observed difference was in the positioning of E84. In DHDPS-WT and DHDPS-WT PS, the E84 side chain is directed up out of the allosteric site, while in all other constructs this side chain points down into the allosteric site (Figure 4.18). E84 also sits slightly higher in these two structures and in DHDPS-WT L E84 compared with the other structures, though this difference is likely negligible. The only other difference was the phenylalanine substitution in DHDPS-S48F apo, which has already been discussed.

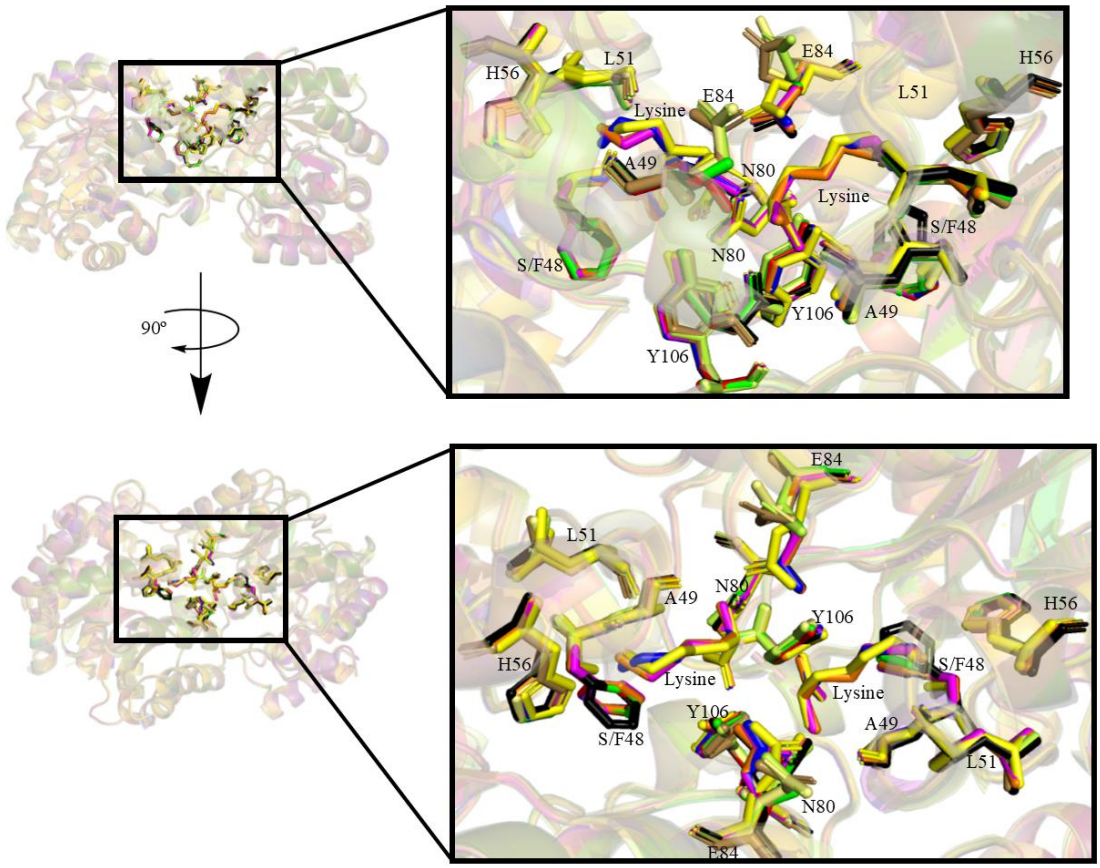

Figure 4.18: *Alignment of the dimer of all DHDPS-S48F and DHDPS-WT structures. Key residues within the allosteric site are highlighted in two different views. The top images show a standard view, while the bottom images are rotated 90º to show the top of the dimer. Structures are coloured as follows: DHDPS-S84F PS, red; DHDPS-S84F LP, pink; DHDPS-S84F LPS, blue; DHDPS-S84F P, green; DHDPS-S84F L, orange; DHDPS-S84F apo, black; DHDPS-WT, yellow-green; DHDPS-WT L, yellow; DHDPS-WT P, bright yellow; DHDPS-WT PS, brown.*

4.6 Mapping the Water Channel

As the water channel is the focus of this study, it is also important to analyse the water molecules in the water channel. Each monomer has a water channel, so we examined the monomeric forms of the DHDPS-S48F and DHDPS-WT structures.

An alignment of all the DHDPS-S48F structures is shown in Figure 4.19. The movement caused by the phenylalanine substitution in all structures except DHDPS-S48F apo appeared to allow some water molecules into the water channel, which is blocked in DHDPS-S48F apo (Figure 4.19). Water molecules were also observed in the allosteric binding site in the structures that do not contain lysine (Figure 4.19). Proton exchange may occur down the channel in DHDPS-S84F P and DHDPS-S84F PS as there is no lysine in the allosteric site and the phenylalanine hugs the side of the channel, allowing water entry.

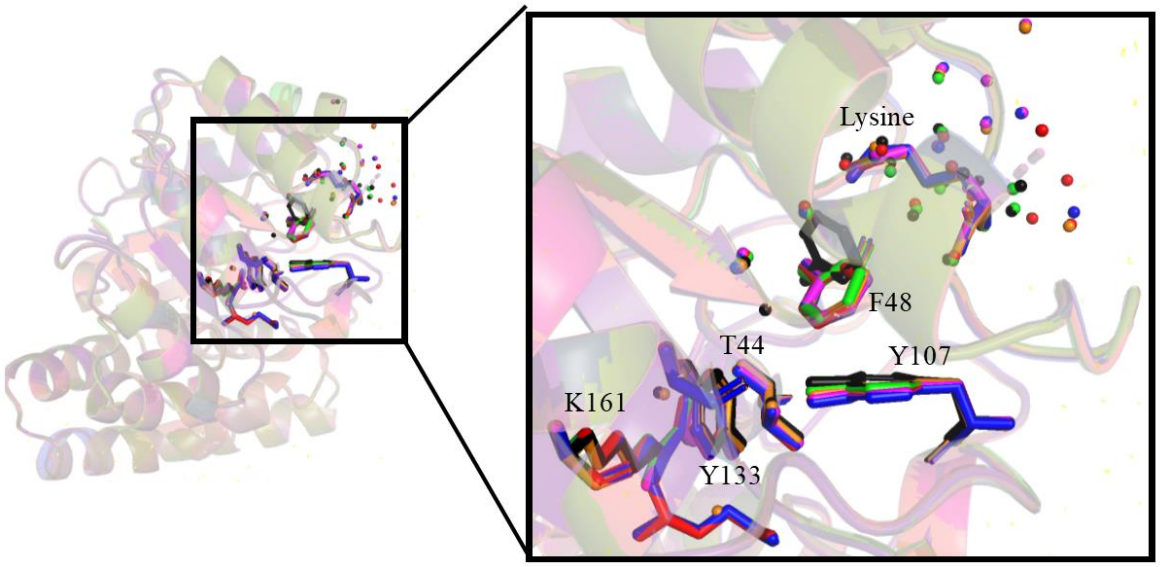

Figure 4.19: *Alignment of the monomer of all DHDPS-S48F proteins. Key residues within the catalytic site are highlighted. Where possible, the lysine in the allosteric binding site is also displayed, as are the water molecules in the water channel. DHDPS-S84F PS is in red, DHDPS-S84F LP is in pink, DHDPS-S84F LPS is in blue, DHDPS-S84F P is in green, DHDPS-S84F L is in orange, and DHDPS-S84F apo is in black.*

The water channel in all of the DHDPS-WT structures is highlighted in Figure 4.20 and shows a greater number of water molecules along the entire length of the channel compared with the previous Figure. Again, water molecules were observed in the allosteric binding site in the absence of lysine. The larger number of water molecules in this channel is even more indicative of proton exchange than the previous figure. Therefore, it concluded that the substitutions do interfere with the channel, but do not block it off completely.

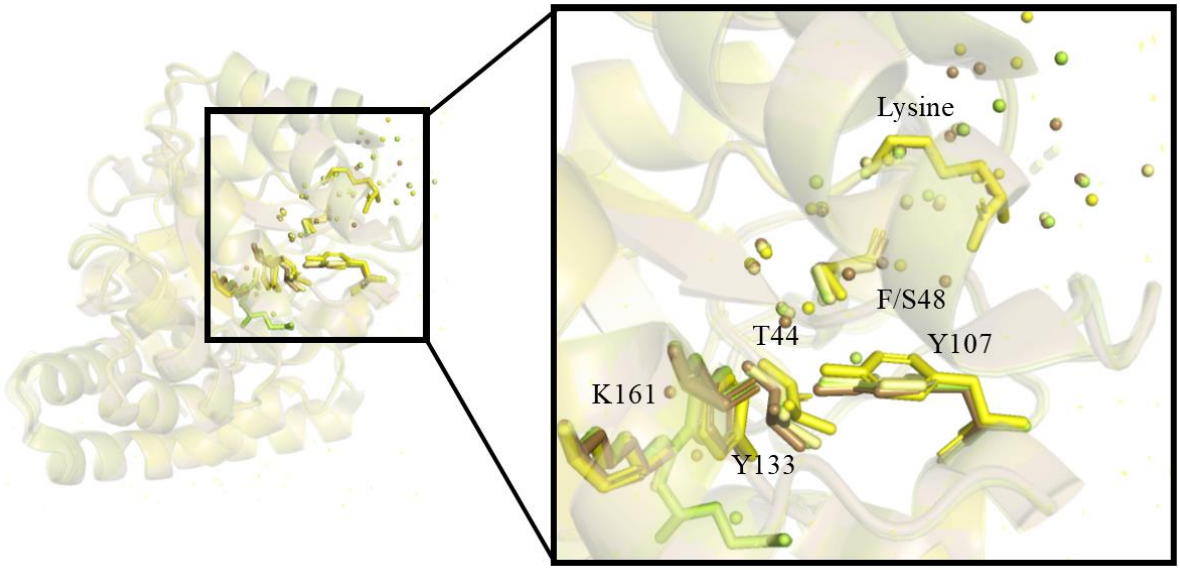

Figure 4.20: *Alignment of the monomer of all DHDPS-WT structures. Key residues within the catalytic site are highlighted. Where possible, the lysine in the allosteric binding site is also displayed, as are the water molecules in the water channel. DHDPS-WT is in yellow-green, DHDPS-WT L is in yellow, DHDPS-WT P is in bright yellow, and DHDPS-WT PS is in brown.*

Finally, we aligned the water channels of all structures (Figure 4.21). The results confirmed that the phenylalanine substitution blocks the water channel, but not as proficiently as hypothesised.

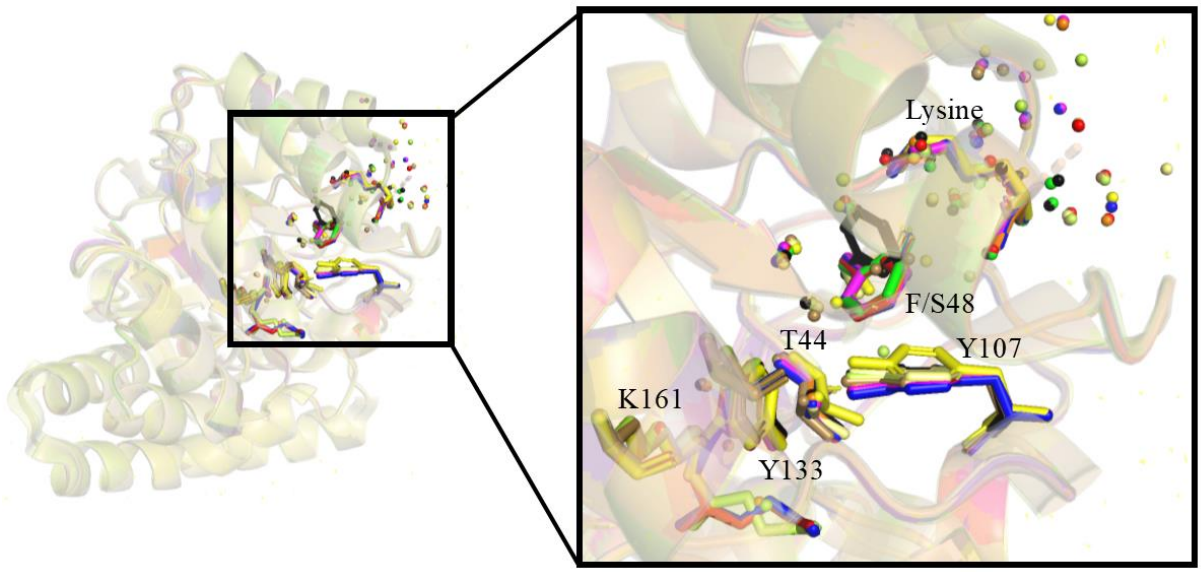

Figure 4.21: *Alignment of the monomers of all DHDPS-S48F and DHDPS-WT structures. Key residues within the catalytic site are highlighted. Where possible, the lysine in the allosteric binding site is also displayed, as are the water molecules in the water channel. Structures are coloured as follows: DHDPS-S84F PS, red; DHDPS-S84F LP, pink; DHDPS-S84F LPS, blue; DHDPS-S84F P, green; DHDPS-S84F L, orange; DHDPS-S84F apo, black; DHDPS-WT, yellow-green; DHDPS-WT L, yellow; DHDPS-WT P, bright yellow; DHDPS-WT PS, brown.*

4.8 Summary

The findings outlined in this chapter confirm that the DHDPS-S48F structures are not significantly different from the wild-type protein, and that the substitution does not appear to interfere with either the catalytic site or the allosteric site. The placement of the phenylalanine side chain is not optimal for blocking the water channel, and therefore has less of an effect on the allosteric site than was intended. In addition, the bulky side chain of the substitution does not appear to hinder the allosteric site, but there is minimal movement of Y106 when the lysine binds. This is consistent with earlier studies on the allosteric site, so is likely not a feature of the substitution. Comparing the catalytic sites of the wild-type and phenylalanine-substitution proteins produced some interesting results. It would seem that the

Y107 residue is significantly lower in the DHDPS-S48F structures than in the wild-type enzyme. However, no differences were observed in the allosteric site apart from the movement of E84, which is likely to be an alternative conformation as the protein is always moving. Further, the carboxyl group in the side chain of E84 remained in a similar position.

4.9 References

1. Mirwaldt, C., Korndorfer, I., and Huber, R. (1995) The Crystal Structure of Dihydrodipicolinate Synthase from *Escherichia coli* at 2.5 Å Resolution, *Journal of molecular biology* ***246***, 227-239.

2. Dobson, R. C., Griffin, M. D., Jameson, G. B., and Gerrard, J. A. (2005) The crystal structures of native and (S)-lysine-bound dihydrodipicolinate synthase from *Escherichia coli* with improved resolution show new features of biological significance, *Acta Crystallographica Section D: Biological Crystallography* ***61***, 1116-1124.

3. Blickling, S., Renner, C., Laber, B., Pohlenz, H.-D., Holak, T. A., and Huber, R. (1997) Reaction mechanism of *Escherichia coli* dihydrodipicolinate synthase investigated by X-ray crystallography and NMR spectroscopy, *Biochemistry* ***36***, 24-33.

4. Dobson, R. C., Valegård, K., and Gerrard, J. A. (2004) The crystal structure of three site-directed mutants of *Escherichia coli* dihydrodipicolinate synthase: further evidence for a catalytic triad, *Journal of molecular biology* ***338***, 329-339.

5. Winn, M. D., Ballard, C. C., Cowtan, K. D., Dodson, E. J., Emsley, P., Evans, P. R., Keegan, R. M., Krissinel, E. B., Leslie, A. G., and McCoy, A. (2011) Overview of the CCP4 suite and current developments, *Acta Crystallographica Section D: Biological Crystallography* ***67***, 235-242.

6. Battye, T. G. G., Kontogiannis, L., Johnson, O., Powell, H. R., and Leslie, A. G. (2011) iMOSFLM: a new graphical interface for diffraction-image processing with MOSFLM, *Acta Crystallographica Section D: Biological Crystallography* ***67***, 271-281.

7. Evans, P. R. (2011) An introduction to data reduction: space-group determination, scaling and intensity statistics, *Acta Crystallographica Section D: Biological Crystallography* ***67***, 282-292.

8. McCoy, A. J., Grosse-Kunstleve, R. W., Adams, P. D., Winn, M. D., Storoni, L. C., and Read, R. J. (2007) Phaser crystallographic software, *Journal of applied crystallography* ***40***, 658-674.

9. Murshudov, G., Vagin, A., and Dodson, E. (1996) Application of maximum likelihood refinement, *Proceedings of Daresbury Study Weekend 4*.

10. Murshudov, G. N., Vagin, A. A., and Dodson, E. J. (1997) Refinement of macromolecular structures by the maximum-likelihood method, *Acta Crystallographica Section D: Biological Crystallography* ***53***, -255.

11. Pannu, N. S., Murshudov, G. N., Dodson, E. J., and Read, R. J. (1998) Incorporation of prior phase information strengthens maximum-likelihood structure refinement, *Acta Crystallographica Section D: Biological Crystallography* ***54***, 1285-1294.

12. Murshudov, G. N., Vagin, A. A., Lebedev, A., Wilson, K. S., and Dodson, E. J. (1999) Efficient anisotropic refinement of macromolecular structures using FFT, *Acta Crystallographica Section D: Biological Crystallography* ***55***, 247-255.

13. Winn, M., Isupov, M., and Murshudov, G. N. (2001) Use of TLS parameters to model anisotropic displacements in macromolecular refinement, *Acta Crystallographica Section D: Biological Crystallography* ***57***, 122-133.

14. Steiner, R. A., Lebedev, A. A., and Murshudov, G. N. (2003) Fisher's information in maximum-likelihood macromolecular crystallographic refinement, *Acta Crystallographica Section D: Biological Crystallography* ***59***, 2114-2124.

15. Winn, M. D., Murshudov, G. N., and Papiz, M. Z. (2003) Macromolecular TLS refinement in REFMAC at moderate resolutions, In *Methods in enzymology*, pp 300-321, Elsevier.

16. Skubák, P., Murshudov, G. N., and Pannu, N. S. (2004) Direct incorporation of experimental phase information in model refinement, *Acta Crystallographica Section D: Biological Crystallography* ***60***, 2196-2201.

17. Vagin, A. A., Steiner, R. A., Lebedev, A. A., Potterton, L., McNicholas, S., Long, F., and Murshudov, G. N. (2004) REFMAC5 dictionary: organization of prior chemical

knowledge and guidelines for its use, *Acta Crystallographica Section D: Biological Crystallography* ***60***, 2184-2195.

18. Emsley, P., Lohkamp, B., Scott, W. G., and Cowtan, K. (2010) Features and development of Coot, *Acta Crystallographica Section D: Biological Crystallography* ***66***, 486-501.

19. da Costa, T. P. S., Muscroft-Taylor, A. C., Dobson, R. C., Devenish, S. R., Jameson, G. B., and Gerrard, J. A. (2010) How essential is the 'essential'active-site lysine in dihydrodipicolinate synthase?, *Biochimie* ***92***, 837-845.

20. Devenish, S. R. A., Gerrard, J. A., Jameson, G. B., and Dobson, R. C. J. (2008) The high-resolution structure of dihydrodipicolinate synthase from *Escherichia coli* bound to its first substrate, pyruvate, *Acta Crystallographica Section F-Structural Biology and Crystallization Communications* ***64***, 1092-1095.

21. Boughton, B. A., Dobson, R. C., and Hutton, C. A. (2012) The crystal structure of dihydrodipicolinate synthase from *Escherichia coli* with bound pyruvate and succinic acid semialdehyde: unambiguous resolution of the stereochemistry of the condensation product, *Proteins: Structure, Function, and Bioinformatics* ***80***, 2117-2122.

22. Blickling, S., and Knablein, J. (1997) Feedback inhibition of dihydrodipicolinate synthase enzymes by L-lysine, *Biological Chemistry* ***378***, 207-210.

Chapter Five: Analysis of the DHDPS-S48W Structures

5.1 Introduction

In Chapter Four, six structures containing phenylalanine mutations at residue 48 were examined. These structures did not show major differences from the wild-type enzyme and looked to be able to function normally, as the mutation did not interfere with either the catalytic or allosteric site. In this chapter, DHDPS-S48W structures are examined to determine how the tryptophan substitution interferes with the key residues of either the allosteric or catalytic site. Tryptophan has the largest side chain of the 20 amino acids, with one six-membered ring connected to one five-membered ring (Figure 5.1). The size of tryptophan makes it a perfect candidate for this study because the larger side-chain is more likely to effectively block the water channel than the phenylalanine discussed in Chapter Four. However, it is also more likely to interfere with key residues in the catalytic and allosteric sites.

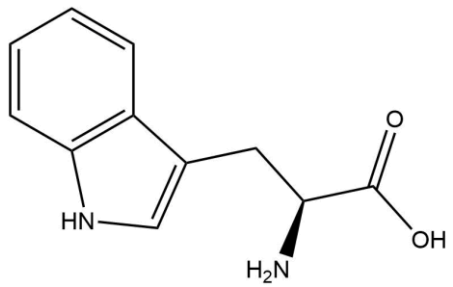

Figure 5.1: *The structure of tryptophan*

In this chapter, the DHDPS-S48W structures are examined to determine whether the lack of activity shown in Chapter Three is caused by blockage of the water channel or by a large hydrophobic mass interfering with the key residues of catalysis.

These structures were created using the same process used to generate the phenylalanine structures, which is outlined in Chapter Four (Section 4.2).

5.2 Features of the Tryptophan Structures

The structures descried in this chapter all contain a S48W point mutation and are in a dimeric form, with each chain being identical and 292 residues in length. Figure 5.1 shows that the density around residue 48 is consistent with that of tryptophan.

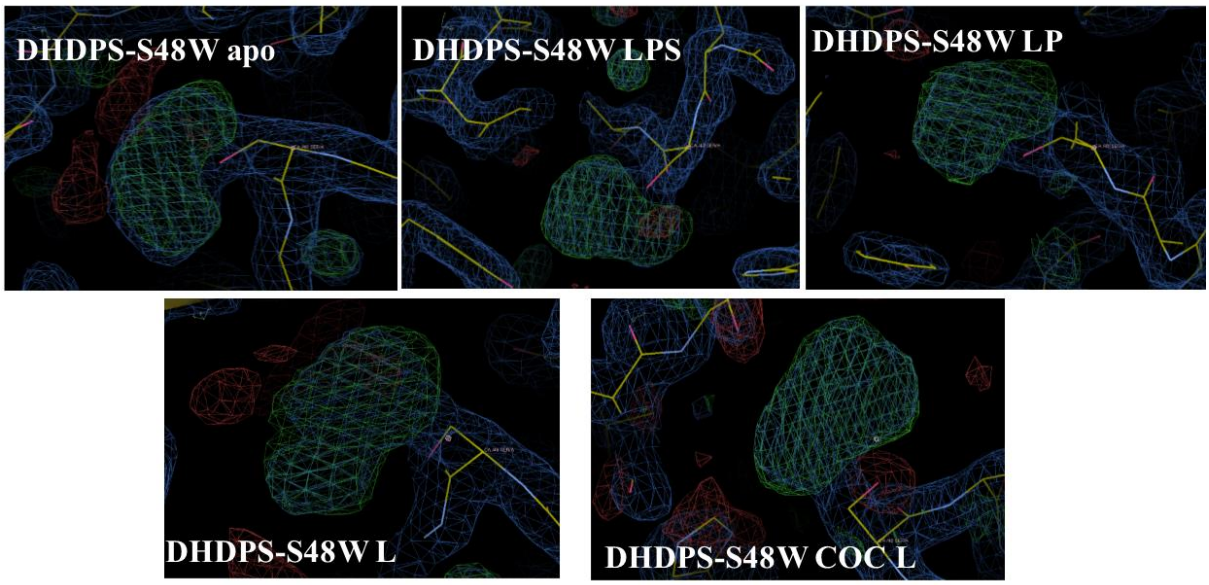

Figure 5.2: *Residue 48 of Chain A in all structures shows density consistent with tryptophan.*

Five structures containing the tryptophan point mutation were generated, including an apoenzyme (DHDPS-S48W apo) and five structures with various bound molecules, including: pyruvate and lysine (DHDPS-S48W LP), pyruvate, an succinic semi-aldehyde, and lysine (DHDPS-S48W LPS), lysine (DHDPS-S48W L), and lysine that had been co-crystallised rather than soaked (DHDPS-S48W COCL). Lysine did not appear in any of the structures; therefore, crystals were both soaked in lysine and co-crystallised with lysine. In the former process, the crystals are allowed to form before the addition of high concentrations of lysine upon preparation of the crystals. Lysine-co-crystallised crystals were processed in the same manner as the other crystals, with the only difference being the addition of lysine.

Figure 5.3 shows an alignment of all seven of the tryptophan structures, from the tetramer down to the monomer. The results showed that the quaternary and tertiary structures stay intact and that the substitution does not cause any major changes in the structure (Figure 5.3). The structures (in different colours) all align well and must therefore all be similar in structure.

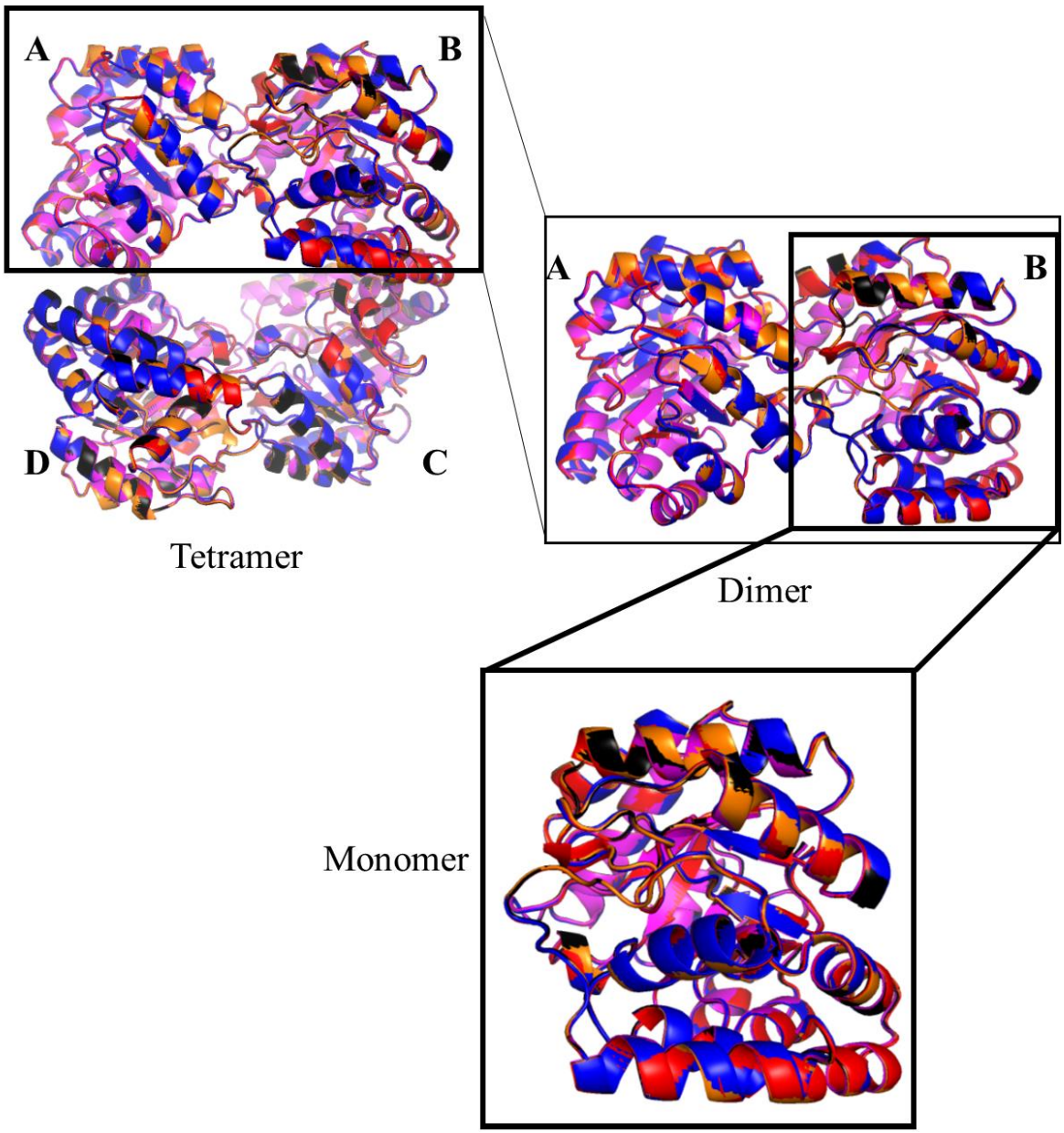

Figure 5.3: *Alignment of all generated DHDPS-S48W structures at the level of tetramer, dimer, and monomer. The structures are coloured as follows: DHDPS-S48W apo, black; DHDPS-S48W LP, red; DHDPS-S48W LPS, blue; DHDPS-S48W L, orange; DHDPS-S48W COC L, pink.*

Although the quaternary and tertiary structures of all the generated structures were the same, some minor differences were observed in the secondary structures. The four major differences in the secondary structures are enlarged in Figure 5.4. The top left section shows that, unlike the other structures, DHDPS-S48W LPS forms loops instead of a helix at the end of the structure. These loops follow the structure of the helix, but the bond lengths do not qualify as a helix. The top right section shows that DHDPS-S48W apo and DHDPS-S48W L have shorter beta sheets than the other structures. Again, the loops still follow the direction of the beta sheets but the bonds differ slightly. The bottom left section shows a small alpha helix in DHDPS-S48W LP, whereas the other structures all have loops in this section. This indicates that DHDPS-S48W LP has the correct bond lengths for an alpha helix, whereas the others do not. Finally, the bottom right section shows beta sheets of different sizes. DHDPS-S48W LPS has a loop that follows the same path as the beta sheet in the other structures but is clearly not as straight as a sheet. Furthermore, DHDPS-S48W COC L and DHDPS-S48W apo have shorter beta sheets than DHDPS-S48W L and DHDPS-S48W LP.

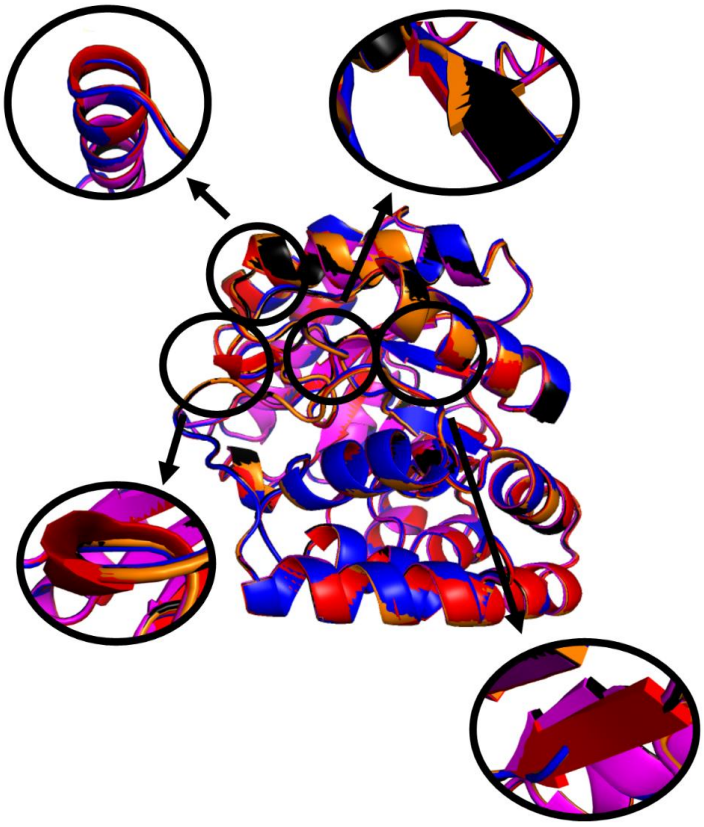

Figure 5.4: *DHDPS-S48W secondary structures displayed at the monomer level. The structures are coloured as follows: DHDPS-S48W apo, black; DHDPS-S48W LP, red; DHDPS-S48W LPS, blue; DHDPS-S48W L, orange; DHDPS-S48W COCL, pink.*

Although the DHDPS-S48W quaternary and tertiary structures looked to be intact, they were aligned with DHDPS-WT to ensure that there were no significant differences (Figure 5.5). The DHDPS-WT structures are from four different sources: DHDPS-WT L was generated in this study, DHDPS-WT is from Dobson *et al.*[1], DHDPS-WT P is from Devenish *et al.*[2], and DHDPS-WT PS is from Boughton *et al.*[3]. Alignments showed no differences between the quaternary and tertiary structures, although slight differences in secondary structure were observed. These were primarily at the beginning and the end of the alpha helices. There was little variation in the beta sheets.

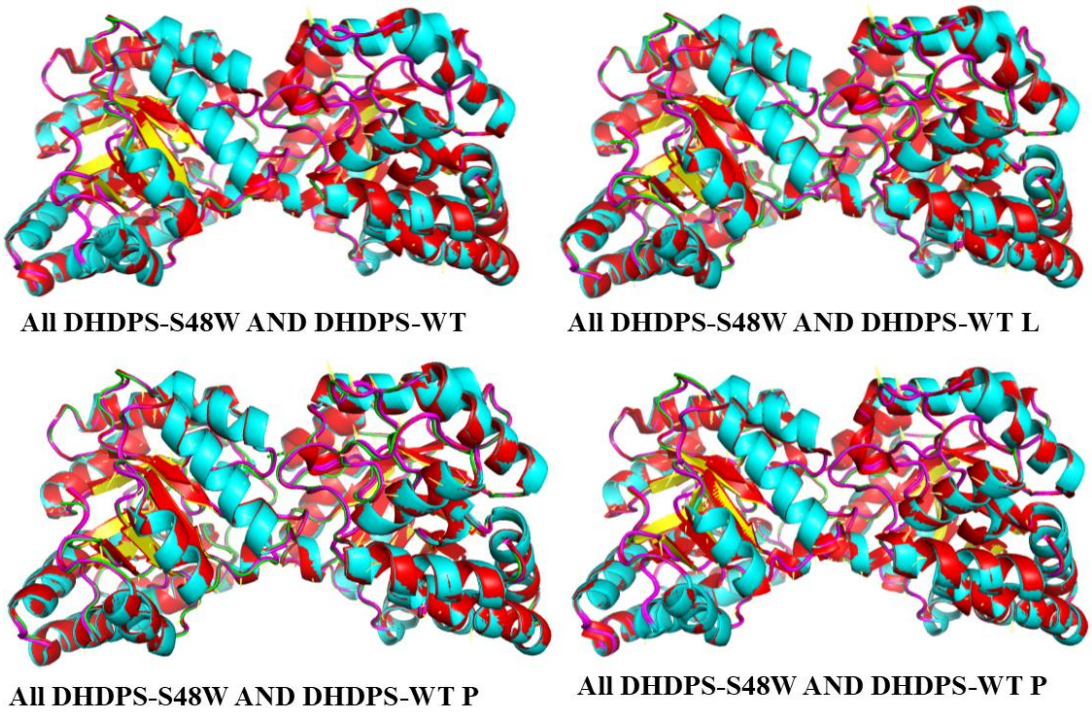

Figure 5.5: *Dimers of all of the DHDPS-S48W structures compared with four different DHDPS-WT structures from four different sources: DHDPS-WT (from Dobson et al.[1]), DHDPS-WT L (this study), DHDPS-WT P (from Devenish et al.[2]), and DHDPS-WT PS (from Boughton et al.[3]). All of the DHDPS-WT structures are shown with red alpha helices, yellow beta sheets, and green loops. The DHDPS-S48W structures have blue alpha helices, red beta sheets, and pink loops.*

Few differences were observed among the DHDPS-S48W secondary structures, and the quaternary and tertiary structures were identical. The variations in the secondary structures did not appear to be in the interfaces of the monomers. Figure 5.5 shows the A/B interface. The hydrophobic stacking of Y107 and Y106 keeps the two monomers together (highlighted in Figure 5.6). There was little variation among the Y107 residues, although some of the residues sit higher than others. However, this variation is not likely to be significant. There was no observed variation in the Y106 structures.

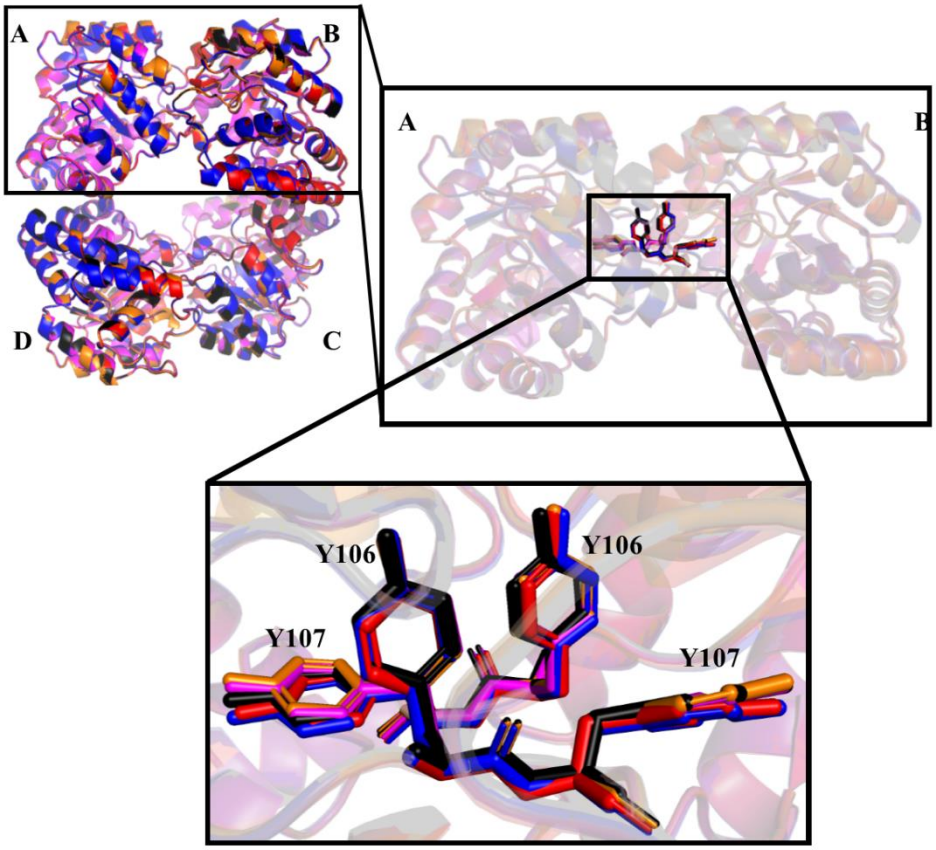

Figure 5.6: *The A/B interfaces of all the DHDPS-S48W structures, with enlargements from the tetramer, to the dimer, to the key residues. The structures are coloured as follows: DHDPS-S48W apo, black; DHDPS-S48W LP, red; DHDPS-S48W LPS, blue; DHDPS-S48W L, orange; DHDPS-S48W COCL, pink.*

The B/C interface of all the structures was also examined. The secondary structures revealed no variations in the area of the B/C interface. The key residues of the interface are shown in Figure 5.7, and the two dimers are thought to be connected via L167, T168, L197, and Q196 [1, 4]. The figure shows no variance in the residues.

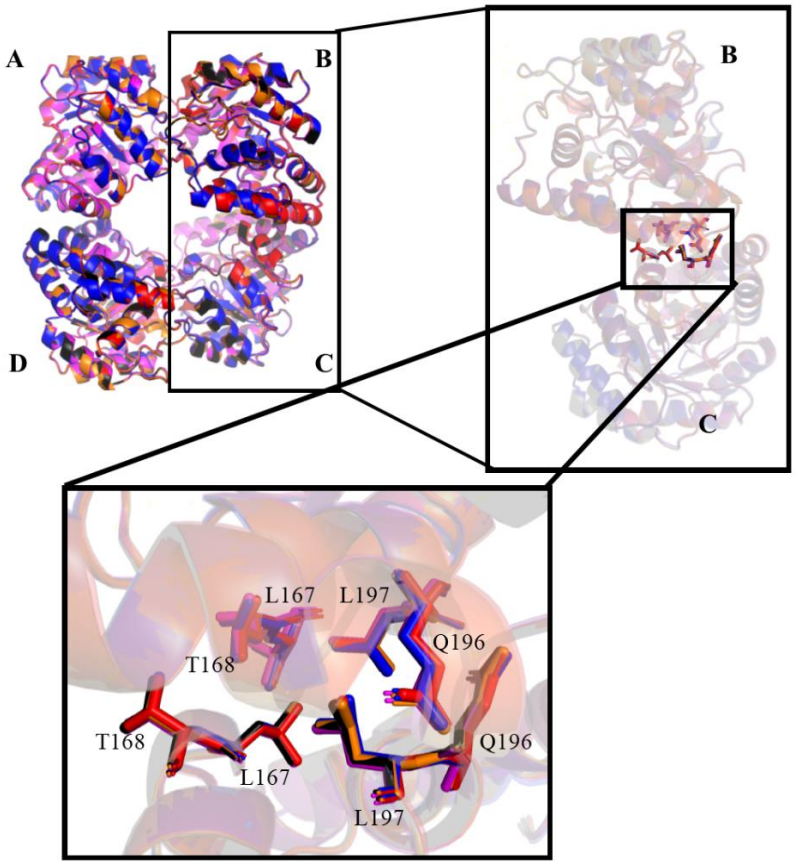

Figure 5.7: *The B/C interface of all of the aligned structures, from the tetramer, to the dimer, to the key residues. The structures are coloured as follows: DHDPS-S48W apo, black; DHDPS-S48W LP, red; DHDPS-S48W LPS, blue; DHDPS-S48W L, orange; DHDPS-S48W COCL, pink.*

The overall structure of the DHDPS-S48W proteins looked very similar despite the small number of differences in the secondary structure. As discussed in Chapter Four, the differences in the structures could also be indicative of different protein configurations. Figure 5.8 highlights the substitutions in all of the DHDPS-S48W structures and shows that there was no detectable variance in the positioning of the substitution.

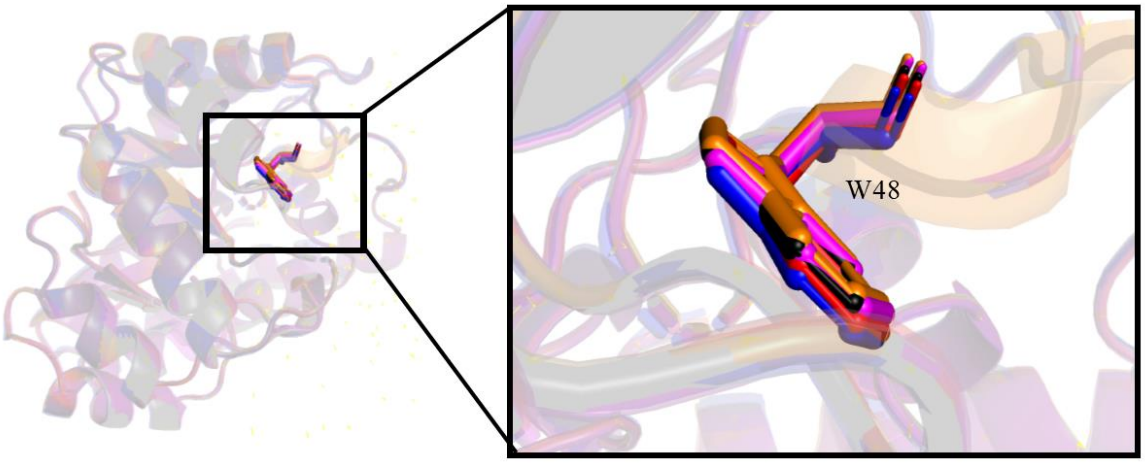

Figure 5.8: *Alignment of the monomer of all of the DHDPS-S48W structures. The substitution is highlighted and enlarged. The structures are coloured as follows: DHDPS-S48W apo, black; DHDPS-S48W LP, red; DHDPS-S48W LPS, blue; DHDPS-S48W L, orange; DHDPS-S48W COCL, pink.*

The movement of the substitution can be tracked by examining the B-factor profile of the protein. Figure 5.9 shows the B-factor scores for all the residues in both chains of the DHDPS-S48W structures. Residue 48 is indicated. The B-chain of DHDPS-S48W LP contained the highest B-factor score, 46.5. The lowest value, 29.7, was observed in the B-chain of DHDPS-S48W LPS. On average, the B-factor scores of the DHDPS-S28W structures were higher than those of the DHDPS-S48F structures. Figure 5.6 shows all the residues in each of the side chains in the same conformation. These side chains may be mobile, but they are generally crystallised in the most favourable conformation.

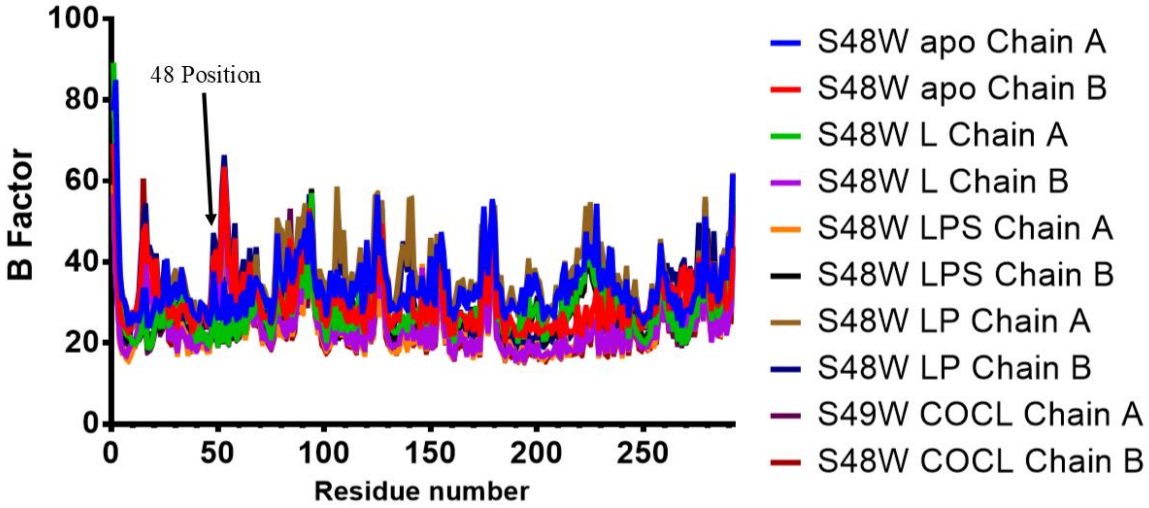

Figure 5.9: *B-factor profiles of all residues in both chains of all of the DHDPS-S48W structures. Each chain is coloured differently, with the key shown on the right. The arrow shows the position of residue 48.*

All the DHDPS-S48W structures had comparable quaternary and tertiary structures. The differences in secondary structure did not appear to interfere with the key residues of the enzymes, and there was no variation in the placement of the substitutions within the structures. Therefore, it does not appear that the substitutions at residue 48 affect the overall structure of the enzyme. The placement of the substitution is in a perfect position to block the water channel, which is more effective than in the structures outlined in Chapter Four.

Finally, Table 4.1 shows all the statistics for the structures. The Ramachandran plots were similar for the tryptophan substitutions, with Y107 of both chains being outside the normal range which is consistent with other works[1, 5]. All were within 1.7-2.1 Å resolution, have an R_{free} between 0.18-0.22, and are in the space group P 31 2 1, which is consistent with other crystallisation studies of DHDPS[1, 4-7].

Table 5.1**:** *Data processing statistics, including molecular replacement details, B-factors, and Ramachandran scores, for all the tryptophan structures*

Data collection statistics	*S48W_apo*	*S48W_COC*	*S48W_L*	*S48W_PL*	*S48W_LPS*
Wavelength (Å)	0.95369	0.95369	0.95369	0.95369	0.95369
Number of images	360	360	360	360	360
Oscillations (°)	0.5	0.5	0.5	0.5	0.5
Space group	P 31 2 1	P 31 2 1	P 31 2 1	P 31 2 1	P 31 2 1
Cell parameters a,b,c (Å)	121.16 121.16 111.97	120.51 120.51 111.03	121.1 121.1 111.8	121.1 121.1 111.3	121.1 121.1 111.2
α,b,y (°)	90 90 90	90 90 120	90 90 120	90 90 120	90 90 120
Resolution range (Å)	38.28–2.00 (2.07–2.00)	104.37–1.83(1.87–1.82)	41.07–1.91 (1.95–1.91)	39.65–2.07 (2.13–2.07)	111.230–1.930 (1.94-1.90)
Unique reflections	64272	78186	73768 (4271)	57870 (4451)	70938 (10096)
Mean I/σ (I)		11.6 (0.9)	19.3 (3.6)	10.1 (2.3)	17.9 (4.0)
Completeness (%)	99.6 (99.3)	99.8 (96.2)	99.6 (94.1)	100.0 (99.9)	99.8 (98.5)
Rmerge	0.068 (0.410)	0.151 (2.426)	0.080 (0.645)	0.145 (0.934)	0.085 (0.588)
Rp.i.m	0.064 (1.139)	0.069 (1.149)	0.025 (0.206)	0.047 (0.330)	0.028 (0.194)
Rr.i.m	0.169 (2.731)	0.165 (2.697)	0.084 (0.678)	0.152 (0.992)	0.081 (0.665)
CC1/2	0.996 (0.659)	0.995 (0.618)	0.999 (0.892)	0.997 (0.667)	0.093 (0.645)
Multiplicity	11.1 (10.4)	11.2 (9.9)	11.1 (10.3)	10.4 (8.9)	11.1 (10.9)
Molecular replacement					
Mol/asym. Unit	2	2	2	2	2
LLG	250.7	135.4	258.4	2831.8	985
Rwork/Rfree	0.2418/0.2684	0.3983/0.4169	0.2275/0.2569	0.2160/0.2451	0.2283/0.2521
Refinement details					
Rwork/Rfree (%)	0.1820/0.2226	0.1649/0.2002	0.1589/0.1893	0.1723/0.2086	0.1528/0.1808
No. of atoms §					
Total	4829	5011	4858	4616	4822
Macromolecules	2	2	2	2	2
Ligands	6	6	4	4	5
Water	472	563	505	402	500
Protein residues	292	292	292	292	292
B Factors (Å)					
Macromolecules	32.364	23.931	24.678	31.413	24.31
Ligands	51.177	55.233	40.222	33.952	29.01
Solvent	38.411	35.471	34.241	36.574	34.277
Ramachandran plot residues (%)					
Most favoured regions	98.64	98.79	98.15	98.29	98.65
Additionally allowed regions	1.19	0.91	1.68	1.37	1.35
Disallowed regions	0.17	0.09	0.17	0.34	0
All-atom clash score	3.85	7.48	2.47	4.96	3.39

5.3 The Catalytic Site

The catalytic site is where the reaction takes place and is found at the centre of each monomer in the β_8 barrel. The residues that guide catalysis include a catalytic triad[5] and K161, which binds to the substrate in order for the chemistry to take place[7]. To confirm that any changes in the kinetic data are due to blocking of the water channel and not steric hinderance of catalysis by tryptophan, we examined the two structures containing the tryptophan mutation that had substrates bound to the active site, namely DHDPS-S48W LP and DHDPS-S48W LPS.

5.3.1 Structures with bound substrate

DHDPS-S48W LP and DHDPS-S48W LPS monomers and catalytic sites were first aligned (Figure 5.10). The figure demonstrates how the tryptophan substitution at residue 48 does not interfere with either the catalytic triad or with the binding of substrates to K161. The Figure also shows that in both DHDPS-S48W LP and DHDPS-S48W LPS, the pyruvates bind in the same place, confirming that the substitution does not interfere with the binding site of the substrates. There was also no observed variation in any of the residues.

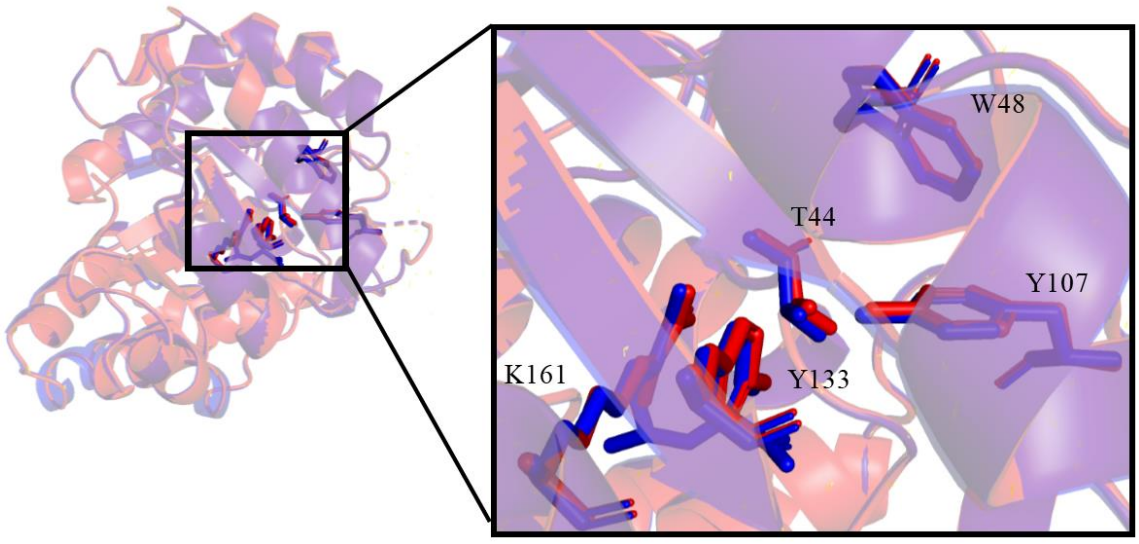

Figure 5.10: *Alignment of the monomers of DHDPS-S48W LP and DHDPS-S48W LPS. The catalytic sites are highlighted. DHDPS-S48W LP is in red and DHDPS-S48W LPS is in blue.*

The catalytic sites and monomers of DHDPS-S48W LP and DHDPS-S48W LPS were then aligned with DHDPS-WT P from Devenish *et al.*[2] and DHDPS-WT PS from Boughton *et al.*[3] (Figure 5.11). The results showed that pyruvate binds in the same place in all the structures. However, there was variation in the positioning of the final carbon in succinic acid semialdehyde in DHDPS-S48W LPS and DHDPS-WT PS, which agrees with the findings outlined in the previous chapter using the DHDPS-S48F structures containing succinic acid semialdehyde. However, as the polar sites remained in the same position, the observed difference may just be indicative of an alternative conformation, or the result of differences in modelling between the current study and that of Boughton *et al*. Apart from the succinic acid semialdehyde, all other residues were located in the same place, showing that the tryptophan substitution does not alter the key residues in the catalytic site.

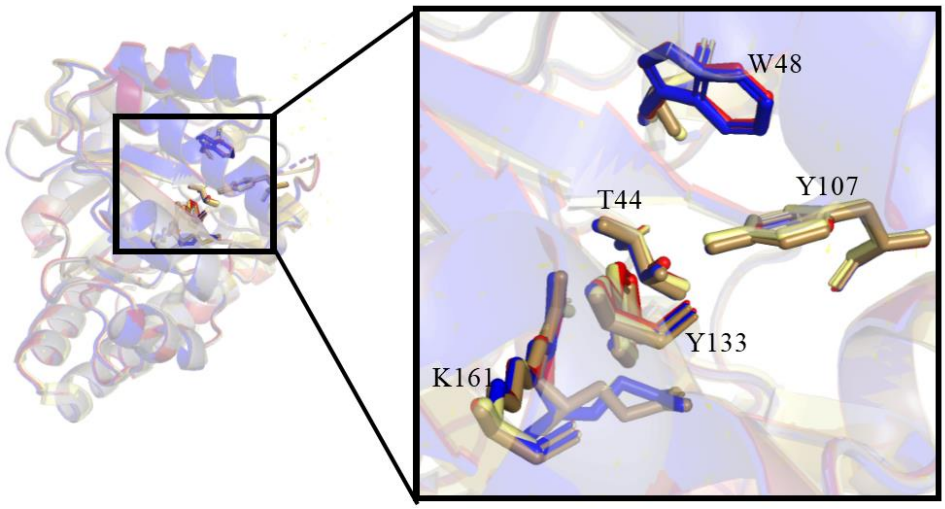

Figure 5.11: *Alignment of the catalytic sites of DHDPS-S48W LP, DHDPS-S48W LPS, DHDPS-WT P (from Devenish et al.[2]), and DHDPS-WT PS (from Boughton et al.[3]). DHDPS-S48W LP is in red, DHDPS-S48W LPS is in blue, DHDPS-WT P is in light yellow, and DHDPS-WT PS is in brown.*

5.3.2 Structures without bound substrate

Three of the five DHDPS-S48W structures DHDPS-S48W apo, DHDPS-S48W L, and DHDPS-S48W COCL, do not contain bound substrate. The catalytic sites of these structures were aligned and are shown in Figure 5.12. Little variation was observed between the three structures, apart from very slight variation at Y107, which was not likely to be significant.

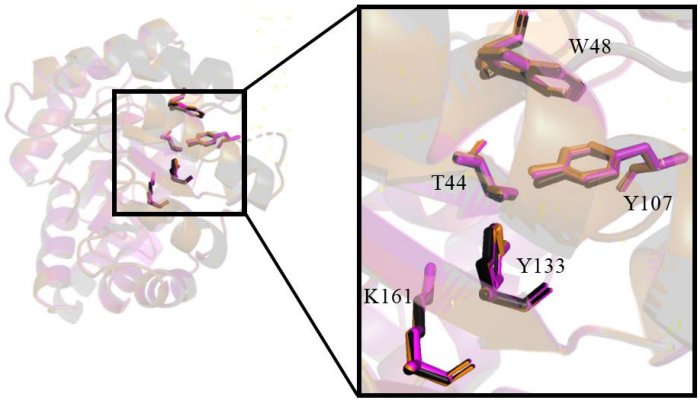

Figure 5.12: *Alignment of the monomers and catalytic sites of DHDPS-S48W apo (black), DHDPS-S48W L (orange), and DHDPS-S48W COCL (pink).*

These structures were then compared with DHDPS-WT L (crystallised for this study) and DHDPS-WT from Dobson *et al.*[1] (Figure 5.13). Just as in the previous alignment, the only major difference between the structures was at Y107. The differences were more significant here, with Y107 from DHDPS-WT L sitting higher than in the other structures and appearing slightly twisted. All other differences were only very slight.

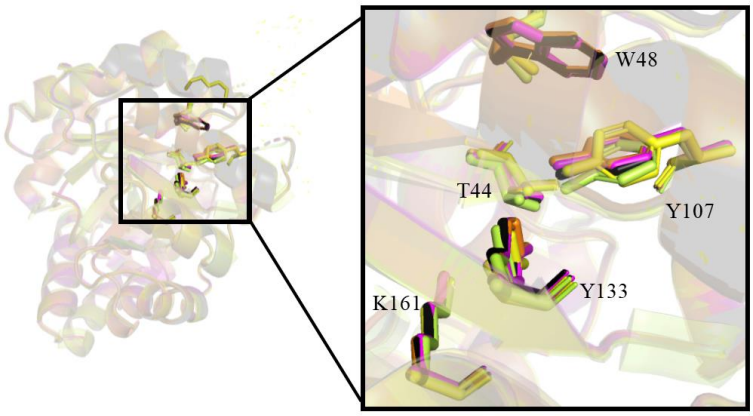

Figure 5.13: *Alignment of the monomers and catalytic sites of DHDPS-S48W apo (black), DHDPS-S48W L (orange), DHDPS-S48W COCL (pink), DHDPS-WT from Dobson et al. (green-yellow), and DHDPS-WT L (yellow).*

5.3.3 Comparison of Structures with and without bound substrate

The structures with bound substrate indicated that the mutation does not interfere with the catalytic site. To confirm that substrate binding does not cause any movement in the key residues, the structures with and without bound substrate were compared.

Figure 5.14 shows an alignment of all five DHDPS-S48W structures. There was slight variation at Y107. This movement did appear to alter the position of the polar site of the residue; however, as the difference was only slight, it may not be significant. Binding of the substrates to DHDPS-S48W LPS and DHDSP-S48 LP did not appear to alter the position of K161. Therefore, the figure suggests that the tryptophan substitution does not interfere with the binding of the substrates or the catalytic site as a whole.

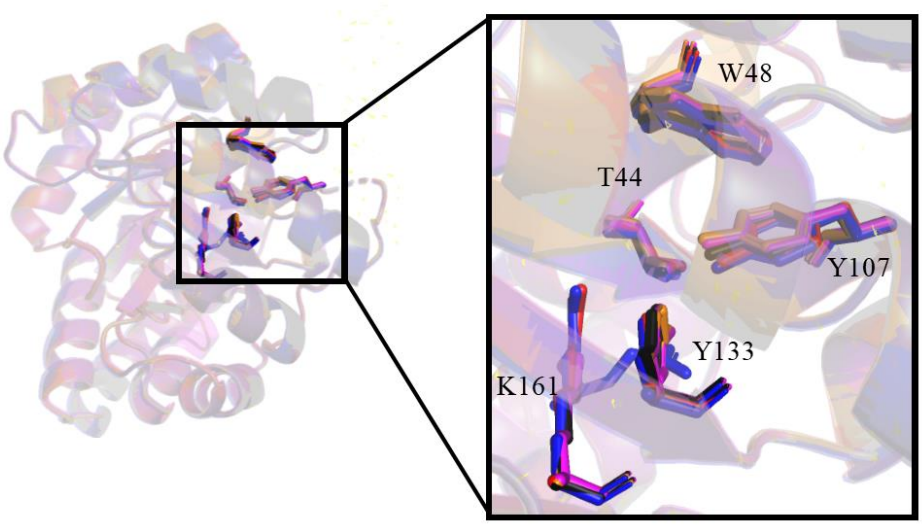

Figure 5.14: *Alignment of the monomers of all of the DHDPS-S48W structures. The catalytic site is highlighted. The structures are coloured as follows: DHDPS-S48W apo, black; DHDPS-S48W LP, red; DHDPS-S48W LPS, blue; DHDPS-S48W L, orange; DHDPS-S48W COCL, pink.*

These structures were then compared with all the DHDPS-WT structures. Figure 5.15 shows the alignment of all the structures, with the key residues of the catalytic site highlighted. There were very few differences between the residues, except for Y107 from DHDPS-WT L, which was slightly twisted. This agrees with the findings shown in Figure 5.12. This difference appears to be an anomaly, as it is not present in the other DHDPS-WT structures. Dobson *et al.*[1] noted that the binding of lysine may cause movement of Y106, altering the hydrophobic stacking and subsequently altering Y107. This may explain the twisting seen here, as none of the DHDPS-S48W structures bind lysine. This movement was noted in Chapter Four but was not as significant. Despite the twisting, the polar point sits in a similar position to the other structures.

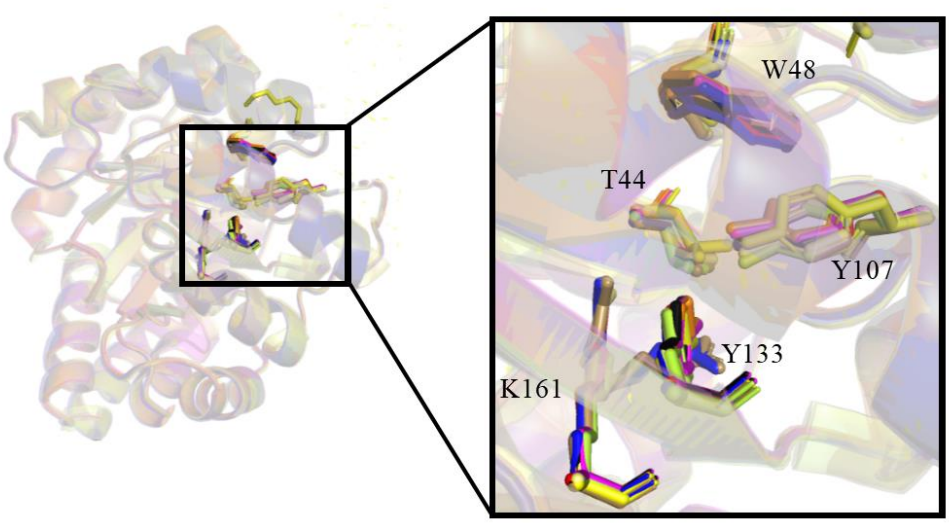

Figure 5.15: *Alignment of the monomers of all DHDPS-S48W and DHDPS-WT structures. The catalytic site is highlighted. The structures are coloured as follows: DHDPS-S48W apo, black; DHDPS-S48W LP, red; DHDPS-S48W LPS, blue; DHDPS-S48W L, orange; DHDPS-S48W COCL, pink; DHDPS-WT P, light yellow; DHDPS-WT PS, brown; DHDPS-WT, green-yellow; DHDPS-WT L, yellow.*

5.3.3 Summary

It does not appear that the catalytic site is altered by the inclusion of the tryptophan substitution at residue 48. Figures 4.5 and 4.6 show that the substrates have no trouble binding to the catalytic site. There is also no evidence that the substitution interferes with the key residues in the catalytic site, or that it stops catalysis from taking place, as both pyruvate and succinic acid semialdehyde bind to K161.

5.4 The Allosteric Site

In Chapter Four, the allosteric site was analysed by looking at the residues in close enough proximity to form bonds with the lysine. The placement of these residues was then compared with that of residues in the structures that do not contain lysine in the allosteric site. All the tryptophan structures were originally designed to contain lysine (apart from DHDPS-S48W apo), as it was noted that the apoenzyme can distinguish the difference between +/− ligands. Furthermore, there were few differences between the phenylalanine structures with substrates (DHDPS-S48F P and DHDPS-S48F PS) and those that also contained lysine (DHDPS-S48F LP and DHDPS-S48F LPS). Therefore, it was determined there was no need for both when crystallising the DHDPS-S48W series. Unfortunately, there was no lysine in the allosteric site of any of the structures. The allosteric sites of the four structures meant to contain lysine are shown in Figure 5.16. Each structure shows H56 in the middle, which would usually sit above bound lysine. However, there is density below.

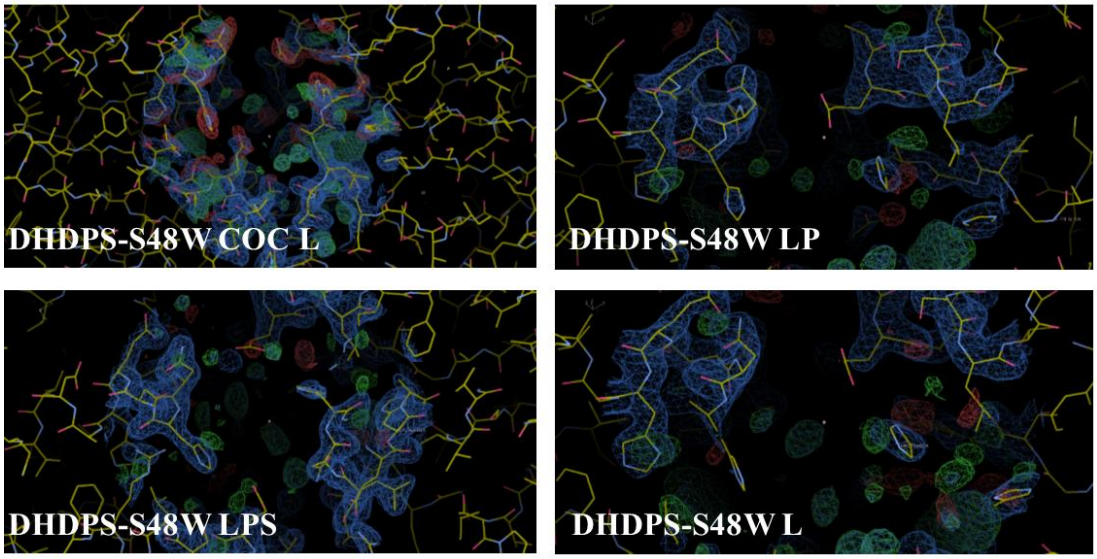

Figure 5.16: *The allosteric sites of DHDPS-S48W COCL, DHDPS-S48W LP, DHDPS-S48W LPS, and DHDPS-S48W L. The lack of density shows there is no lysine in the sites.*

The structure containing only bound lysine was generated three times to ensure there was no human error (a representative image is shown as the three replicates were almost identical). None of the structures showed densities in the allosteric site. As there was no lysine present when soaking the crystal (which is the conventional method[1, 8]), co-crystallisation with 20 mM of lysine in the drop was attempted. Two separate crystals derived from separate drops were diffracted, but no density was found in the allosteric site

of either protein (only one structure shown as they were identical). Therefore, we concluded that DHDPS-S48W cannot bind lysine. This will be discussed further in Chapter Six.

The allosteric sites of all the DHDPS-S48W structures meant to contain lysine are shown in Figure 5.17. One difference was observed in the E84 side chain, which was slightly offset.

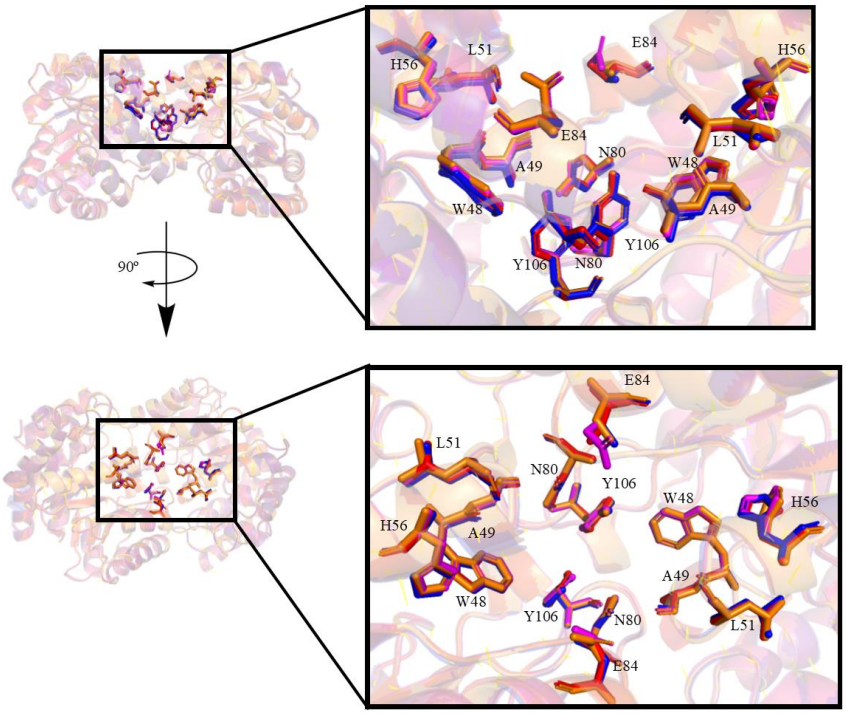

Figure 5.17: *Alignment of the dimers of DHDPS-S48W LP, DHDPS-S48W LPS, DHDPS-S48W L, and DHDPS-S48W COCL. The allosteric site is highlighted. The top panel shows a side view of the dimer with chain A on the left, while the bottom panel shows the allosteric site from above with chain A on the left. The structures are coloured as follows: DHDPS-S48W LP, red; DHDPS-S48W LPS, blue; DHDPS-S48W L, orange; DHDPS-S48W COCL, pink.*

Comparison of the allosteric sites of these structures with those of the DHDPS-WT structures could help to determine why the allosteric sites of the DHDPS-S48W structures weren't capable of holding a lysine. The resulting alignment is shown in Figure 5.18. The results showed that the DHDPS-S48W structures that were exposed to lysine were more similar to the DHDPS-WT structure. The most obvious difference occurred at E84, which has its side chains pointing in different directions. The E84 side chains of all structures apart from DHDPS-WT L were directed upwards away from the dimer, while those of DHDPS-WT L were directed towards the dimer as if to bind lysine. The other main variation was in Y106 which, in DHDPS-WT L, held a different conformation than all other structures in the Figure. This movement may be due to the lysine binding to the allosteric site as predicted in Dobson *et al.*[1]. Very little variation was observed in the other residues.

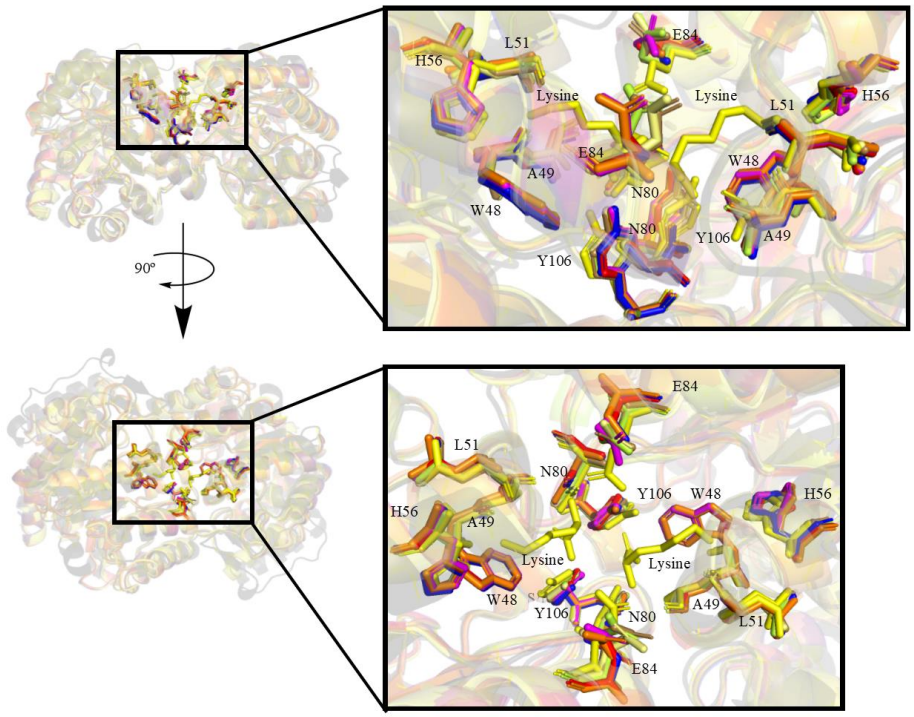

Figure 5.18: *Alignment of the dimers of all DHDPS-S48W and DHDPS-WT structures. The allosteric site is highlighted. The top panel shows a side view of the dimer with chain A on the left, while the bottom panel shows the allosteric site from above with chain A on the left. The structures are coloured as follows: DHDPS-S48W apo, black; DHDPS-S48W LP, red; DHDPS-S48W LPS, blue; DHDPS-S48W L, orange; DHDPS-S48W COCL, pink; DHDPS-WT P, light yellow; DHDPS-WT PS, brown; DHDPS-WT, green-yellow; DHDPS-WT L, yellow.*

5.5 Mapping the Water Channel

The substitution was introduced to block the water channel and observe whether this alters catalysis. Chapter Three showed that the substitution does alter catalysis, but it remained unclear as to whether the substitution sufficiently blocks the water channel. Figure 5.19 shows the water channel of chain B of all the DHDPS-S48W structures. The lysine of DHDPS-WT L is labelled to indicate the location of the allosteric site. The figure shows that the water channel is sufficiently blocked by the substitutions as there are very few water molecules in the channel. In addition, there does not appear to be any way for the water molecules on the top of the channel to transfer protons to those inside the channel. The water molecules do collect around the lysine binding site, which is represented by the DHDPS-WT L lysine.

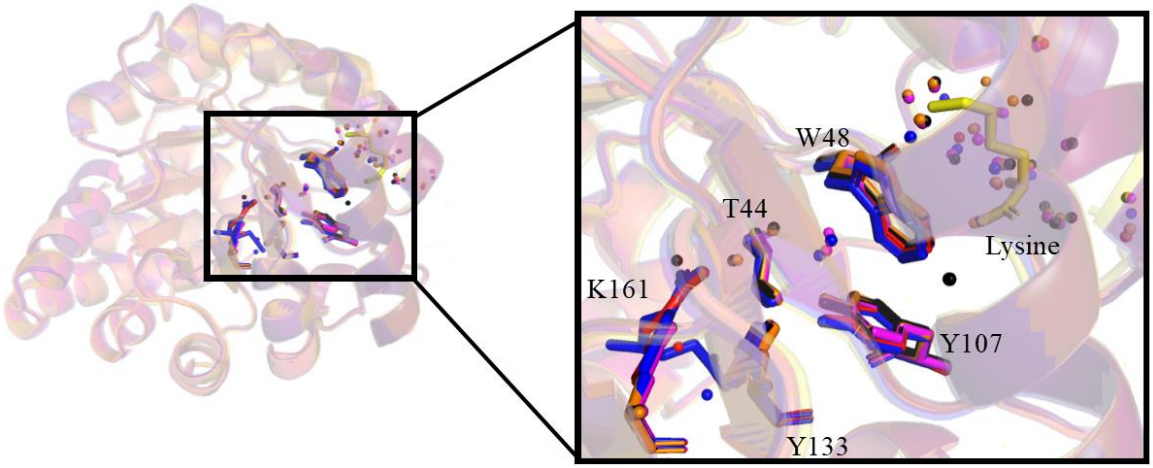

Figure 5.19: *Alignment of the monomers of all of the DHDPS-S48W structures. The key residues within the catalytic site are highlighted. The lysine from DHDPS-WT L is labelled in the lysine binding site to indicate the location of the allosteric site (yellow). DHDPS-S48W COCL is in pink, DHDPS-S84W LP is in red, DHDPS-S84W LPS is in blue, DHDPS-S84W L is in orange, and DHDPS-S84W apo is in black.*

Figure 5.19 showed that the water molecules were located in similar positions for all of the structures, but that few water molecules were located near the tryptophan. Comparing the water channels of these structures with those of the DHDPS-WT structures would show if the tryptophan interferes with the water channel.

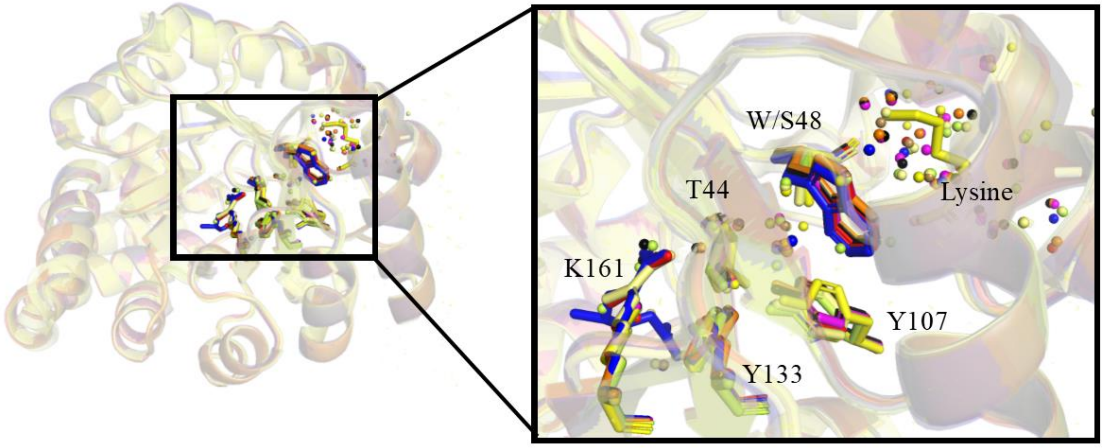

Figure 5.20: *Alignment of the monomers of all of the DHDPS-S48W structures and all the DHDPS WT structures. The key residues within the catalytic site are highlighted. DHDPS-S48W COCL is in pink, DHDPS-S84W LP is in red, DHDPS-S84W LPS is in blue, DHDPS-S84W L is in orange, and DHDPS-S84W apo is in black. DHDPS-WT is yellow-green, DHDPS-WT L is yellow, DHDPS-WT P is bright yellow, and DHDPS-WT PS is brown.*

Figure 5.20 shows an alignment of the water channels of all the DHDPS-S48W and DHDPS-WT structures. The lysine in the DHDPS-WT L structure shows the position of the allosteric site. The figure shows an abundance of water molecules in the DHDPS-WT structures in proximity to the location of the substitution. In contrast, the figure shows that the tryptophan substitution interferes with the channel, blocking the entry of water molecules into the channel.

5.5 Summary

The tryptophan substitution structures are similar to the wild-type enzyme, only differing at the allosteric site at residue E84, and Y106, and at the catalytic site at residue Y107. The movement of E84 may interfere with lysine binding in the allosteric site. Interestingly, the difference at Y107 only appears to be significant in DHDPS-WT, and is more likely due to the twisting of Y106 as a result of lysine binding, as was hypothesised by Dobson *et al.*[1]. Despite this, the catalytic site does bind to both pyruvate and succinic acid semialdehyde.

The analysis of these mutated structures provides evidence that the tryptophan mutation does not interfere with catalysis, but may interfere with allostery as the allosteric inhibitor, lysine, cannot bind.

The tryptophan substitution blocks the water channel by lying flat on the channel. This was the main goal of the substitution, and this series of structures confirms that the tryptophan substitution is better able to block the water channel than the phenylalanine substitution examined in Chapter 4.

5.6 References

1. Dobson, R. C., Griffin, M. D., Jameson, G. B., and Gerrard, J. A. (2005) The crystal structures of native and (S)-lysine-bound dihydrodipicolinate synthase from *Escherichia coli* with improved resolution show new features of biological significance, *Acta Crystallographica Section D: Biological Crystallography* ***61***, 1116-1124.

2. Devenish, S. R. A., Gerrard, J. A., Jameson, G. B., and Dobson, R. C. J. (2008) The high-resolution structure of dihydrodipicolinate synthase from *Escherichia coli* bound to its first substrate, pyruvate, *Acta Crystallographica Section F-Structural Biology and Crystallization Communications* ***64***, 1092-1095.

3. Boughton, B. A., Dobson, R. C., and Hutton, C. A. (2012) The crystal structure of dihydrodipicolinate synthase from *Escherichia coli* with bound pyruvate and succinic acid semialdehyde: unambiguous resolution of the stereochemistry of the condensation product, *Proteins: Structure, Function, and Bioinformatics* ***80***, 2117-2122.

4. Blickling, S., Renner, C., Laber, B., Pohlenz, H.-D., Holak, T. A., and Huber, R. (1997) Reaction mechanism of *Escherichia coli* dihydrodipicolinate synthase investigated by X-ray crystallography and NMR spectroscopy, *Biochemistry* ***36***, 24-33.

5. Dobson, R. C., Valegård, K., and Gerrard, J. A. (2004) The crystal structure of three site-directed mutants of *Escherichia coli* dihydrodipicolinate synthase: further evidence for a catalytic triad, *Journal of molecular biology* ***338***, 329-339.

6. Mirwaldt, C., Korndorfer, I., and Huber, R. (1995) The Crystal Structure of Dihydrodipicolinate Synthase from *Escherichia coli* at 2.5 Å Resolution, *Journal of molecular biology* ***246***, 227-239.

7. da Costa, T. P. S., Muscroft-Taylor, A. C., Dobson, R. C., Devenish, S. R., Jameson, G. B., and Gerrard, J. A. (2010) How essential is the 'essential'active-site lysine in dihydrodipicolinate synthase?, *Biochimie* ***92***, 837-845.

8. Laber, B., Gomisruth, F. X., Romao, M. J., and Huber, R. (1992) *Escherichia-coli* dihydrodipicolinate synthase - identification of the active-site and crystallization, *Biochemical Journal* ***288***, 691-695.

Chapter Six: Discussion and Conclusions

6.1 Introduction

In the previous four chapters the results of the study have been presented. This chapter will explore the results in the context of this hypothetical mechanism of allostery. This study hypothesises that the water channel that bridges the allosteric site down and the catalytic site, is essential part of the allosteric mechanism. The water channel is thought to transfer a proton from bulk solvent to the catalytic site for pyruvate to form a schiff base. To test this, two substituted enzymes were created that each contained a point mutation at the 48 position. One contains a phenylalanine substitution and the second has a tryptophan substitution. The phenylalanine and tryptophan were placed at the 48 position which positions the overly bulky side chains of these two amino acids in the water channel. This was to mimic the way the lysine blocks the channel in the hypothesis. These were crystallised to ensure the mutations were not interfering with the catalytic or allosteric site sterically, they would just simply be blocking the channel (Chapters Four and Five). Kinetics studies were done to observe whether the mutants' activity was less than the wild type (Chapter Three).

6.2 Purification and Mass Spectrometry

Chapter two was dedicated to recognising that the enzyme had been purified and that what was purified was indeed the mutated enzyme. The purification gels in chapter two gave evidence that a protein around 30,000 Da was purified. This is consistent with DHDPS. To further back up this mass spectrometry was conducted. The mass spectrometry results are consistent with the phenylalanine and tryptophan substitutions. This was enough evidence to move on with the kinetic and crystallographic studies.

6.3 Kinetics

The kinetic studies were to show how active DHDPS-S48F and DHDPS-S48W were, and how that activity compared to DHDPS-WT with and without the lysine. Kinetic studies have been conducted on point substituted DHDPS before, these studies protocols were used here[1, 2]. It was clear after the DHDPS-S48W activity tests were done that it was far less active then both DHDPS-WT and DHDPS-S48F. Figure 6.1 shows the kinetic data fitted to the Michaells-Menten model. DHDPS-WT is much more active than the substituted enzymes.

The data supports the hypothesis. Both DHDPS-S48F and DHDPS-S48W are less active then the DHDPS-WT. DHDPS-S48F with lysine has a similar rate to that of DHDPS-WT with lysine just slightly more active. DHDPS-S48W with and without lysine has the same activity. This suggests that the lysine does not bind to this mutant at this concentration of lysine, or that lysine has no effect.

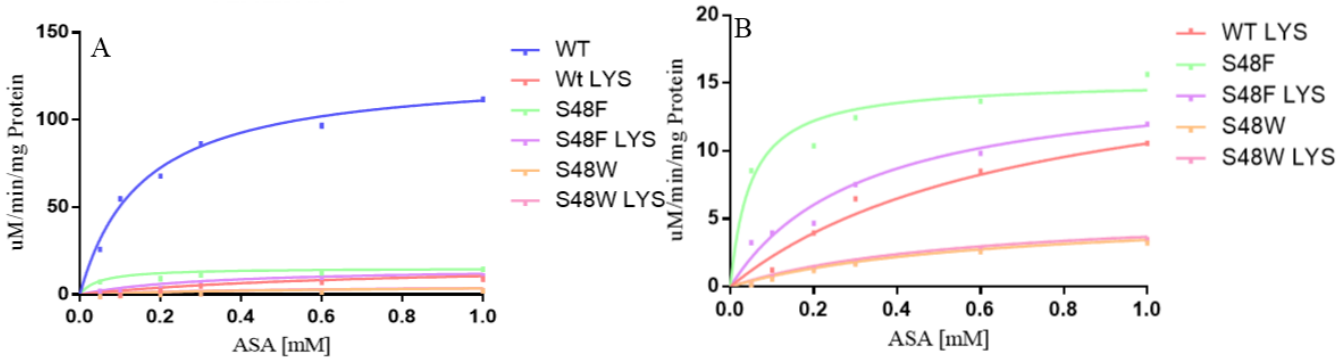

Figure 6.1: *Kinetics graphs of DHDPS-WT, DHDPS-S48F, and DHDPS-S48W with and without lysine. Each data set is coloured, with a key on the right of each graph. Graph B does not include the DHDPS-WT data.*

Each of the enzymes carrying the substitution has less activity then DHDPS-WT. However, their activity is similar to DHDPS-WT with lysine; this is consistent with the hypothesis, as the substitutions are to mimic lysine binding. The data here also suggests that DHDPS-S48W does not bind lysine, since lysine had no effect on rate. Alternatively, it binds lysine, but binding has no effect on catalysis. The data shows DHDPS-S48F has a slightly higher rate with lysine then DHDPS-WT with lysine. Therefore, it may not bind to lysine as readily as DHDPS-WT.

An activity assay with saturating substrate concentration but altering lysine concentration may show lysine binds to DHDPS-S48W, in higher lysine concentration then 2.5 mM.

Unfortunately, due to time constraints and depleting amounts of *S*-ASA this was unable to be done for this study.

The kinetic data does support the hypotheses, but it also raises questions that the crystal structures need to answer. Questions such as why do the substituted enzymes not bind lysine as well? and does the substitution at the 48 position interfere with catalysis in some other fashion?

6.4 Crystal structures

Chapter Four analysed the six structures containing phenylalanine, while Chapter Three analysed the five structures containing tryptophan. These included structures with ligands bound, including the substrates and lysine. The catalytic site and the allosteric site were analysed along with the general area of the water channel. The substitution site was also analysed.

6.4.1 Features of the Structures

The substitutions did not seem to create any major change in the over all structure. The quaternary and tertiary structure of the substituted enzymes are unchanged. The Ramachandran scores of the structures were all in allowed regions apart from Y107 which is commonly found outside allowed regions for other DHDPS-WT structures as well[3]. The substitutions did not seem to interfere with the over all structure of the enzymes.

It was noted in Chapter Four that the phenylalanine substitution did not cover the water channel as well as the tryptophan substitution when substrates or lysine were present. The phenylalanine ring sits in the water channel in a way that makes the hydrophobic ring less of a steric hindrance than the tryptophan ring which sits flat. This is shown in Figure 6.2 where the majority of the phenylalanine structures do not have the ring flat on the water channel potentially allowing protons to pass.

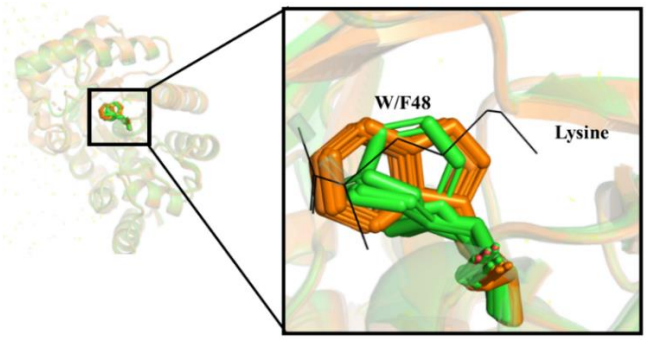

Figure 6.2: *All of the DHDPS-S48W and DHDPS-S48F structures aligned*

The B factor for position 48 of both DHDPS-S48F and DHDPS-S48W is higher relative to the rest of the structure, indicating there is more movement in the side chain (Figure 6.3). However, there are favourable regions for these side chains to sit in. Clearly the position of the phenylalanine in all the structures bar one, is a very favourable position. All the tryptophan structures have the side chain in one position, suggesting that that position is common and therefore more favourable. It is important to remember that the side chains of the amino acids in proteins are dynamic. An enzyme is not static as the crystal structures depict

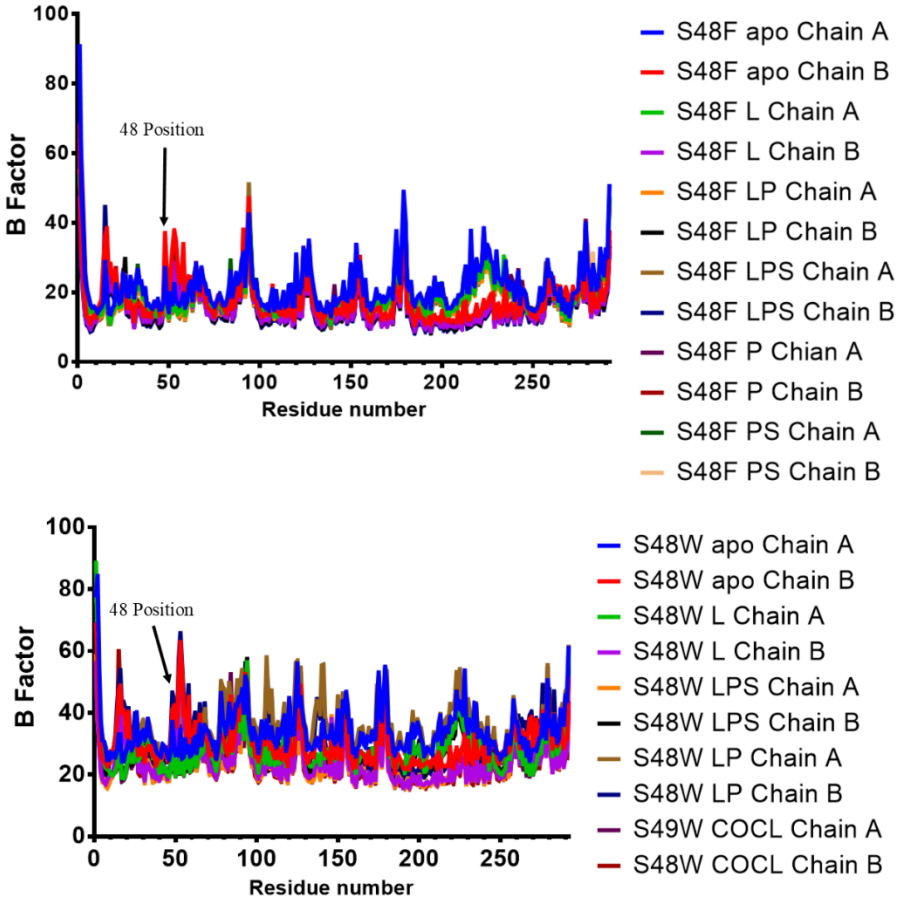

Figure 6.3: *The B factor graphs of DHDPS-S48Fstructures (top) and DHDPS-S48W structures (bottom).*

6.4.2 Catalytic Site

The catalytic site of each of the mutations was analysed by looking at the key residues. This includes the catalytic triad, T44, Y107, and Y133, and K161. These residues are responsible for the chemistry in DHDPS, so their movement would alter the chemistry of the enzyme.

For each of the substituted enzymes there where structures that had ligands bound. These were studied to see whether the substrates would bind, and if the catalytic site still allowed enough room for them to bind. The point of the substitutions is to block the water channel but there was a chance that they may also hinder the binding of the substrates in the catalytic site. This was not an issue as all the substrates did bind. Both the substitutions had both substrates bind to K161 in their catalytic site. This suggests that the substitutions are not sterically affecting substrate binding. The position of the substrates on the substituted enzymes is compared to the structure solved by Boughton *et al*[4] which also contains pyruvate and succinic semi-aldehyde bound to lys161. When all three structures are compared substrates have the same conformation. This can been seen in Figure 6.4 where the substituted structures are aligned with Boughton *et al*[4] which shows only a slight variation in succinic semi-aldehyde. This variation may be due to the higher resolution of their structure. Overall the substitutions in the water channel do not interfere with the binding of the substrates. Therefore, the catalytic site should conduct its self as normal even with the substitutions at the 48 position.

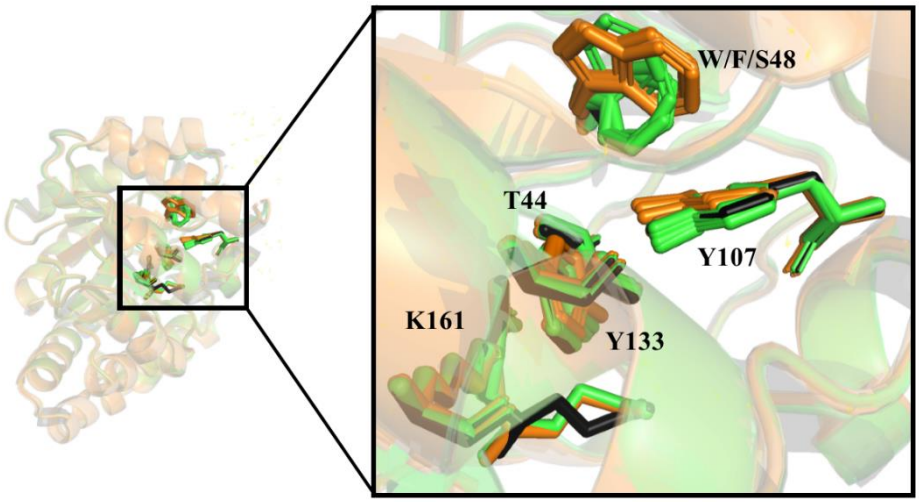

Figure 6.4: *The catalytic site of all the structures with the DHDPS-S48F in green, DHDPS-S48W in orange and Boughton et al*[4] *structure in black.*

As the mutations are mimicking the closing of the water channel by lysine, and the hypothesis states that the lysine blocks proton exchange for schiff base formation. Succinic acid semialdehyde binding proves that the schiff base is forming. This goes against the hypothesis as the schiff base is being allowed to form. However, as stated in Chapter One, when lysine is bound to the allosteric site the rate of reaction is only decreased and not stopped completely. The Catalytic site is open (Figure 6.5). This allows substrates to entre

and could also allow protons in to the catalytic site when the water channel is blocked. This would explain how the schiff base can still form when the lysine is bound, and the mutation is in the water channel.

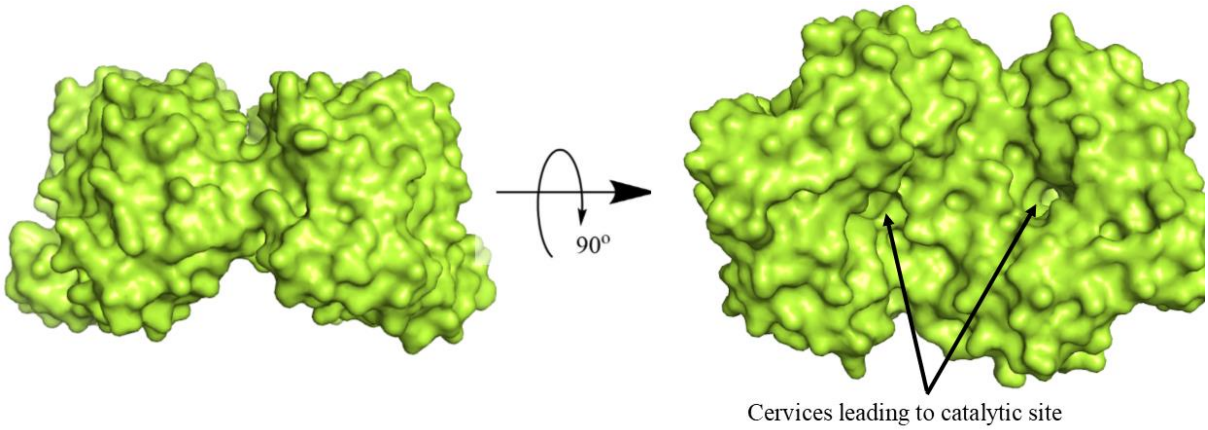

Figure 6.5: *The dimer of DHDPS-WT rotated 90º to show the bottom where the crevices that leads to the catalytic site are.*

The catalytic site of the substituted structures suggests the substitutions at the 48 position do not interfere with the chemistry of the catalytic site. The addition of the succinic acid semialdehyde confirms the schiff base is forming. This confirms that protons are entering the catalytic site therefore the addition of the substations is not stopping catalysis. This mimics the natural state, as when lysine binds to the allosteric site catalysis doesn't stop. This is likely due to the catalytic site being open which would allow protons to enter the catalytic site and allow the schiff base to be formed.

6.4.3 Allosteric Site

The allosteric site is defined by the lysine that sits inside of it. The residues that could hold the lysine are identified as E84, H56, L51, N80, A49, F/W/S48, and Y106

The tryptophan structures do not have lysine in the allosteric site, despite lysine being added to the crystal. This was done several times with two different techniques, but nether technique gave a lysine bound structure. For this reason, it is difficult to compare the tryptophan allosteric site with DHDPS-WT and the DHDPS-S48F structures allosteric site, as the residues may not alter as they would if lysine was bound.

Blinking *et al*[5, 6] hypothesised that E84 binds to lysine when it is in the allosteric site. The data here supports that. There was a difference in the E84 of DHDPS-WT and DHDPS-S48F which had a different conformation of the first carbon in the side chain, but the polar carboxyl group of each residue sat in a similar position. The movement of one carbon is to be expected, as the enzymes are dynamic. The DHDPS-S48W E84 side chain is positioned upwards away from the allosteric site (see Figure 6.6). This is most likely due to there being no lysine in the allosteric site. DHDPS-WT from Dobson *et al.*[3] has the same positioning in there E84 which suggests the side chain moves upon lysine binding. Therefore, it is unlikely this is a result of the substitution.

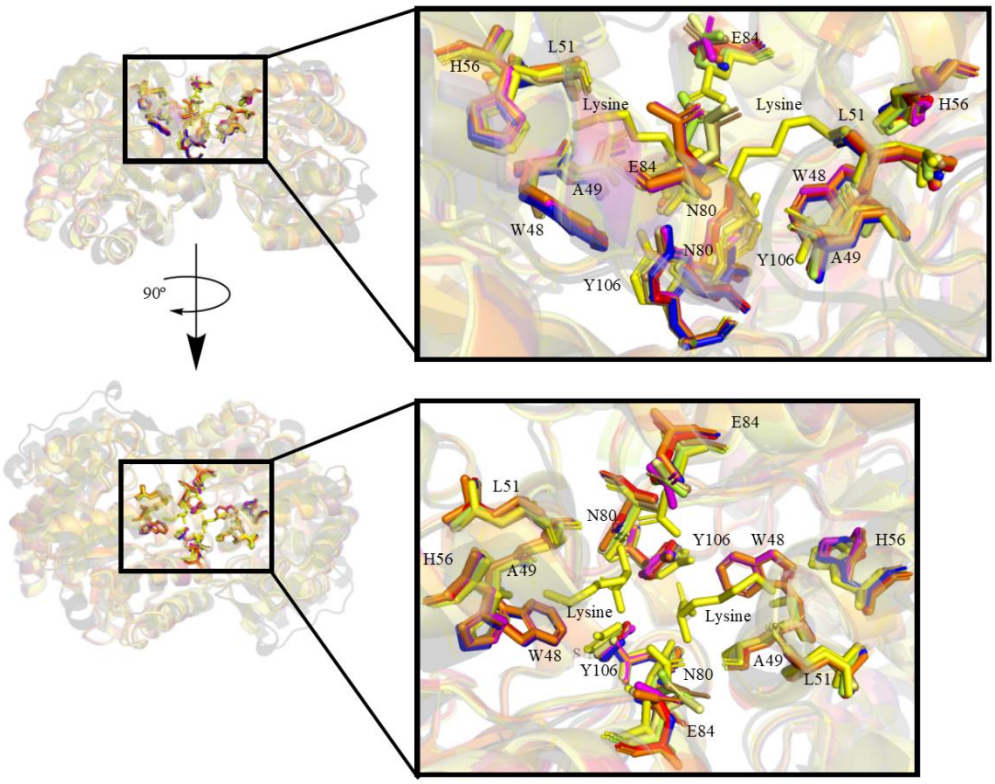

Figure 6.6: *All DHDPS-S48W and DHDPS-WT structures are aligned, and the allosteric site is highlighted from the dimer. The top show the side view of the dimer with chain A on the left, the bottom of the figure is the allosteric site from above with chain A still on the left. The structures are coloured as follows: DHDPS-S48W apo in black, DHDPS-S48W LP in red, DHDPS-S48W LPS in blue, DHDPS-S48W L in orange, and DHDPS-S48W COCL in pink, DHDPS-WT P in light yellow, and DHDPS-WT PS in brown, DHDPS-WT from in green-yellow, and DHDPS-WT L in yellow.*

DHDPS-S48F, L, LPS, and LP allosteric site all align well with the DHDPS-WT L from Dobson *et al.*[3] (Figure 6.7). Dobson *et al.*[3] noted that when lysine binds to the allosteric site it alters Y107 slightly, which in turn alters Y106. All the DHDPS-S48F structures contain lysine see this, although the Y107 are not as twisted as in DHDPS-WT L. The large side chain of tryptophan could be interfering with the movement of Y107 as it looks to be quite dynamic from the B factor scores. This could stop Y106 from moving and, in turn, affect lysine binding to the allosteric site. This could also be happening in the DHDPS-S48F structures but on a smaller scaled as the side chain is not as large as tryptophan's the side chain.

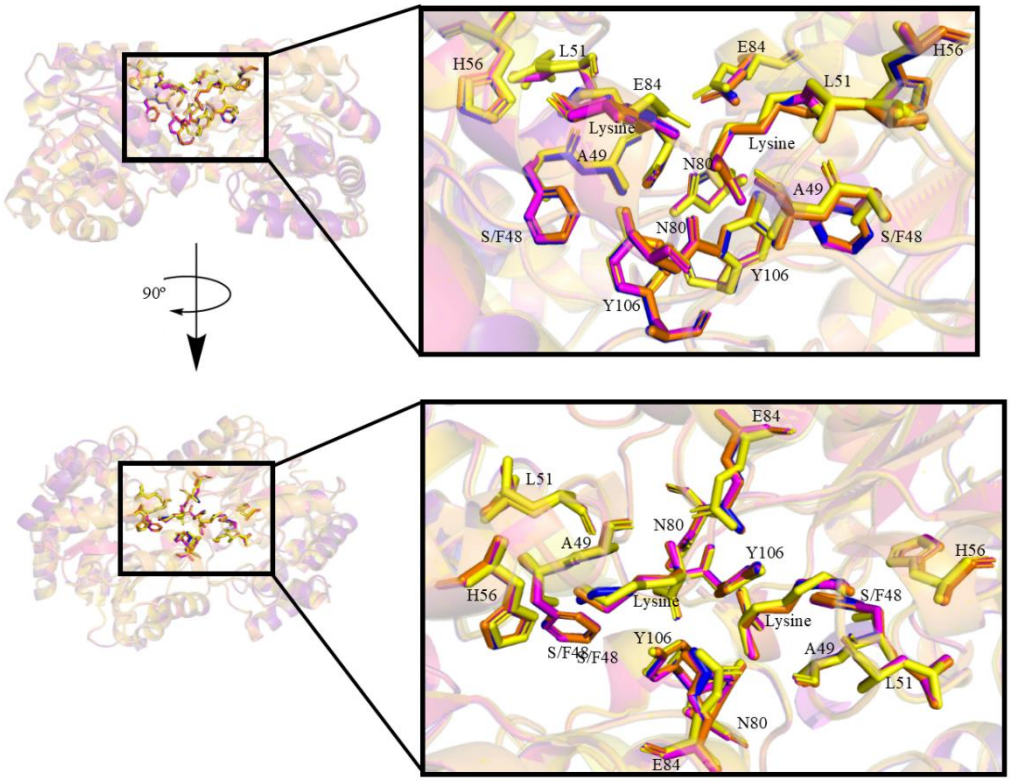

Figure 6.7: *All the DHDPS-S48F substitutions containing lysine in the allosteric site and DHDPS-WT L aligned with the key residues of the allosteric site highlighted from the dimer. DHDPS-WT L is in yellow, DHDPS-S84F LP is in pink, DHDPS-S84F LPS is in blue, and DHDPS-S84F L is orange.*

Dobson *et al*[3] also showed that the main chain oxygen on the S48 bound the lysine in the allosteric site. Although in these structures the 48 position has the substitution, the main chain can still interact. The Nε on the DHDPS-S48F lysine can interact with the F48 main chain O atom.

6.4.4 The Water Channel

The water channels of the substituted enzymes tell two different stories. As stated previously the phenylalanine substitution in the majority of the DHDPS-S48F structures were not in an optimal position to interfere with the water channel. This is consistent with the finding that the DHDPS-S48F enzyme is more active than the DHDPS-S48W due to there still being proton transfer within the water channel. This is supported by Figure 6.8, The dotted lines follow the green waters of DHDPS-S48F which show a clear path from bulk solvent into the catalytic triad. This information explains why DHDPS-S48F is more active then DHDPS-S48W. This Figure shows that the DHDPS-S48W substitution blocks the water channel best, DHDPS-S48F also blocks the water channel well, when the substitution is in an optimal position (such as DHDPS-S48 apo's is).

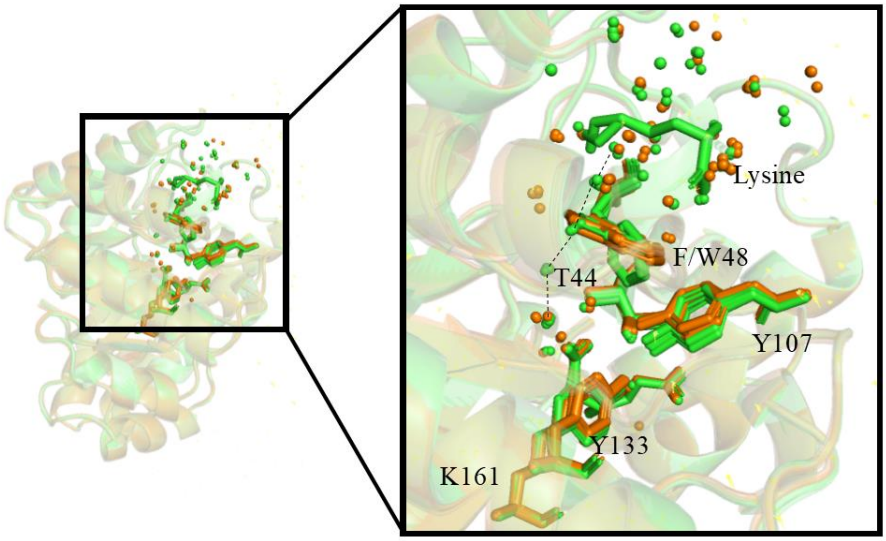

Figure 6.8: *The waters channel of all DHDPS-S48F structures (green), and all DHDPS-S48W (orange) structures aligned. The dotted lines show a path of green waters which pass the substitution, making them able to chaperone a proton.*

6.5 Conclusions

The hypothesis of this study was that the water channel that runs between the active site and the allosteric site of DHDPS plays a key role in the allosteric mechanism. The data in this study supports this hypothesis. The kinetic data shows both the substituted enzymes, DHDPS-S48F and DHDPS-S48W, have less activity than the native (DHDPS-WT). The crystal structures show the substitutions do not seem to interfere with the key residues of the enzymes. As DHDPS-S48W does not bind lysine it may not be as reliable as DHDPS-S48F, as it may interfere with the allosteric site residue Y106 and the catalytic site residue Y107. But there is little evidence of DHDPS-S48F interfering with the key residues apart

from the movement of the substitution itself. The DSF data of DHDPS-S48F also agrees with DHDPS-WT which shows how little the phenylalanine in DHDPS-S48F affects the enzyme as a whole.

More research can be done to further support this hypothesis, such as the depleting lysine kinetic assays, and further analysis of DSF, but what evidence has been compiled supports the hypotheses. Mapping the uncharted water channel of DHDPS has shown that it likely plays a key role in allostery.

6.7 References

1. Dobson, R. C., Valegård, K., and Gerrard, J. A. (2004) The crystal structure of three site-directed mutants of *Escherichia coli* dihydrodipicolinate synthase: further evidence for a catalytic triad, *Journal of molecular biology* ***338***, 329-339.

2. da Costa, T. P. S., Muscroft-Taylor, A. C., Dobson, R. C., Devenish, S. R., Jameson, G. B., and Gerrard, J. A. (2010) How essential is the 'essential'active-site lysine in dihydrodipicolinate synthase?, *Biochimie* ***92***, 837-845.

3. Dobson, R. C., Griffin, M. D., Jameson, G. B., and Gerrard, J. A. (2005) The crystal structures of native and (S)-lysine-bound dihydrodipicolinate synthase from *Escherichia coli* with improved resolution show new features of biological significance, *Acta Crystallographica Section D: Biological Crystallography* ***61***, 1116-1124.

4. Boughton, B. A., Dobson, R. C., and Hutton, C. A. (2012) The crystal structure of dihydrodipicolinate synthase from *Escherichia coli* with bound pyruvate and succinic acid semialdehyde: unambiguous resolution of the stereochemistry of the condensation product, *Proteins: Structure, Function, and Bioinformatics* ***80***, 2117-2122.

5. Blickling, S., Renner, C., Laber, B., Pohlenz, H.-D., Holak, T. A., and Huber, R. (1997) Reaction mechanism of *Escherichia coli* dihydrodipicolinate synthase investigated by X-ray crystallography and NMR spectroscopy, *Biochemistry* ***36***, 24-33.

6. Blickling, S., and Knablein, J. (1997) Feedback inhibition of dihydrodipicolinate synthase enzymes by L-lysine, *Biological Chemistry* ***378***, 207-210.

7. Niesen, F. H., Berglund, H., and Vedadi, M. (2007) The use of differential scanning fluorimetry to detect ligand interactions that promote protein stability, *Nature protocols* ***2***, 2212.

8. Mirwaldt, C., Korndorfer, I., and Huber, R. (1995) The Crystal Structure of Dihydrodipicolinate Synthase from *Escherichia coli* at 2.5 Å Resolution, *Journal of molecular biology* ***246***, 227-239.

9. Domigan, L. J., Scally, S. W., Fogg, M. J., Hutton, C. A., Perugini, M. A., Dobson, R. C. J., Muscroft-Taylor, A. C., Gerrard, J. A., and Devenish, S. R. A. (2009) Characterisation of dihydrodipicolinate synthase (DHDPS) from *Bacillus anthracis*, *Biochimica et Biophysica Acta (BBA) - Proteins and Proteomics* ***1794***, 1510-1516.

Chapter Seven: Experimental

7.1 Molecular biology and microbiology techniques

7.1.1 Strains and plasmids

Escherichia coli AT997 (*dapA*$^{-}$) was used for the expression of both DHDPS-S48F and DHDPS-S48W, while *E. coli* XL 1-Blue (*dapA*$^{+}$) was used for expression and purification of DHDPS-WT. BL21 (DE3) *E. coli* were used for the expression of DHDPR. All of the *E. coli* strains used in this study, along with their corresponding antibiotic resistance profiles, are outlined in Table 7.1.

Table 7.1 *Plasmids used in this study*

***E. coli* Strain**	**Antibiotic Resistance**
AT997 pJG001-S48W	Ampicillin and tetracycline
AT997 pJG001-S48F	Ampicillin and tetracycline
XL 1-Blue pJG001	Ampicillin
BL21 (DE3) pET151 Eco-DHDPR	Ampicillin

7.1.2 Bacterial cultures

All bacteria were cultured under sterile conditions. Agar was prepared using distilled water and was sterilised via autoclaving. Plates were poured next to a flame in a fume hood that had been sterilised with ethanol. When necessary, antibiotics were added to cooled, sterilised agar immediately prior to pouring. To confirm the sterility of the environment, control plates which contained no bacteria were added to the incubator to confirm there was no contamination.

7.1.3 Media

Luria agar (100 mL):

- 1.5 g of agar
- 2.5 g of Luria broth base
- Distilled water (to 100 mL)

All constituents were added to a conical flask, mixed, and then immediately sterilised by autoclave (provided via the School of Biology, University of Canterbury).

Luria broth (LB) (100 mL):

- 2.5 g of Luria broth base
- Distilled water (to 100 mL)

All constituents were added to a conical flask, mixed, and then immediately sterilised by autoclave.

7.1.4 Preparation of glycerol stocks

Bacterial cells were cultured on an agar plate supplemented with the appropriate antibiotic. A single colony was used to inoculate 10 mL of liquid LB medium containing the appropriate antibiotic, and the culture was incubated overnight at 37°C. Equal volumes (usually 500 µL) of sterilised 50% (v/v) glycerol and bacterial culture were then mixed in a 1.5-mL tube and immediately frozen in liquid nitrogen. All glycerol stocks were stored at −80°C.

7.1.5 Plasmid purification

Plasmids were purified using a GenElute Plasmid Miniprep Kit (Sigma-Aldrich), according to the manufacturer's instructions.

7.1.6 Preparation of competent cells

Frozen *E. coli* AT997 cells were streaked onto an LB agar plate containing no antibiotics, and incubated at 37°C for ~16 h. A single colony was then inoculated into 10 mL of liquid LB medium and incubated overnight at 37°C. The 10-mL culture was used to inoculate a 100-mL volume of fresh LB medium, which was cultured at 37°C to an optical density at 600 nm of 0.6. The culture was then immediately stored on ice, and the cells were transferred to 50-mL centrifuge tubes and centrifuged at 3000 rpm for 5 min at 4°C. The supernatant was discarded, and the cell pellet was resuspended in 30 mL of ice-cold 0.1 M $CaCl_2$. The resuspended cells were incubated on ice for 30 min and then centrifuged at 3000 rpm for 5 min at 4°C. The supernatant was discarded, and the cell pellet was resuspended in 2 mL of ice-cold 0.1 M $CaCl_2$. Glycerol (50% v/v) was then added to the resuspended cell pellet to a concentration of 15% v/v, and the resulting competent cells were stored in 100-µL aliquots at −80°C[1].

7.1.7 Transformation of competent cells

Competent cells were thawed and stored on ice prior to use. A 5-μL volume of purified pJG001-S48W plasmid DNA was added to the cells, which were incubated on ice for a further 30 min. The cells were heat-shocked at 42°C for 45 s and then immediately placed on ice. A 950-μL volume of liquid LB medium was added to the cells, which were then incubated at 37°C for approximately 1 h with vigorous shaking. The cells were then streaked onto LB agar plates containing appropriate antibiotics and incubated overnight at 37°C[2].

7.2 Biochemical Techniques

7.2.1 Buffers

Buffers used to purify DHDPS and DHDPR, for enzyme kinetics assays and for protein crystallography are outlined in Table 7.2. Buffers were prepared using milli-Q water, and the pH of each buffer was measured using a standard pH meter with a Russell combination electrode. All buffers were filter-sterilised prior to use.

Table 7.2: *Buffers used in this study.*

BUFFER	INGREDIENTS	USE
BUFFER A	20 mM Tris (pH 8, adjusted using HCl)	All steps in the purification of DHDPS; size exclusion chromatography during DHDPR purification
BUFFER B	20 mM Tris 1 M NaCl (pH 8, adjusted using HCl)	Anionic chromatography during DHDPS purification
BUFFER C	20 mM Tris 0.5 M ammonium sulphate (pH 8, adjusted using HCl)	Hydrophobic chromatography during DHDPS purification
LOW IMIDAZOLE	50 mM NaH_2PO_4 50 mM imidazole 300 mM NaCl (pH 8, adjusted using NaOH)	Affinity chromatography during DHDPR purification
HIGH IMIDAZOLE	50 mM NaH_2PO_4 500 mM imidazole 300 mM NaCl (pH 8, adjusted using NaOH)	Affinity chromatography during DHDPR purification
HEPES BUFFER	200 mM HEPES (pH 8)	Enzyme kinetics assays
CRYSTALLISATION BUFFER	2 M K_2HPO_4 (pH 9.8, 9.9 or 10, adjusted using KCl)	Crystallography

7.2.2 Preparation of crude DHDPS and DHDPR protein extracts

The only difference between the DHDPS and DHDPR cultures is the DHDPR cultures were induced with IPTG when they reached an OD_{600} of 0.6. DHDPS was not induced as DHDPS is constitutively expressed. Bacterial cultures were incubated overnight and then harvested via centrifugation at 4000 rpm for 10 min at 4°C. The supernatant was discarded, and the cell pellet was resuspended in Buffer A. The cells were then sonicated on ice in three 10-min sessions, with a cool down period of 10 min between each session. Fresh ice was added to the ice bath prior to each sonication session. The sonicated cells were then centrifuged at 4000 rpm for 20 min at 4°C. This protocol was adapted from da Costa *et al.*[3]

7.2.3 Purification of DHDPS

The technique used for purifying DHDPS was modified from the method described by Mirwaldt *et al.*[4], which had been adapted from Lamber *et al.*[5].

7.2.4.1 Heat shock

Crude protein extract was aliquoted into 1.5-mL Eppendorf tubes, incubated at 70°C for 2 min, and then immediately put back on ice. Samples were then centrifuged at 14000 rpm for 10 min at 4°C and the supernatants were collected for further processing.

7.2.4.2 Anion exchange chromatography

The pooled aliquots from the heat shock step were loaded onto a Q-Sepharose column that has been pre-equilibrated with three bed volumes of Buffer A. Another three bed volumes of Buffer A were then run through the column. Buffer A containing 1 M NaCl was then added at a gradient increasing to 100% NaCl over 1 h to elute the protein, and the resulting fractions were examined via sodium dodecyl sulphate polyacrylamide gel electrophoresis (SDS-PAGE) to determine which fraction contained the enzyme.

7.2.4.3 Hydrophobic interaction chromatography

Ammonium sulphate was added to the pooled fractions at a concentration of 0.5 M, and the resulting solution was loaded onto a phenyl-Sepharose column that had been pre-equilibrated with three bed volumes of buffer C. The column was then washed with three bed volumes of buffer C. To elute the enzyme, Buffer A was added at a gradient increasing to 100% over 1 h. Fractions were then collected and examined by SDS-PAGE.

7.2.4.4 Size exclusion chromatography

The pooled fractions from the hydrophobic interaction chromatography were loaded onto a HiLoad Superdex 200 PG column pre-equilibrated with three bed volumes of Buffer A. The column was run for one column volume. Fractions were then examined by SDS-PAGE to determine in which fraction the enzyme eluted.

7.2.4 Purification of DHDPR

DHDPR was purified using a protocol described by Kefala *et al.*[6], which included affinity chromatography.

7.2.5.1 Nickel affinity chromatography

Crude protein extract was loaded onto a HisTrap FF column equilibrated with Low Imidazole Buffer. Once the flow through had run though and the UV line had plateaued,

High Imidazole Buffer was added for 10 min to elute the enzyme. Fractions were then analysed by SDS-PAGE to determine the fraction in which the enzyme eluted .

7.2.5.2 Buffer exchange
Selected fractions from HisTrap chromatography were then run through a HiPrep 26/10 Desalting Column to exchange the protein from High Imidazole Buffer into Buffer A. Alternatively, dialysis was used to desalt the protein following elution from the HisTrap column. The eluted protein was loaded onto a semi-permeable membrane which was then incubated in 4 L of Buffer A with constant agitation.

7.2.5.3 Size exclusion chromatography
Protein from either column-based buffer exchange or dialysis were concentrated to 2 mL and loaded onto a HiLoad Superdex 200 PG column that had been equilibrated with three column volumes of Buffer A. The column was run for one column volume. Fractions were examined by SDS-PAGE to identify the fraction in which the enzyme eluted.

7.2.5 Mass spectrometry
Both the tryptophan and phenylalanine mutant proteins, along with wild-type DHDPS, were examined by mass spectrometry. To prepare the samples for analysis, all proteins were concentrated to 10 mg/mL in Buffer A and then diluted to 1 mg/mL with dH_2O. Mass spectrometry was carried out by School of Chemistry, University of Canterbury.

7.2.6 Differential scanning fluorimetry
Twenty microliters of 1:100 diluted SYPRO Orange were added to 60 µL of protein (1 mg/mL) and 20 µL of buffer with or without lysine (4 mM). Duplicate samples, with and without lysine, were prepared for each of the proteins (DHDPS-WT, DHDPS-S48F, and DHDPS-S48W). The samples were loaded into the fluorimeter and heated from 20°C to 100°C for 1 hour. The florescence of the SYPRO Orange was recorded over the heating process and a graph of fluorescence versus temperature was produced.

7.2.7 Kinetic studies

Kinetic studies were conducted for both mutants (DHDPS-S48F and DHDPS-S48W) as well as DHDPS-WT, and were carried out with and without lysine. This was to observe whether there was a difference in activity between the substituted enzymes and the native (DHDPS-WT). A coupled assay was used with DHDPR, which catalysed the reaction after the DHDPS reaction. The reaction mechanism is shown in Figure 7.1.

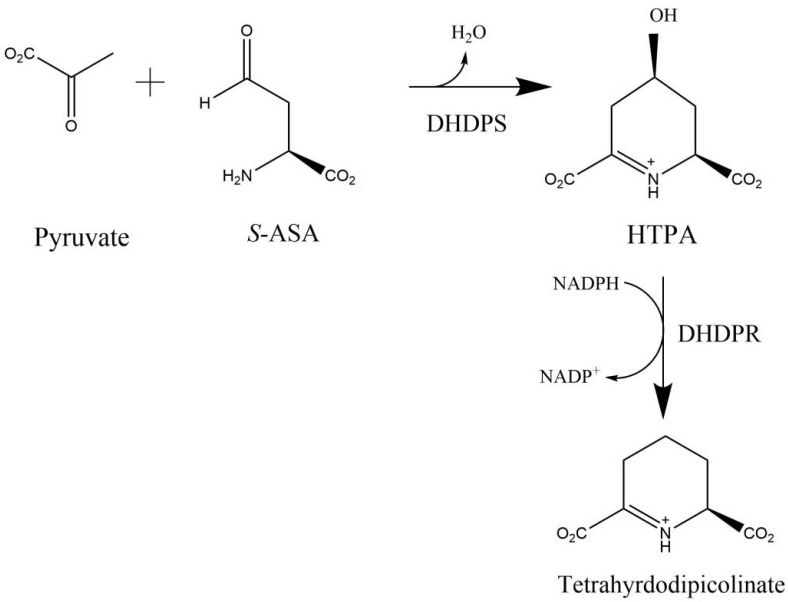

Figure 7.1: *The coupled assay performed in the kinetic studies. Showing the reactants of DHDPS change to HTPA, which is immediately reduced by DHDPS via NADPH.*

The degradation of NADPH was measured. Therefore, DHDPR needed to be in excess to ensure the DHDPS reaction was being recorded. A kinetic curve was generated using varying concentrations of aspartate β-semialdehyde (*S*-ASA). The concentrations of all reagents used in the assays are outlined in Table 7.3.

Table 7.3: *Reagents used in the DHDPS-coupled assay, their stock concentrations and the volumes and concentrations used in each reaction. The concentration of ASA was varied to generate a kinetic curve.*

REAGENT	STOCK CONCENTRATION (MM)	VOLUME IN CUVETTE (ML)	CONCENTRATION IN CUVETTE (MM)
HEPES BUFFER	200	500	100
NADPH	5.4	37.5	0.203
DHDPR		62.5	
DISTILLED H_2O		352.5	
PYRUVATE	25	25	2.5
***S*-ASA**	25	10	0.25
DHDPS TEST		12.5	
TOTAL		1000	

Duplicate assays were conducted using lysine. In these assays, 25 µL of lysine (100 mM) were added to the reaction mix, resulting in a final lysine concentration of 2.5 mM. The volume of dH_2O was adjusted accordingly.

7.2.8 Crystallography

7.2.8.1 Preparation of samples for crystallisation

All proteins were crystallised using the hanging drop method, with drop sizes varying from 4–5 µL. Two different methods were used (Mirwaldt *et al.*[4] and Dobson *et al*.[7]), with the ratios of the separate components of the drops altered depending on the method. K_2HPO_4 buffer (2 M) was tested at pH 9.8, 9.9, and 10.

The drops (4 µL) prepared using the Mirwaldt *et al.* technique contained:

- 2-1.5 µL of 10 mg/mL DHDPS
- 0.6 µL of 6% N-octyl-β-D-glucopyranoside
- 1.3 µL of 2 M K_2HPO_4

The drops (4 µL) prepared using the Dobson *et al*. technique contained:

- 2.5 µL of 10 mg/mL DHDPS
- 0.5 µL of 6% N-octyl-β-D-glucopyranoside
- 1 µL of 2 M K_2HPO_4

All abbreviations used in tables 7.5 and 7.6 are summarized in Table 7.4.

The plate set-ups for the crystallisation of DHDPS-S48W and DHDPS-WT are outlined in Tables 7.4 and 7.5, respectively. The sections that were not co-crystallised with lysine had lysine added after the crystals had formed, as per the method of Dobson *et al* [7].

Table 7.4: *Hanging drop plate set-up for the crystallisation of DHDPS-S48W using different crystallisation methods*

Protein volume	***Mirwaldt or Dobson***	***Condition 1***	***Condition 2***	***Condition 3***	***Condition 4***	***Condition 5***	***Condition 6***
2 µL of protein	M	WT (pH 9.8)	WT (pH 9.8) Lysine	WT (pH 9.9)	WT (pH 9.9) Lysine	WT (pH 10)	WT (pH 10) Lysine
1.5 µL of protein	M	WT (pH 9.8)	WT (pH 9.8) Lysine	WT (pH 9.9)	WT (pH 9.9) Lysine	WT (pH 10)	WT (pH 10) Lysine
2.5 of µL protein	D	WT (pH 9.8)	WT (pH 9.8) Lysine	WT (pH 9.9)	WT (pH 9.9) Lysine	WT (pH 10)	WT (pH 10 Lysine
2 µL of protein	D	WT (pH 9.8)	WT (pH 9.8) Lysine	WT (pH 9.9)	WT (pH 9.9) Lysine	WT (pH 10)	WT (pH 10 Lysine

Table 7.5: *Hanging drop plate set-up for the crystallisation of DHDPS-WT using different crystallisation methods*

Protein Volume	***Mirwaldt or Dobson***	***Condition 1***	***Condition 2***	***Condition 3***	***Condition 4***	***Condition 5***	***Condition 6***
2 µL of protein	M	S48W (pH 9.8)	S48W (pH 9.8) Lysine	S48W (pH 9.9)	S48W (pH 9.9) Lysine	S48W (pH 10)	S48W (pH 10) Lysine
1.5 µL of protein	M	S48W (pH 9.8)	S48W (pH 9.8) Lysine	S48W (pH 9.9)	S48W (pH 9.9) Lysine	S48W (pH 10)	S48W (pH 10) Lysine
2.5 µL of protein	D	S48W (pH 9.8)	S48W (pH 9.8) Lysine	S48W (pH 9.9)	S48W (pH 9.9) Lysine	S48W (pH 10)	S48W (pH 10) Lysine
2 µL of protein	D	S48W (pH 9.8)	S48W (pH 9.8) Lysine	S48W (pH 9.9)	S48W (pH 9.9) Lysine	S48W (pH 10)	S48W (pH 10) Lysine

DHDPS-S48F was crystallised prior to my involvement, but all structures presented in the study were solved by me, all using the same method.

7.2.8.2 Diffraction data analysis

All X-ray diffraction data used in this thesis were collected at the Australian Synchrotron Facility (Clayton, VIC, Australia) using MX1 and MX2 beamlines. All structures were solved using CCP4 software[8], with iMOSFLM[9] used to process the diffraction data. The aimless CCP4 suite[10] was then used to scale the data, and molecular replacement was conducted using PHASER[11]. Resulting pdb and mtz files were refined using REFMAC5[12-20] and were altered using the Crystallographic Object-Oriented Toolkit[21].

7.3 References

1. Dagert, M., and Ehrlich, S. (1979) Prolonged incubation in calcium chloride improves the competence of *Escherichia coli* cells, *Gene* ***6***, 23-28.

2. Van der Rest, M., Lange, C., and Molenaar, D. (1999) A heat shock following electroporation induces highly efficient transformation of *Corynebacterium glutamicum* with xenogeneic plasmid DNA, *Applied Microbiology and Biotechnology* ***52***, 541-545.

3. da Costa, T. P. S., Muscroft-Taylor, A. C., Dobson, R. C., Devenish, S. R., Jameson, G. B., and Gerrard, J. A. (2010) How essential is the 'essential'active-site lysine in dihydrodipicolinate synthase?, *Biochimie **92***, 837-845.

4. Mirwaldt, C., Korndorfer, I., and Huber, R. (1995) The Crystal Structure of Dihydrodipicolinate Synthase from *Escherichia coli* at 2.5 Å Resolution, *Journal of molecular biology **246***, 227-239.

5. Laber, B., Gomisruth, F. X., Romao, M. J., and Huber, R. (1992) *Escherichia-coli* dihydrodipicolinate synthase - identification of the active-site and crystallization, *Biochemical Journal **288***, 691-695.

6. Kefala, G., Janowski, R., Panjikar, S., Mueller-Dieckmann, C., and Weiss, M. S. (2005) Cloning, expression, purification, crystallization and preliminary X-ray diffraction analysis of DapB (Rv2773c) from *Mycobacterium tuberculosis*, *Acta Crystallographica Section F: Structural Biology and Crystallization Communications **61***, 718-721.

7. Dobson, R. C., Griffin, M. D., Jameson, G. B., and Gerrard, J. A. (2005) The crystal structures of native and (S)-lysine-bound dihydrodipicolinate synthase from *Escherichia coli* with improved resolution show new features of biological significance, *Acta Crystallographica Section D: Biological Crystallography **61***, 1116-1124.

8. Winn, M. D., Ballard, C. C., Cowtan, K. D., Dodson, E. J., Emsley, P., Evans, P. R., Keegan, R. M., Krissinel, E. B., Leslie, A. G., and McCoy, A. (2011) Overview of the CCP4 suite and current developments, *Acta Crystallographica Section D: Biological Crystallography **67***, 235-242.

9. Battye, T. G. G., Kontogiannis, L., Johnson, O., Powell, H. R., and Leslie, A. G. (2011) iMOSFLM: a new graphical interface for diffraction-image processing with MOSFLM, *Acta Crystallographica Section D: Biological Crystallography **67***, 271-281.

10. Evans, P. R. (2011) An introduction to data reduction: space-group determination, scaling and intensity statistics, *Acta Crystallographica Section D: Biological Crystallography **67***, 282-292.

11. McCoy, A. J., Grosse-Kunstleve, R. W., Adams, P. D., Winn, M. D., Storoni, L. C., and Read, R. J. (2007) Phaser crystallographic software, *Journal of applied crystallography* ***40***, 658-674.

12. Murshudov, G., Vagin, A., and Dodson, E. (1996) Application of maximum likelihood refinement, *Proceedings of Daresbury Study Weekend 4*.

13. Murshudov, G. N., Vagin, A. A., and Dodson, E. J. (1997) Refinement of macromolecular structures by the maximum-likelihood method, *Acta Crystallographica Section D: Biological Crystallography* ***53***, 240-255.

14. Pannu, N. S., Murshudov, G. N., Dodson, E. J., and Read, R. J. (1998) Incorporation of prior phase information strengthens maximum-likelihood structure refinement, *Acta Crystallographica Section D: Biological Crystallography* ***54***, 1285-1294.

15. Murshudov, G. N., Vagin, A. A., Lebedev, A., Wilson, K. S., and Dodson, E. J. (1999) Efficient anisotropic refinement of macromolecular structures using FFT, *Acta Crystallographica Section D: Biological Crystallography* ***55***, 247-255.

16. Winn, M., Isupov, M., and Murshudov, G. N. (2001) Use of TLS parameters to model anisotropic displacements in macromolecular refinement, *Acta Crystallographica Section D: Biological Crystallography* ***57***, 122-133.

17. Steiner, R. A., Lebedev, A. A., and Murshudov, G. N. (2003) Fisher's information in maximum-likelihood macromolecular crystallographic refinement, *Acta Crystallographica Section D: Biological Crystallography* ***59***, 2114-2124.

18. Winn, M. D., Murshudov, G. N., and Papiz, M. Z. (2003) Macromolecular TLS refinement in REFMAC at moderate resolutions, In *Methods in enzymology*, pp 300-321, Elsevier.

19. Skubák, P., Murshudov, G. N., and Pannu, N. S. (2004) Direct incorporation of experimental phase information in model refinement, *Acta Crystallographica Section D: Biological Crystallography* ***60***, 2196-2201.

20. Vagin, A. A., Steiner, R. A., Lebedev, A. A., Potterton, L., McNicholas, S., Long, F., and Murshudov, G. N. (2004) REFMAC5 dictionary: organization of prior chemical

knowledge and guidelines for its use, *Acta Crystallographica Section D: Biological Crystallography* ***60***, 2184-2195.

21. Emsley, P., Lohkamp, B., Scott, W. G., and Cowtan, K. (2010) Features and development of Coot, *Acta Crystallographica Section D: Biological Crystallography* ***66***, 486-501.